Simulation and Optimization of Unsteady Flow and Water Temperature in Reservoir Regulated Rivers

by

JOHN C. CARRON

B.S., The Colorado College, 1989

M.S., University of Colorado, 1993

A dissertation submitted to the

Faculty of the Graduate School of the

University of Colorado in partial fulfillment

of the requirement for the degree of

Doctor of Philosophy

Department of Civil, Architectural, and Environmental Engineering

2000

This dissertation entitled:

Simulation and Optimization of Unsteady Flow and Water Temperature

in Reservoir Regulated Rivers

by

JOHN C. CARRON

has been approved for the Department of

Civil, Architectural, and Environmental Engineering

_____

Hari Rajaram

_____

Diane McKnight

_____

John Pitlick

Date _____

The final copy of this dissertation has been examined by the

signators, and we find that both the content and the form

meet acceptable presentation standards of scholarly work in

the above mentioned discipline.

© John C. Carron 2000
All Rights Reserved

Carron, John (Ph.D., Civil, Environmental, and Architectural Engineering)

Simulation and Optimization of Unsteady Flow and Water Temperature in Reservoir Regulated Rivers

Dissertation directed by Professor Hari Rajaram

The use of short-term transient releases and selective withdrawal structures in reservoir operations are helpful, and often required, to meet multiple water temperature objectives downstream. Optimization techniques can be used to identify release patterns which meet these temperature objectives. Use of transient reservoir releases may also result in a reduction of water use for instream temperature objectives when compared to traditional steady-state minimum flow designations.

This thesis aims to develop methods for the simulation and optimization of short-term reservoir releases and release temperatures, with the objective of meeting location-specific stream temperature targets downstream. A coupled unsteady flow and heat transport model is developed. Significant components of the model development include a comparison of numerical methods appropriate for advection dominated systems, and field work at the Green River study site to identify and quantify key model parameters. The simulation model forms the basis for evaluating the impact of unsteady flows on stream temperatures, and also serves to evaluate the optimal control techniques. A bound-constrained optimization method is used successfully to develop release strategies which minimize objective functions based on temperature and flow targets. A first-order second-moment model of system uncertainties is also developed. The uncertainty techniques are used to evaluate the impacts of forecast errors on stream temperatures. Errors in atmospheric conditions are shown to have a significant impact on our ability to accurately predict stream temperatures.

For Traci and Calen.

Acknowledgments

This thesis would not have been possible without the help of many people. My committee chair, Dr. Rajaram, has been an inspiring mentor. Thank you to the other members of my committee, Edith Zagona, John Pitlick, Jana Milford, and Diane McKnight. There are many people at the Center for Advanced Decision Support for Water and Environmental Systems (CADSWES) who deserve recognition; among them are Rene Reitsma, Arnaud Dumont, and Jackie Sullivan. A million “thank you’s” to Janet Yowell, guru of FrameMaker and purveyor of humor. Terry Fulp and Larry Crist of the U.S. Bureau of Reclamation were instrumental in getting this work funded. Larry Crist, and Steve Brayton of the Utah Division of Wildlife Resources provided a wealth of information about Flaming Gorge and the Green River. Numerous other persons provided equipment, data, and valuable feedback. These include George Smith of the U.S. Fish and Wildlife Service, Tom Ryan, Larry Miller, Rich Stodt and Dave Matthews of the U.S. Bureau of Reclamation, and Bob Harding of Brown’s Park National Wildlife Refuge.

Completing a dissertation is as much about perseverance as it is about knowledge. My friends and colleagues Rene Reitsma, Arnaud Dumont and Dan Weiler helped me persevere by administering frequent doses of squash, mountain biking, trips to the mountains, and other useful distractions.

Finally, I owe an enormous thank you to Traci, my wife and best friend. I could not have completed this work without your love, support, and considerable patience.

CONTENTS

1. Introduction 1
Thesis 1
Background 1
Literature Review 3
Coupled Unsteady Flow and Water Quality Models 4
Optimization of Reservoir Releases 7
Uncertainty Propagation 11
Objectives and Contributions 14

2. Governing Equations for Unsteady Flow and Heat Transport 17
Unsteady Flow and Heat Transport 17
External Forcings 22
Atmospheric Heat Transfer 23
Streambed Heat Transfer 24

3. Numerical Methods 27
Introduction 27
Finite Difference Methods 28
The QUICKEST Finite Difference Method 30
Verification of Numerical Methods 31
Simulation of an Advective Front 31
Simulation of Heat Transport and Kinematic Flow Waves 34

4. Stream Temperature Modeling and Control Implications 36
Calibration and Verification of the Green River Model 36
Influence of Short-Term Flow Fluctuations and Prospects for Temperature Control 42
Flow Transients in the Green River 43
Temperature Control on the Stanislaus River 45

Multiple Temperature Constraints on the Green River 47
Factors Limiting Temperature Control in Regulated Rivers 50

5. Control and Optimization Theory 55
Introduction 55
Overview of Optimization of Nonlinear Systems. 55
Theory of Bound-Constrained Optimization 56
Quasi-Newton Solution for Bound-Constrained Optimization 57
Verification of Solutions 63

6. Optimal Control of Reservoir Operations 64
Introduction 64
Formulation of Objective Function 66
Feasible Solutions using Unsteady Releases 69
Feasible Solution for Pikeminnow Habitat Objective. 70
Feasible Solution for Trout Habitat Objective 73
Optimal Solution for Pikeminnow and Trout Habitat Objectives 75
Results for Maximum Air Temperatures 75
Results for Average Air Temperatures 77
Optimization using Selective Withdrawal 82
Optimal Release Temperature for Hydropower Operations 86
Optimization using both Unsteady Releases and Selective Withdrawal 88
Influence of Different Control Intervals on Optimal Solutions. 89
Strategies for Meeting Temperature Objectives 92

7. Impacts of Uncertain Atmospheric Forcings and Stream Depth
on Temperature Prediction 94
Introduction 94
Uncertainty Propagation 96
Estimation of Parameter Errors 99
Impacts of Uncertainty on Stream Temperature Prediction 105
Temperature Management Implications 110

8. Summary and Conclusions 111

9. References 114

Appendix A. Overview of Heat Exchange Processes 124
Introduction 124
Conductive Heat Transfer 125

Radiative Heat Transfer 125
Convective Heat Transfer and Boundary Layer Theory 126
Solar (Shortwave) Radiation 130
Atmospheric Longwave Radiation 130
Back Radiation from Water Body 131
Evaporation 131
Conduction/Convection 133
Streambed Heat Flux 133
Data Requirements 136
Streambed Heat Diffusivity Field Work 138

Appendix B. Numerical Methods 141
The QUICKEST Finite Difference Method 141
The ELLAM Finite Element Method 144
The MacCormack FCT Finite Difference Method 146

FIGURES

3.1. Performance of numerical methods in tracking an advective front. 32
3.2. Performance of numerical methods in tracking an advective front. 33
3.3. QUICKEST solution for coupled flow and heat transport. 35
4.1. Green River and Flaming Gorge Dam. 37
4.2. Calibration of QUICKEST model to SSARR model of Green River. 39
4.3. Calibration and verification of Green River temperature model. 41
4.4. Flaming Gorge releases during the model calibration period. 42
4.5. Impacts of transient releases on stream temperatures of Green River 44
4.6. Impacts of transient releases on stream temperatures of Green River. 45
4.7. Comparison of temperatures in the Stanislaus River 47
4.8. Comparison of temperatures in the Green River below Flaming Gorge Dam.....49
4.9. Impacts of atmospheric conditions and release temperatures 51
4.10. Non-dimensional comparison of heating rates for 4 rivers 54
6.1. Graphical depiction of objective function forms. 68
6.2. Feasible control solution for Pikeminnow objective. 71
6.3. Temperature and objective function values for Pikeminnow objective. 72
6.4. Feasible control solution for trout habitat objective. 73
6.5. Temperature and objective function values for trout objective. 74
6.6. Optimal reservoir releases for problem described by Eq. 6.6. 76
6.7. Progression of stream temperature values at the objective locations. 77
6.8. Objective function values for exponential objective function of Eq. 6.6.....78
6.9. Optimal reservoir releases for problem described by Eq. 6.6. 79
6.10. Progression of stream temperature values at the objective locations. 80
6.11. Objective function values for exponential objective function of Eq. 6.6.....81

6.12. Optimal release temperatures for steady reservoir releases. 84

6.13. Stream temperatures at constraint locations.....85

6.14. Objective function values for optimal release temperatures. 86

6.15. Daily maximum stream temperatures below Flaming Gorge Dam 87

6.16. Optimal control sequence using 3-hour control intervals. 90

6.17. Optimal control sequence using 3-hour control intervals plus a ramping objective to minimize fluctuations. 92

7.1. Regression of Eta model forecast incident solar radiation onto values predicted by the Green River model. 101

7.2. Regression of Eta model forecast air temperatures with observed data 102

7.3. Correlation between Air Temperature and Solar Radiation errors 104

7.4. Maximum daily standard deviations below Flaming Gorge Dam. 105

7.5. Accumulation of errors in stream temperature prediction 106

7.6. Relative Impacts of uncertain variables 108

7.7. Comparison of standard deviation to the mean value resulting from a 20% increase in flow, 105 km (top and 46 km (bottom).....109

A.1. Sediment temperature and water temperature data from Brown's Park National Wildlife Refuge 139

A.2. Detail of A.1.....140

B.1. Quadratic weighting scheme 142

TABLES

3.1. Mass Conservation Comparison of Numerical Methods 33
6.1. Comparison of solutions for combined flow and temperature control. 89
6.2. Comparison of solutions for 3 and 6 hour control intervals.....91
7.1. Modeled standard deviations of independent variables as a percentage of the mean value. 103
A.1. Data Requirements for Model Components.....137

CHAPTER 1

INTRODUCTION

1.1 THESIS

The use of short-term transient releases and selective withdrawal structures in reservoir operations are helpful, and often required, to meet multiple water temperature objectives downstream. Optimization techniques can be used to identify release patterns which meet these temperature objectives. Use of transient reservoir releases may also result in a reduction of water use for instream temperature objectives when compared to traditional steady-state minimum flow designations.

1.2 BACKGROUND

Development and management of large reservoirs has historically focused on flood control, hydroelectric generation, and consumptive uses such as municipal, agricultural, and industrial supply. Increasingly, concerns over adverse impacts of reservoir operations on downstream aquatic and riparian ecosystems have led to a re-evaluation of the objectives for which reservoirs are managed (Lillehammer and Saltveit, 1984; National Research Council, 1987; U.S. Department of the Interior, 1993 and 1995). Reservoir induced changes in flow regime and water quality significantly alter these downstream environments from their natural pre-dam state. Morphological changes such as reduced bed-load movement and increased stability of banks

and sand bars also impact the composition and abundance of aquatic species. Riparian species which rely on floods for undergrowth scouring and deposition of sediment often yield to faster growing invasive species. Reservoir tailwaters often support game fish, a secondary benefit of impoundment. However, these fisheries often thrive at the expense of native warm-water fish which are marginalized or eliminated by the dramatic temperature changes and modified flow regimes (U.S. Department of the Interior, 1995). Tailwater temperatures are typically much colder than ambient water temperatures in unregulated streams during summer months, and somewhat warmer during winter (Bolke and Waddell, 1975; Faye et al., 1979). Concerns about such adverse impacts, and the desire to minimize them, has led to increasingly complex management problems.

Managing reservoir releases to control downstream temperature is not a new idea. Various researchers have examined potential methods for reducing adverse impacts of reservoir operations. Water temperature is one of the most important factors influencing stream habitats, as it both directly (e.g., by retarding growth, temperature shock) and indirectly (e.g., through impacts on reaeration and decay rates) affects aquatic habitats (Ward and Stanford, 1979; Lillehammer and Saltveit, 1982). The ability to control river water temperatures depends on many factors, both physical and institutional. Meteorology, physiology, geography, riparian conditions (e.g., shading), geology and hydrology will impact rates of heat flux. Institutional constraints and objectives, such as ramping rates, minimum and maximum flow rates, flood control operations, and hydroelectric generation, will further limit controllability.

We should make an important statement with respect to minimum flows before continuing. There will often be cases in which minimum flows are not only designated for temperature management, but also, for example, for maintaining stream depth over specific fish habitat, such as spawning beds. In these cases, reduction of flows may lead to acceptable stream temperatures, but violate other constraint characteristics.

Reduction of flows for temperature maintenancemust thus be considered within this larger context.

In most reservoir-regulated rivers, temperature control is achievable only through modification of reservoir releases (Webb and Walling, 1988; Malatre and Gosse, 1995; Woodward-Clyde Consultants, 1986; Zimmerman and Dortch, 1989). Reservoirs with selective withdrawal mechanisms are capable of releasing water from different depths within the reservoir. Depending on the degree of thermal stratification at the selective withdrawal structure, this can provide an additional means of controlling downstream temperatures (Theurer et al., 1982; Sartoris, 1976; Fontane et al., 1982).

Rivers which are regulated by reservoir releases may exhibit dramatic changes in flow velocity and depth over periods as short as a few hours, as flows are modified to meet hydroelectric demands, flood control, and water delivery requirements. Because of the potential for rapidly changing river conditions, it may be difficult to accurately predict flow and water quality conditions using steady-state modeling approaches. Strong nonlinearities resulting from varied releases are apparent in travel time (stream velocity), flow depth, and stream heat capacity. In this work we address the issue of controllability of water temperatures in rivers which are regulated by reservoir releases. We are particularly interested in the rate at which water temperature increases downstream of reservoirs subject to different release rates, release temperatures, and atmospheric conditions. These factors have a direct influence on our ability to meet specific temperature objectives, which may vary both spatially and in time.

1.3 LITERATURE REVIEW

This section provides an overview of previous research in the primary topics covered by this work: Coupled unsteady flow and water quality modeling, optimal control, and uncertainty propagation. Contributions by this work to each of these areas

are also outlined.

Coupled Unsteady Flow and Water Quality Models

Existing models which couple flow and water quality constituents usually sacrifice some level of sophistication for ease of use, calibration, or reduction of computational effort. Models of river hydrodynamics are numerous; therefore I will provide a brief, and by no means comprehensive, overview. The focus is directed toward models which couple unsteady hydrodynamic simulation with water quality constituents.

Much of the early impetus for modeling river flows and water quality resulted from concerns about impacts from municipal and industrial effluents into natural waters. There is a large body of work, beginning in the late 1960's, concerned with measuring and predicting effects of thermal discharges from electrical generating stations (e.g., Edinger et al., 1968; Edinger et al., 1974; Paily and Macagno, 1976; Hills and Viskanta, 1976; Brocard and Harleman, 1976; Faye et al., 1979; Jobson, 1973; Jobson, 1985; Bravo et al., 1993). There is another significant, though smaller, body of literature describing modeling efforts in river systems subject to regulated flows (e.g., Bolke and Waddell, 1975; Jobson and Keefer, 1979; Ferrick et al. 1983; U.S. Department of the Interior, 1995).

Edinger et al. (1968) and (1974) provide a broad overview of air/water heat exchange, thermal stratification, and mixing theory. Their work is widely cited in the literature and in textbooks (e.g., Thomann and Mueller (1987), Chapra (1997)). Brady et al. (1969) and Edinger et al. (1974) develop methods using equilibrium temperatures for water bodies. They show that both daily and annual variations from the equilibrium (mean) stream temperature can be modeled using a time-varying bulk heat exchange coefficient. Jobson (1977) develops a semi-analytical solution for simulating heat transfers into and out of the streambed, based on representing the bed as a homogenous slab of finite thickness with a no-flux boundary condition at the lower boundary,

and a convective flux term at the bed-water interface. The model used in this work relies heavily on the theories presented in Edinger's and Jobson's works. They are discussed in depth in the section on heat forcing functions. Kim (1993) and Byars (1994) applied coupled flow and heat transport models to Boulder Creek, a small, highly transient stream in Colorado. Kim also examined heat exchanges at the streambed / water interface using a vertical discretization of the streambed in each computational element.

Jobson (1985) employs a linear unsteady transport approximation in modeling flow, temperature and several other constituents in the Chattahoochee River, Georgia, which is subject to both flow regulation and powerplant effluent. Ferrick et al. (1984) develop and apply a diffusion wave model to highly variable tailwater flows. They use the numerical diffusion implicit it their discretization scheme to approximate the true physical diffusion in the system. Brocard and Harleman (1976) studied waste heat injections into Conowingo Reservoir on the Susquehanna River. They used finite difference techniques for the hydraulics, and a variable-mesh finite element approach for the temperature model to capture large temperature gradients near effluent outflows.

Bravo et al. (1993) employ a stochastic state-space representation to estimate stream temperatures downstream of the Joliet power station on the Des Plaines River, Illinois. They use a hybrid numerical approach, using the method of characteristics for the advective term, and a Crank-Nicholson scheme for the diffusion and heat exchange terms. Holly et al. (1990) developed the CHARIMA model for simulating unsteady flow, sediment, and heat transport in river systems. In CHARIMA, the hydrodynamics are based on a dynamic wave approximation of the St. Venant equations, while an advection-diffusion scheme is employed for the heat transport model. Bradley et al. (1998) use CHARIMA to estimate temperature exceedence probabilities due to heating from thermal plants.

Several public domain models are available for simulating river hydraulics and

water temperature. QUAL2E is perhaps the most commonly used stream water quality modeling tool. The model operates in steady-state or “quasi-dynamic” modes, and can simulate advection and dispersion of up to 15 water quality constituents. The quasi-dynamic mode allows the user to examine diurnal changes in constituent concentrations (for example, as a result of changing respiration rates) but does not allow for fully dynamic hydraulic simulation, since boundary conditions and forcings must be static. The Water Quality for River-Reservoir Systems (WQRRS) model developed by the U.S. Army Corps of Engineers provides a common interface for river hydraulics, river water quality, and reservoir water quality modeling. The hydraulic routing module allows users the choice of several variations on the St. Venant equations, the Muskingum method, and the modified Puls method, in both steady and unsteady flow regimes. The water quality module, however, assumes steady state conditions, but can model aerobic degradation and diffusion of non-reactive constituents. The Stream Network Temperature (SNTEMP) model developed by the U.S. Geological Survey predicts stream temperatures in streams with complex topologies, based on flow, riparian (shading), and meteorological conditions. The models run on a daily or larger timestep, and output mean daily water temperature and an estimated maximum daily temperature.

This work uses a diffusion wave approximation to the St. Venant equations. It is a nonlinear, unsteady, one-dimensional representation of both the river hydraulics and stream temperature. Highly transient reservoir releases, which are of interest in this work, add significant numerical difficulties, primarily from the occurrence of moving fronts caused by sudden changes in release volume. The timing of short-term transient releases will be shown to have a significant impact on variations in downstream temperatures in later chapters. We use a highly accurate numerical scheme - the Quadratic Upstream Interpolation for Convective Kinematics with Estimate Streaming Terms, or QUICKEST - developed by Leonard (1979). The scheme is based on a finite

difference control volume discretization of the river channel, and uses quadratic interpolation at each cell wall to achieve highly accurate solutions around advecting fronts. Although research addressing the problem of modeling advective fronts is not new, it does continue to generate interest (e.g., Sivapalan et al., 1997; Rutschmann and Hager, 1996; Vag et al., 1996). The application of the QUICKEST numerical method to flow and river water quality modeling below reservoirs has not been reported in the literature. There are also no known published works which examine impacts of diurnal flow modifications on stream temperatures and their potential use for reducing water use.

Optimization of Reservoir Releases

We should start by making a distinction here between the kind of control problems we are dealing with and problems which can be addressed using theories of real-time or optimal feedback control. Real-time control schemes have been employed in water resource systems to provide direct feedback to reservoir operators, wastewater treatment facilities, and thermal plants. Systems which are amenable to solutions of this type are generally constrained at the location of the source outflow into the water body. For control purposes, these systems can monitor chemical or thermal properties, identify potential violations, modify plant operations, and cause a more or less instantaneous impact on conditions at the constraint location. Contrast this to a situation where a temperature constraint exists a significant distance - and hence, travel time - downstream of a control location. Feedback of an impending violation of the constraint will not prevent the violation from occurring, because any control which is subsequently enacted will have a significant time delay before those benefits are felt downstream. The solution to our problem, therefore, must utilize forecasts of system states and forcing variables. We seek short-term (1-2 day) optimal control solutions based on these predicted future conditions.

The literature regarding optimization and control of reservoir releases is

immense. We therefore limit our discussion of previous work to some general comments about the more common approaches, and to work which specifically addresses the problem of meeting temperature constraints under unsteady flow conditions. When looking at optimization or control problems in managing rivers for water quality constituents, the need for a coupled system model becomes apparent. The release of water from a reservoir typically provides the only control on the system (reservoirs with selective withdrawal mechanisms have two). However, the ability of a reservoir to control the downstream character of the river is limited. Influences of unregulated inflows from tributary streams, losses or gains from groundwater, and atmospheric heating and cooling eventually become the dominant forces determining the character of the stream. Stream reaches in which water temperature is directly influenced by managed releases, what Sinokrot and Stefan (1993) call “thermal transition reaches”, are the focus of this work. We cannot hope to control the character of the river beyond that point at which the “memory” of the release has been eliminated. The variables we wish to influence (temperature), are directly influenced by the timing and magnitude of the releases, and on the atmospheric and ground heat fluxes.

Control theory has its roots in the fields of mechanical, chemical, and aerospace engineering. Optimization has long been the domain of operations research. Dreyfus (1965) proposes that “optimization” or “optimal control” be applied to problems with a well-defined objective function, which is a sub-set of the larger theory of system control, where the “objective” may be a qualitative goal, such as non-oscillatory behavior, convergence, or growth. In the latter case, there may be a large set of possible solutions.

Some of the more well known optimization techniques include linear programming (LP), dynamic programming (DP), nonlinear programming (NLP), and their derivatives (e.g., stochastic DP, chance-constrained LP, etc.), genetic algorithms, neural network, and fuzzy-logic. Control methodologies, including the well known Linear

Quadratic Gaussian (LQG) control scheme and its derivatives (which are closely related to DP theory), are often differentiated from optimization schemes by the inclusion of a feedback mechanism, typically in the form of a Kalman filter or equivalent error minimization method. LQG, in fact, can be thought of as a series of dynamic programming solutions which are re-evaluated at each time increment in which a new system observation becomes available. The reader is referred to Yeh (1985) for a general overview of optimization methodologies. Yakowitz (1982) provides an overview of DP methods, while Bazaraa et al., (1993) provide an overview of NLP methodologies. Overviews of control theory can be found in Barnett and Cameron (1985) and Auslander et al. (1974).

Optimization and control techniques for managing reservoir and river systems have been in use since the mid 1960s. Much of the original work focused on the areas of reservoir design, flood control, and optimal waste load allocation. More recent trends have seen the inclusion of water quality, recreation, and ecosystem viability as management objectives.

Krajewski et al. (1993) address the problem of controlling thermal heating of rivers under uncertainty. They use output from multiple simulation runs to generate a cost surface, and then find its minimal value to locate the optimal control. Jaworski et al. (1970) use DP techniques to optimize reservoir releases for dissolved oxygen and temperature objectives, while simultaneously considering water-in-storage values. Nicholson et al. (1970) use DP to control water quality in rivers using both source control and reservoir low-flow augmentation. Cardwell and Ellis (1993) use Stochastic DP to determine optimal waste-load allocations for a set of 5 point sources distributed along a river reach. Wasimi and Kitanidis (1983) use LQG methods to control systems of reservoirs under flood conditions. Marino and Loaiciga (1985,1986) similarly use quadratic penalty functions with feedback to control reservoirs in California's Central Valley Project. Georgakakos (1984), and Georgakakos and Marks (1987) extend the

LQG methodology to include nonlinear systems. Their ELQG method relies on a linearization of the governing equations around local mean values in time and space, and solves constrained LQG type problems using an iterative solution technique to ensure compliance with the constraints.

Correia and Andrade (1988) use network optimization techniques to optimize reservoir operations during both wet and dry seasons near Sao Paulo. They examine trade-offs between water delivery and hydropower generation subject to meeting instream water quality objectives downstream. Fontane et al. (1981) and Wilhelms and Schneider (1986) use objective-space dynamic programming (OSDP) to develop reservoir discharge strategies which minimize deviations from target release temperatures. These models predict the annual thermal stratification cycle in a reservoir, and generate a single long-term control strategy, which they conclude to be preferable to optimization over weekly or monthly periods.

Recent work by Piasecki and Katopodes (1997a, 1997b) applies adjoint equation theory to sensitivity analysis and control of contaminant releases in rivers and estuaries. They develop their model in the context of controlling multiple contaminant sources with multiple constraint locations in a two dimensional river / estuary model. Adjoint methods have also been applied to problems in atmospheric science (Hall and Cacuci, 1982; Kapitza, 1991), groundwater systems (Yeh and Sun, 1990), petroleum reservoir modeling (Chavent et al., 1975) and to optimal design for nuclear power plants (Marchuk, 1986).

We require an optimization method that can be used for systems which are nonlinear in both the governing equations and objective function. The methods should allow designation of constraints on the control variables (flow and temperature), and should allow for spatial and temporal discretization of the objective function. These requirements greatly reduce the set of optimization techniques which we may choose from.

In the present work, we apply a bound-constrained optimization technique. This method may be considered a subset of nonlinear programming which is characterized by constraints which are only in the form of bounds on the variables (i.e., no inequality or equality constraint functions). Bound-constrained techniques are particularly appropriate in systems which are undefined outside of the variable bounds. This feature is important in the present work because the physical system is either undefined or infeasible for controls outside the constraint bounds (e.g., negative reservoir releases or releases greater than the outlet works are physically capable of). We employ a quasi-Newton solution approach to the bound-constrained optimization problem, using a publicly available optimization software tool (L-BFGS-B; Zhu et al., 1997). The solution to the optimization problem is generated by repeated approximation of the gradient and Hessian matrix values of the objective function by perturbing the control vectors. To verify the optimal solutions, we employ a quadratic root-finding algorithm. The algorithm is also used to solve simple one-control optimization problems for which the BFGS solver is too complex. The use of optimization techniques for short-term predictive control of water temperatures downstream of hydropower reservoirs using unsteady flows has not been previously reported.

Uncertainty Propagation

Uncertainty manifests itself in many ways in complex models of hydrologic systems. Errors in data observations, in model parameters, and as a result of discretization of continuous systems all point to the need to quantify the amount of uncertainty carried through the modeling process. It is not sufficient to understand the magnitude of the uncertainties. We need to be able to quantify how uncertainties propagate through the system, and how sensitive the system is to errors in individual model parameters and forcings.

There are numerous methods available for quantifying uncertainty in hydro-

logic models. Simple goodness-of-fit criteria may be obtained by comparing observed and predicted values of the dependent variables. Perhaps the most common criteria is a sum-of-squares measurement, which is often used as a minimizing function when calibrating models. These types of uncertainty analysis suffer from relying on observed data which may only represent a portion of the actual range of possible system states, or which is too small to be statistically significant. Also, static measures of uncertainty are inappropriate for non stationary systems with time-varying dynamics. Monte-Carlo type simulations predict model output variability by examining variable distributions resulting from a large number of deterministic model runs, with input variables sampled from appropriate distributions. This approach is useful when knowledge of variable distributions is good, and when the computational expense of multiple model runs is not prohibitive. Analytical formulations based on a first-order second moment perturbation approach allow the model uncertainties to be computed in tandem with the mean values. This approach is more efficient in terms of computing resources, but can require complex derivations of covariance equations, and is strictly correct only for linear systems with Gaussian uncertainty distributions. However, they have been used extensively for nonlinear systems, based on linearizing the uncertainty propagation equations. In these cases, they still provide useful second moment information which may be used to construct confidence bounds. Detailed explanations of these methods may be found in Jazwinski (1970), Gelb (1974), and Bras and Rodriguez-Iturbe (1985).

McLaughlin (1983) develops a state-space representation of distributed parameter systems and uses a first-order error approximation to propagate covariance values through the system. Marino and Loaiciga (1986) use a Linear Quadratic Gaussian approach to model manager’s aversions to risks introduced into the system by uncertain model inputs and parameters. They also use the uncertainty propagation model in conjunction with a Kalman filtering process for parameter estimation and real-time

reservoir control during flood events. Bradley et al. (1998) use the CHARIMA model (Holly et al., 1990) to develop exceedence probabilities for water temperatures impacted by thermal plant operations. Their probabilities are derived from the deterministic model by equating the probability to the fraction of time which the temperature exceeds a specified level.

The Bedford-Ouse study (Whitehead and Young, 1979; Whitehead, 1983) uses time-series analysis to model residual errors in its deterministic model, and uses Monte Carlo type simulations to generate output probability density functions. Similarly, Koivo and Tanttu (1983) use a self-tuning predictor variation of a multivariate ARMA (auto-regressive moving average) model to estimate dissolved oxygen and BOD. Their approach is essentially a Kalman-type filter applied to statistical (autoregressive) models. Ibbitt (1972) studied the effects of introducing random errors into (assumed) error-free data to compute sensitivities in parameter values for precipitation, evaporation, and streamflow. Moss (1991) uses a hydrologic “random walk” to estimate hydrologic conditions under varying climatic conditions in large scale hydrologic models.

Warwick and Roberts (1992) use Monte Carlo simulations to develop uncertainty bounds for a waste load allocation model. They found that uncertainty in Kjeldahl nitrogen concentrations had the largest impact on permissible waste loading levels. Brown (1987) develops methods for incorporating uncertainty analysis techniques, such as sensitivity analyses and Monte Carlo simulation, into the EPA’s QUAL2E model. Examples from that work illustrate the potential spatial variability of sensitivities to specific parameter and input uncertainties.

In this dissertation, governing equations are developed for system uncertainties using a first-order, second-moment (FOSM) approach. The approach has been used previously in water quality studies by Hoybye (1998), Protopapas and Bras (1993) for soil moisture modeling, and Melching et al. (1991) for evaluation of rainfall-runoff

models. The approach is often employed in systems represented by relatively simple governing equations, as the derivation for more complex systems is prohibitive. The FOSM method generates equations for variances and covariances, which are simulated in a manner similar to the original simulation model. The user provides estimates of variance and covariance values for independent variables and boundary conditions. In this work, estimates of the variances and covariances are developed from regression of ground-based observations of meteorological data with forecasts generated by the Eta mesoscale climate model. These statistics allow us to quantify confidence bounds on temperature predictions when using Eta model forecasts in an operational setting. The governing equations for uncertainty will be modeled using the QUICKEST numerical scheme. The application of FOSM approaches to modeling temperature uncertainty in reservoir-regulated rivers is novel. Also, the use of the QUICKEST scheme for this type of uncertainty modeling has not been previously reported.

1.4 OBJECTIVES AND CONTRIBUTIONS

This thesis aims to develop methods for the simulation and optimization of short-term reservoir releases and release temperatures, with the objective of meeting location-specific stream temperature targets downstream. A coupled unsteady flow and heat transport model is developed. Significant components of the model development include a comparison of numerical methods appropriate for advection dominated systems, and field work at the Green River study site to identify and quantify key model parameters. The simulation model forms the basis for evaluating the impact of unsteady flows on stream temperatures, and also serves to evaluate the optimal control techniques. A bound-constrained optimization method is used to develop release strategies which minimize objective functions based on temperature and flow targets. A first-order second-moment model of system uncertainties is also developed. The uncertainty techniques are used to evaluate the impacts of weather forecast errors on

stream temperatures. Errors in atmospheric conditions are shown to have a significant impact on our ability to predict stream temperatures.

To summarize, this dissertation makes contributions in the following areas:

- Impact of short-term fluctuations in reservoir releases on downstream water temperature. The research quantifies the impacts of short-term release modifications, particularly with respect to diurnal variations induced by atmospheric conditions. Field work conducted during 1998 identified parameter values for sediment heat conductivity. A comparison of three numerical methods identified the QUICKEST method as a highly accurate and efficient finite difference scheme. The QUICKEST scheme is used to simulate the coupled unsteady flow and temperature equations. The methods are applied to the Green River below Flaming Gorge Dam. Results of this work are being used to develop release strategies for the Colorado Pikeminnow recovery program in the Green and Yampa Rivers in Dinosaur National Monument.

- Controllability of water temperature in regulated rivers using variable reservoir release rates and temperatures. The research employs a bound-constrained optimization technique to develop reservoir release rates which are optimal with respect to a set of physical and operational objectives, including downstream water temperature, release volume, and ramping rates (the rate at which reservoir releases are changed). The results indicate that the bound-constrained method produces optimal release strategies, and that in many situations, even with the use of selective withdrawal, diurnally varying releases are required in order to meet multiple temperature objectives.

- Impact of uncertain weather forecasts and flow depth on prediction of water temperatures. A First-Order, Second-Moment (FOSM) approach is utilized to develop governing equations for air temperature, solar radiation, stream depth, and water

temperature (co)variances. Ground-based meteorological data are used to calibrate and test the simulation model. In an operational setting, however, predictions of stream temperatures must rely on meteorological forecasts of future conditions. We develop statistical relationships between these forecasts and the ground-based observations. The resulting statistics are used in the uncertainty model to quantify confidence bounds on stream temperature predictions. The use of imprecise meteorological forecasts is shown to have a significant impact on stream temperature prediction.

CHAPTER 2

GOVERNING EQUATIONS FOR UNSTEADY FLOW AND HEAT TRANSPORT

2.1 UNSTEADY FLOW AND HEAT TRANSPORT

Releases from reservoirs are inherently more predictable than unregulated stream flow, because they are almost completely controllable. However, release rates may potentially vary by more than an order of magnitude in a short period. Sudden increases or decreases in releases are not uncommon as reservoir operators adjust releases to meet electric generation needs or flood control requirements. Fluctuating releases result in large variations in stream velocity, surface area, and water depth downstream. These variations can have a significant impact on water quality. Modeling reservoir releases using unsteady flow algorithms allows us to take advantage of these variations when generating optimal releases, and generally provides a more accurate representation of the system.

Numerous researchers have addressed the issues of reservoir release and downstream temperature modeling. These efforts range from relatively simple 1-D steady flow approximations of mean daily flow (e.g., Sartoris, 1976; Wunderlich and Shiao, 1984; Woodward Clyde, 1986) to multi-dimensional and unsteady flow approximations (e.g., Faye et al., 1979; Jobson and Keefer, 1979; Zimmerman and Dortch, 1989). A closely related problem, that of the impacts of thermal effluent, has also been widely

studied (e.g., Jobson, 1973; Edinger et al., 1974; Paily et. al., 1974; Hills and Viskanta, 1976; Bowles et. al., 1977). These two classes of problems are quite similar, with both governing equations and control issues sharing many of the same features.

Most physically-based models are based on approximations to the unsteady one-dimensional St. Venant equations for continuity,

$$U\frac{\partial A}{\partial x} + A\frac{\partial U}{\partial x} + \frac{\partial A}{\partial t} - q = 0 \tag{2.1}$$

and momentum conservation,

$$\frac{\partial U}{\partial t} + U\frac{\partial U}{\partial x} + g\left(\frac{\partial y}{\partial x} - \frac{\partial z}{\partial x} + S_f\right) = 0 \tag{2.2}$$

where U = average wave velocity, A = cross-sectional area, x = longitudinal direction, g = gravity acceleration, t = time, q = lateral inflow (per unit length), y = flow depth, z = bed elevation, S_f = friction slope.

Although Eq. 2.1 and Eq. 2.2 cannot in general be solved analytically, many numerical solutions are available. As shown, the equations are data intensive, and in many situations are unnecessarily complex. With a cursory understanding of the physical system being modeled, it is common to neglect one or more terms in the St. Venant equations. These simplifications result in approximations such as the kinematic wave and diffusion wave models. For regulated rivers subject to unsteady flows, numerical approximations must operate across a wide range of flow conditions often characterized by sharp-fronted, short-period waves. Previous authors (e.g., Ponce et. al., 1978; Henderson, 1963; Ferrick et. al., 1983; Cappelaere, 1997) provide analyses of the validity of various approximations. These analyses indicate that inertial terms in these systems are relatively small. Henderson notes that it is reasonable to expect large water surface slope terms, particularly in rivers with mild bottom slopes during periods of changing releases. The diffusion wave approximation has been shown to accu-

rately capture transient flow characteristics in reservoir tailwaters (Henderson, 1963). It is a valid approximation for the rivers modeled in this thesis, for a wide range of flow rates, based on the guidelines described by Ponce (1978). The diffusion wave approximation with no gains or losses is given by:

$$\frac{\partial Q}{\partial t} + \frac{\partial Q}{\partial A}\frac{\partial Q}{\partial x} - \frac{\partial}{\partial x}\left(D\frac{\partial Q}{\partial x}\right) = 0 \tag{2.3}$$

where $D = Q/2BS_0$, B = mean channel width, and S_0 = bed slope.

The one-dimensional heat transport equation for rivers can be expressed as (Jobson and Keefer, 1979; Sinokrot and Stefan, 1993):

$$\frac{\partial}{\partial t}(TA) + \frac{\partial}{\partial x}(TQ) - \frac{\partial}{\partial x}\left(D_T\frac{\partial}{\partial x}(TA)\right) = \frac{\Delta HA}{\rho C_p y} \tag{2.4}$$

where T is water temperature, A is the area of cross-section of the flow, D_T is the temperature diffusion/dispersion coefficient, ΔH represents the atmospheric and streambed heat fluxes, ρ is the density of water, C_p is its specific heat, and y is flow depth. The flow rate impacts the heat equation through the transport and heat source terms, since the flow depth (y) and cross-section area (A) are functions of the flow rate (Q). These relationships are made explicit below.

For illustrative purposes, the river geometry is approximated as a wide-rectangular channel. This assumption in no way precludes the use of other approximations for $\frac{dQ}{dA}$, rather it provides a straightforward example. For a wide rectangular channel, Q=Bq, where q=flow per unit width (L^2/t). Substituting Q=Bq into Eq. 2.3, and using Manning's equation to develop a term for $\frac{dQ}{dA}$, we have

$$\frac{\partial q}{\partial t} + [\alpha q^{\beta}]\frac{\partial q}{\partial x} - \left[\frac{1}{2}\frac{q}{S_0}\right]\frac{\partial^2 q}{\partial x^2} = 0 \tag{2.5}$$

with

$$\alpha = \frac{5}{3}\left(\frac{\sqrt{S_0}}{n}\right)^{3/5}$$
$$\beta = \frac{2}{5} \tag{2.6}$$

The advection-dispersion transport equation for water temperature is given by

$$\frac{\partial T}{\partial t} + v_T\frac{\partial T}{\partial x} - \frac{\partial}{\partial x}\left(D_T\frac{\partial T}{\partial x}\right) = \frac{\Delta H}{\rho C_p y} \tag{2.7}$$

where T is water temperature, v_T is water velocity, D_T is the longitudinal diffusion/dispersion coefficient, and $\frac{\Delta H}{\rho C_p y}$ is a heat exchange term representing heat gain (or loss) at the water - air and water - streambed interfaces. For simplicity, and because advection is the dominant physical behavior in most tailwater systems, we have chosen to neglect the diffusion/dispersion term in the following derivation. Water temperatures in regulated rivers will typically vary by much less than 1 ^{o}C per kilometer, even immediately downstream of dams. The longitudinal heat gradient, and thus longitudinal heat diffusion/dispersion, is negligible. It is worth noting, however, that if a reservoir is equipped with a selective withdrawal mechanism capable of operating over short time horizons, inclusion of the diffusion term in equation 2.7 may be necessary, as sudden changes in water temperature could induce longitudinal diffusion/dispersion.

Typically, releases at a control point are known in units of flow (L^3/T), which, for a wide rectangular channel, become flow per unit width (L^2/T) when divided by the channel width. We want to relate this flow to the velocity term in Eq. 2.7. Begin with Mannings equation,

$$Q = \frac{1}{n}AR^{2/3}S_0^{1/2} \tag{2.8}$$

and notice that for a wide rectangular channel, the hydraulic radius R is approximated

by

$$R = \frac{By}{B + 2y} \approx \frac{By}{B} \approx y \tag{2.9}$$

as $B >> y$, where B is the channel width, and y its depth. Inserting Eq. 2.9 into Eq. 2.8 yields the equation for flow per unit channel width

$$q = \frac{1}{n} y^{5/3} S_0^{1/2} \tag{2.10}$$

Now, notice that velocity for a channel of unit width is

$$v = \frac{q}{y} \tag{2.11}$$

Solving for y in Eq. 2.10 and inserting that solution into Eq. 2.11 gives us the relationship between flow and solute velocity:

$$v = \frac{q}{y} = \left[\frac{n}{\sqrt{S_0}}\right]^{-3/5} q^{2/5} \tag{2.12}$$

We can now re-write the advective constituent equation with v from Eq. 2.12:

$$\frac{\partial T}{\partial t} + \left[\left[\frac{n}{\sqrt{S_0}}\right]^{-3/5} q^{2/5}\right]\frac{\partial T}{\partial x} = \frac{\Delta H}{\rho C_p y} \tag{2.13}$$

Eq. 2.5 and Eq. 2.13 are the coupled transport equations for flow and temperature. Note that we have made several assumptions to get to this point. The channel is assumed to be wide and rectangular and flow is considered only in the longitudinal direction. Convective acceleration terms have been ignored. Velocities, diffusion coefficients, and gain and loss terms are averaged over the width and depth of the channel. Other channel geometries may be used in place of the above approximations if appropriate. They add some complexity to the governing equations, but the derivations follow the same line of reasoning.

2.2 EXTERNAL FORCINGS

Atmospheric fluxes are the primary catalyst in determining water temperature, which in turn affects “nearly every physical property of concern in water quality management” (Jobson, 1973). Significant heat flux may also occur into and out of the streambed, and is especially important in shallow streams (Jobson, 1977). Variations in stream water temperatures tend to follow annual and diurnal variations in mean air temperatures. Diurnal variations are caused primarily by heating of the water by incoming longwave and shortwave radiation, and heat transfer into the stream from the streambed. Heat loss occurs through convection and evaporation at the water surface, and through conductive losses into the streambed when the overlying water is warmer than the bed surface. Characteristic time scales of heat transfer in the streambed are on the order of less than 24 hours to a week or more, depending on stream characteristics and atmospheric conditions (Jobson, 1977; Sinokrot and Stefan, 1993). The effects of heat transfer to and from the streambed are not as pronounced as atmospheric fluxes, but may nevertheless significantly dampen diurnal temperature variations.

The subject of heat transfer across the air - water interface has been widely studied. An extensive overview can be found in Edinger et al. (1974). Summaries based in large part on that work include Fischer et al. (1979), Thomann and Mueller (1987), and Chapra (1997). Primary sources and sinks involved in heat exchange between air and water include: shortwave solar radiation, longwave atmospheric radiation, longwave back-radiation, reflected solar and atmospheric radiation, gain or loss of heat due to conduction, and gain or loss of heat due to evaporation or condensation.

The following is based largely on the work of Edinger et al. (1974). Assuming a well mixed vertical column of water, the change in temperature T of a water body is given by

$$\frac{\partial T}{\partial t} = \frac{\Delta H}{\rho C_p y} \tag{2.14}$$

where ΔH is net heat flux, C_p is heat capacity of water, ρ is water density, and y is stream depth.

Atmospheric Heat Transfer

The net heat exchange to / from the water is the sum of atmospheric and stream bed fluxes, $\Delta H = \Delta H_a + \Delta H_b$. The atmospheric flux is given by

$$\Delta H_a = H_{sn} + H_{an} - H_{br} \pm H_c \pm H_e \tag{2.15}$$

with

$$\begin{aligned} H_{sn} &= \text{net solar (shortwave) radiation} \\ H_{an} &= \text{net atmospheric (longwave) radiation} \\ H_{br} &= \text{longwave radiation from water} \\ H_c &= \text{conductive heat transfer} \\ H_e &= \text{evaporative heat transfer} \end{aligned} \tag{2.16}$$

A commonly used functional representation of Eq. 2.15 is

$$\begin{aligned} \Delta H_a = {} & R_s f(\theta_s, cc) + \sigma\varepsilon(T_a + 273)^6(1 - R_l) - \sigma\varepsilon(T_w + 273)^4 \\ & - 0.47 f(u_w)(T_w - T_a) - f(u_w)(e_s - e_a) \end{aligned} \tag{2.17}$$

where

R_s = reflection coefficient for solar radiation

θ_s = incidence angle of solar radiation

cc = fractional cloud cover (0-1)

σ = Stefan-Boltzmann constant (4.9 x 10^{-3} J / (m^2 d K^4))

ε = emmissivity of water (~0.97)

T_a = air temperature (C) **(2.18)**

T_w = water temperature (C)

R_l = reflection coefficient for longwave radiation

u_w = wind speed above water surface

e_s = saturation vapor pressure at the water surface

e_a = vapor pressure of air immediately above water surface

Eq. 2.17 is based in part on physical laws of thermodynamics and in part on empirically derived relationships. The solar radiation term $(R_s f(\theta_s, cc))$ is based on the solar altitude, and a quadratic "extinction" coefficient based on cloud cover. The atmospheric longwave radiation term $(\sigma\varepsilon(T_a + 273)^6(1 - R_l))$ is based on a variation of Brundt's formula (itself based on the Stefan-Boltzmann law), using cloud cover data as a surrogate for air vapor pressure. Longwave radiation $(\sigma\varepsilon(T_w + 273)^4)$ emitted from the stream is also computed using the Stefan-Boltzmann law. Conduction ($0.47 f(u_w)(T_w - T_a)$) is based on the temperature difference between water and air, Bowen's coefficient (0.47 mm Hg/^{o}C), and an empirically derived windspeed function. Evaporation ($f(u_w)(e_s - e_a)$) is based on Dalton's "Law of Partial Pressures", and an empirically derived windspeed function. Further details of each atmospheric term, and its origin, are provided in Appendix A.

Streambed Heat Transfer

Heat transfer between streambed and stream is often neglected as an important process in the dynamics of stream temperature models. However, it has been noted that in many natural waters, particularly those which are shallow (< 3 m) and clear,

streambed heat fluxes significantly impact diurnal heating in the overlying stream (Jobson, 1977). Heat flux into the streambed is typically assumed to be dominated by conduction, though over longer periods it may be complicated by water movement into and out of the bed. Conduction will be the predominant mechanism over shorter periods of time (hours to days) during which convective heat flux via groundwater flow is negligible. Heat flux on the stream side of the streambed/stream interface is somewhat more complicated. In most natural rivers, flow is turbulent, which leads to a well mixed (vertically and laterally) system with a narrow boundary layer at the streambed. The type of approximation used for heat flux across this boundary is dependent on the relative speed with which convective mixing in the river and conduction in the streambed occur. We use an approximation developed by Jobson (1977) which has been shown to give good results (Jobson and Keefer, 1979; Sinokrot and Stefan, 1993). The method assumes that conduction within the bed (as opposed to diffusion/ dispersion in the stream) is the limiting factor in the streambed - water heat flux mechanism. Using this assumption, a transient heat flux equation describing the gain or loss of heat into the streambed over a given time interval can be developed. The net change in total heat in the streambed layer becomes a gain or loss into the stream itself. The streambed heat flux at the bed-water interface is given by

$$\Delta H_b = -k \left. \frac{\partial T_b}{\partial z} \right|_{z=0} \tag{2.19}$$

with

$$\begin{aligned} T_b &= \text{river bed temperature} \\ z &= \text{bed depth (= 0 at water interface)} \\ k &= \text{bed thermal conductivity} \end{aligned} \tag{2.20}$$

Heat stored within the stream bed is modeled using Carslaw and Jaeger’s (1959) expression for temperature distribution within a medium subject to a changing bound-

ary condition (see Jobson, 1977). Field work during the summer of 1998 confirmed values for the streambed conductivity (see Appendix A, Section A.3), and verified applicability of the streambed heat transfer formulation given above. A complete derivation of the sediment heat flux terms is given in Appendix A.

CHAPTER 3

NUMERICAL METHODS

3.1 INTRODUCTION

We now turn to the methods employed to solve the governing equations developed in the previous chapter. The problem of solving these partial differential equations (PDEs) is pervasive throughout engineering and the applied sciences. The choice of numerical techniques used to solve PDEs varies greatly, but is typically determined by the dominant physical behavior in the system being modeled. For advection-diffusion problems, which have both a hyperbolic (advection) and parabolic (diffusion) component, the choice is often based on which of the components dominate the system's behavior. For diffusion dominated systems, most numerical schemes give good results. When advection dominates, however, many schemes suffer from either excessive numerical diffusion or non-physical oscillations in their solutions (see, e.g., Leonard, 1979; Finlayson, 1992; Celia et. al., 1990). Regulated rivers are typically advection dominated, and may also contain multiple advective fronts. These multiple fronts result from propagating flow, water temperature, and other constituents, which travel at different velocities downstream. Numerical simulation of the coupled equations for unsteady flow and heat transport provides a basis for evaluating thermal regimes in regulated rivers. The choice of numerical algorithms for solving these equations is influenced heavily by the dominance of the advection term in both equations.

Several previous works have focused on the development of accurate numerical algorithms for advection dominated problems. These are reviewed in, for example, Leonard (1979), Celia et. al (1989), Finlayson (1992), and Morton (1996). Brocard and Harleman (1976), Bowles et al. (1977), and Bravo et al. (1993) have addressed coupled unsteady flow and temperature modeling in rivers.

In this dissertation, we use an explicit finite-difference scheme - the QUICKEST scheme of Leonard (1979) - to solve the coupled system of partial differential equations. This scheme has been called “the key explicit finite difference scheme for unsteady convection - diffusion” by Morton (1996). It has been applied to coupled flow and transport problems in estuaries (Lin and Falconer, 1997; Portela and Neves, 1993), in chlorine treatment systems (Wang and Falconer, 1998), and coupled hydrodynamic transport and ecological models of ocean currents (Vested et. al., 1996). The QUICKEST scheme is a control volume formulation which employs a three-point upstream-weighted quadratic interpolation for the wall values of the independent variables. Nonlinear velocities are accounted for through an estimated advective term which uses initial conditions at each timestep to approximate average velocities over the step at each wall.

3.2 FINITE DIFFERENCE METHODS

Finite difference schemes used in the solution of advection dominated PDEs may often be generalized as either upstream (backward) or centered difference formulations, or some combination or the two. Specializations of these include the Lax-Wendroff, MacCormack, Preissman/Holly-Preissman, Quadratic Upstream Interpolation for Convective Kinematics (QUICK), and Flux-Corrected Transport (FCT) methods. Finlayson (1992) and Morton (1996) provide extensive overviews of these and many other schemes. We use the MacCormack scheme with a flux correction component as a baseline finite difference scheme against which the QUICKEST scheme is

compared. The MacCormack scheme is generally good for linear systems, and produces good mass conservation, but suffers from an inability to track steep advective fronts accurately.

Many of the “traditional” numerical approaches to the advection problem yield results that are oscillatory, non-mass-conservative, or excessively diffusive. Upstream (upwind) methods derive their gradients in the (negative) direction of flow velocity. Thus, for uni-directional stream flow, they are essentially based on backwards differencing schemes. They provide stable solutions, but are unable to capture moving fronts accurately due to excessive numerical diffusion where gradients are large. Centered difference schemes derive local gradients based on center, left, and right nodal values irrespective of velocity direction. They incur errors in the advection term due to their independence of the nodal value being sought, and often exhibit oscillations as a result (Leonard, 1979; Morton and Sobey, 1993).

Attempts have been made to overcome these problems. Operator splitting techniques are one common approach, based on the simulation of advection and diffusion in two independent steps. For example, the advective term may be solved using a method of characteristics approach, and a centered implicit or explicit scheme used for the diffusion term. Further compounding the problem is our desire to include transient, nonlinear, velocity and diffusion coefficients. When the system under investigation is characterized by unsteady flow, numerous additional problems surface, including discontinuities in the method of characteristics and changes in stability criteria in both time and space.

Many of the problems of finite difference approximations may be avoided altogether through use of finite element techniques. One of the most popular finite element techniques is that based on the Euler Lagrangian Localized Adjoint Method (ELLAM; Herrera, 1984; Celia et. al., 1989). Its most beneficial characteristic is that it uses basis functions that are derived directly from the governing equations being discretized.

This approach provides a natural selection mechanism for the basis functions and results in very good approximations of the system. Implementation of finite element methods is somewhat less intuitive than finite difference methods. The ELLAM method is also compared to the QUICKEST scheme.

The QUICKEST Finite Difference Method

The QUICKEST numerical approximation has been called the best explicit finite-difference scheme available for unsteady, nonlinear convection-diffusion equations (Morton, 1996; etc.). Numerous authors have provided performance comparisons of the QUICKEST scheme to other explicit and implicit finite difference schemes (e.g., Lin and Falconer, 1997; Stamou, 1992).

The unique feature of the method is its use of a three-point upstream-weighted quadratic interpolation for the wall values of the independent variables in a control volume approximation of the governing equations. For one-dimensional flows with consistently positive flows in the x-direction, this results in the use of four nodal values per cell. Nonlinear velocities are accounted for through the estimated streaming term (EST) which uses initial conditions at each timestep to approximate average velocities over the step at each wall. The general form of the approximation is

$$\begin{aligned} q_i^{n+1} = \; & q_i^n + \frac{c_l}{2}\left[(q_{i-1}^n + q_i^n) - c_l(\Delta x)grad_l - \frac{\Delta x^2}{3}(1 - c_l^2 - 3\alpha)curv_l\right] - \\ & \frac{c_r}{2}\left[(q_i^n + q_{i+1}^n) - c_r(\Delta x)grad_r - \frac{\Delta x^2}{3}(1 - c_r^2 - 3\alpha)curv_r\right] + \\ & \alpha\left[\left(\Delta x grad_r - \frac{\Delta x^2}{2}c_r curv_r\right) - \left(\Delta x grad_l - \frac{\Delta x^2}{2}c_l curv_l\right)\right] \end{aligned} \tag{3.1}$$

with

$$
\begin{aligned}
grad_l &= (q_i^n - q_{i-1}^n)/\Delta x \\
grad_r &= (q_{i+1}^n - q_i^n)/\Delta x \\
curv_l &= (grad_r - grad_l)/\Delta x \\
curv_r &= (grad_{r+1} - grad_r)/\Delta x \\
\alpha &= \text{physical diffusion coefficient} \\
c_l, c_r &= \text{courant number } \left(u\frac{\Delta t}{\Delta x}\right) \text{at the left and right cell walls}
\end{aligned}
\tag{3.2}
$$

Appendix C contains complete derivations of this method, and the ELLAM and MacCormack methods.

3.3 VERIFICATION OF NUMERICAL METHODS

We first provide a comparison of the three numerical methods discussed above. The comparison serves to demonstrate the validity of the QUICKEST scheme for advection dominated systems. A second example demonstrates the solution of the coupled unsteady flow and heat transport equations.

Simulation of an Advective Front

A benchmark test of the three numerical methods was developed using a hypothetical hydrograph and channel characteristic. The simulations assume advective transport with no diffusion or losses. As such, it is essentially the kinematic wave routing approximation. For comparison, a pseudo-analytical solution for specific points is generated using the method of characteristics. All three numerical schemes are shown to be highly mass-conservative. The ELLAM and QUICKEST schemes are notably better, however, in capturing the steepening front of the advecting wave. Table 1 contains results for the mass-conservation and run time values of the benchmark tests. Figure 3.1 and Figure 3.2 show results for the three schemes at 1000 meters from the release point, using timestep sizes of 2 and 5 seconds. They also show the solution obtained using the method of characteristics, which is exact when tracking specific

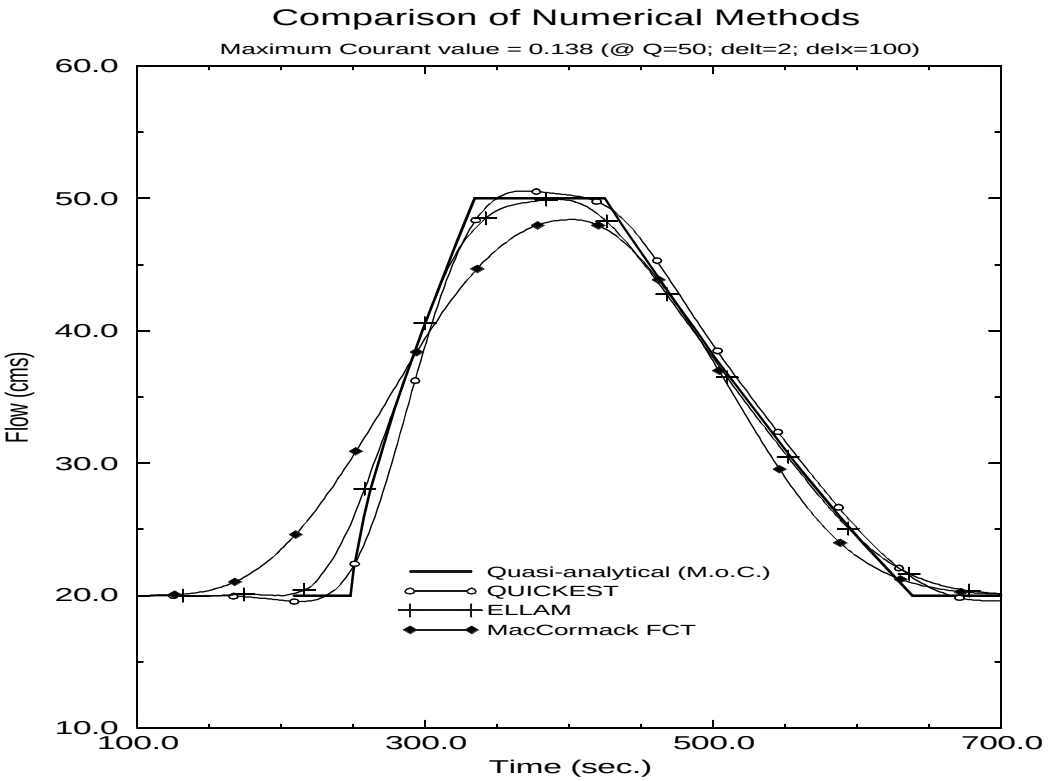

Figure 3.1: Performance of numerical methods in tracking an advective front.

point velocities through time. The maximum Courant numbers for the two simulations occur at 50 cms, and are 0.138 and 0.345 for the 2 and 5 second stepsizes, respectively. Table 3.1 summarizes the mass-conservation results and simulation times for the three methods. The mass conservation characteristics of all three numerical schemes are quite good, with all of the methods for both runs exhibiting deviations of well less than 1.0%. The QUICKEST method achieves nearly as accurate results as the ELLAM scheme. More significantly, it does so with a 70% reduction in computational run-time. The MacCormack scheme has the best mass conservation results, but is significantly worse than either the QUICKEST or ELLAM schemes when comparing the average sum-of-squares error over the simulation period.

We should note that this example is not physically realistic, as the advecting front will in reality be damped by diffusion. However, the example is useful because most of the numerical difficulties in solving advection dominated systems are

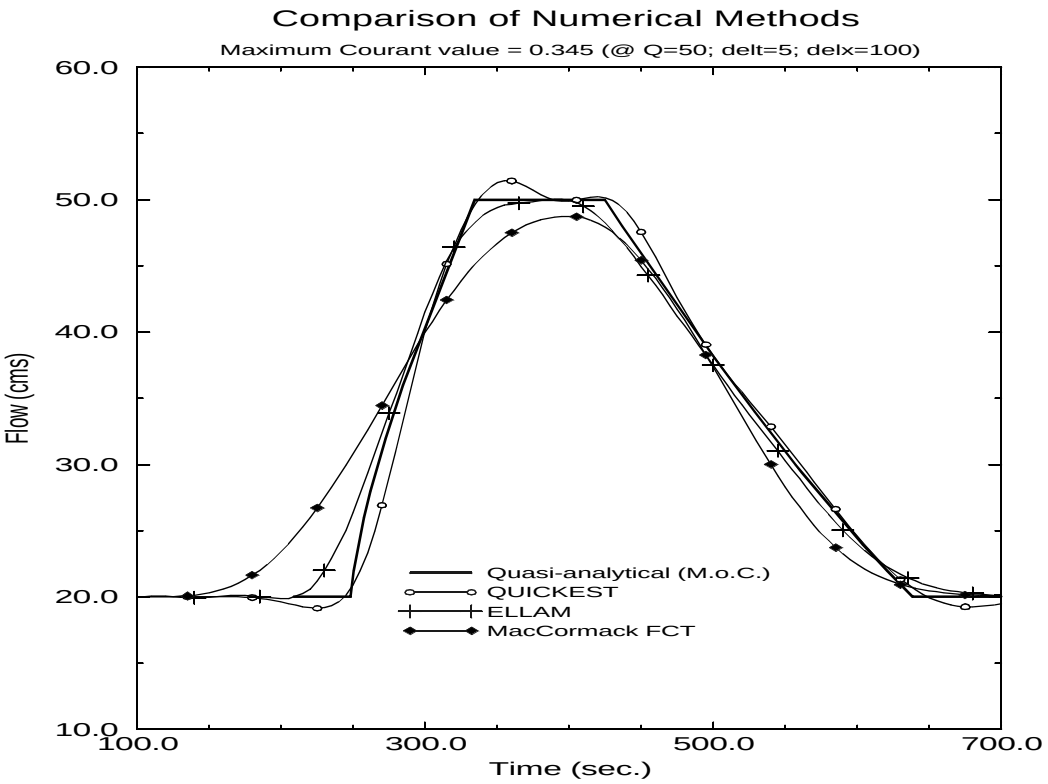

Figure 3.2: Performance of numerical methods in tracking advective front.

Table 3.1: Mass Conservation Comparison of Numerical Methods

	QUICKEST	**ELLAM**	**Mac FCT**	**QUICKEST**	**ELLAM**	**Mac FCT**
	delt = 2	**delt = 2**	**delt = 2**	**delt = 5**	**delt = 5**	**delt = 5**
m^3 = 27200	27159.05	27152.07	27173.91	27166.83	27180.03	27210.59
Error (m^3)	40.95	47.93	26.09	33.17	19.97	10.59
% Error	0.151	0.176	0.096	0.122	0.073	0.039
Normalized Run Time	1.0	3.36	1.06	1.0	3.36	1.06
Average SSE	0.955	0.958	6.180	1.165	1.332	8.464

accentuated in the case of pure advection. We expect the QUICKEST scheme to perform better than in this example when diffusion is included. From the example it is apparent that the QUICKEST scheme is useful for advection dominated systems.

Simulation of Heat Transport and Kinematic Flow Waves

The second example adds a purely advective, conservative (i.e., no heat source terms), heat transport component to the kinematic wave model above. The channel characteristics for this example are taken directly from the Green River study site discussed in detail in the following section. Transient flow and temperature boundary conditions are imposed at the upstream end of the system, which is initially at steady state. Results for the QUICKEST solution are developed for the coupled system. The changes in flow and temperature occur simultaneously, as shown by the dotted hydrograph and thermograph in Figure 3.3. The resulting hydrograph and thermograph are shown at a location 35 km downstream. The solutions are again compared with point-wise quasi-analytical solutions obtained using the method of characteristics. The figure clearly illustrates the different rates at which the kinematic wave front and the temperature front travel. The figure also provides some insight into the effect of the different front velocities. The region of warmer water in the thermograph has been “stretched” by the faster moving wave front. The net effect is that higher temperatures will be observed for a greater length of time the further downstream the observation occurs. It is important to note that heat is conserved in the example. The changing flow depth gives the false impression in Figure 3.3 that there is a net accumulation of heat. We note again that this is a purely hypothetical simulation with no diffusion or heat flux. It does however nicely show the separation of the wave fronts and the spatial variations in stream temperatures caused by unsteady flows.

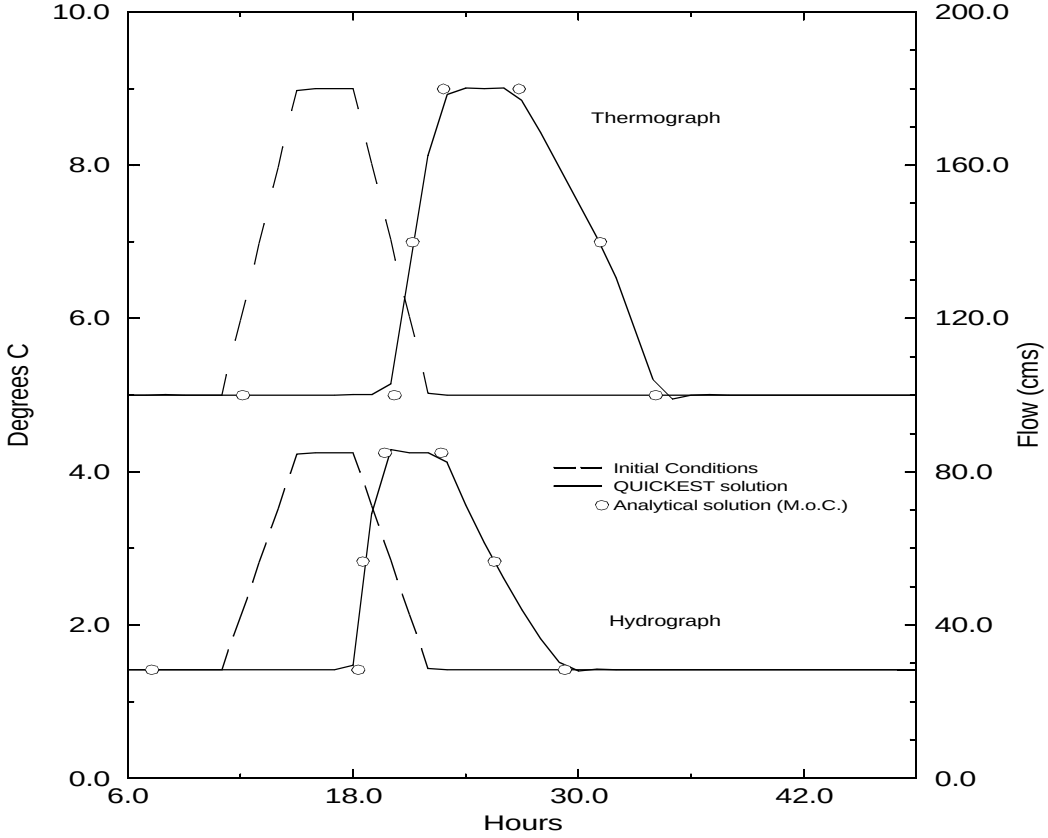

Figure 3.3: QUICKEST solution for coupled flow and heat transport.

CHAPTER 4

STREAM TEMPERATURE MODELING AND CONTROL IMPLICATIONS

The previously described numerical model is now applied to the Green River. We examine the impacts of short-term transient flows on river temperatures. Analysis of these impacts motivated development and application of the optimization techniques which follow in Chapters 5 and 6.

4.1 CALIBRATION AND VERIFICATION OF THE GREEN RIVER MODEL

The Green River is the largest tributary to the Colorado River. Its watershed includes much of western Wyoming, eastern Utah, and Northwestern Colorado. Flaming Gorge Dam impounds the Green River just south of the Utah / Wyoming border. The dam was built to meet water delivery requirements of the Colorado River Compact, for flood control, and for hydroelectric generation. Our study reach extends 105 kilometers below Flaming Gorge Dam to the confluence of the Green and Yampa Rivers in northwestern Colorado (Figure 4.1). The river is deeply incised in canyons in the upper and lower third of this reach, and flows through a 3 - 7 km wide valley in its middle third. The channel is characterized by steep banks and a relatively flat bed, due in large part to 40 years of flow regulation by Flaming Gorge Dam. Significant changes to the Green River resulting from the dam have altered the aquatic and ripar-

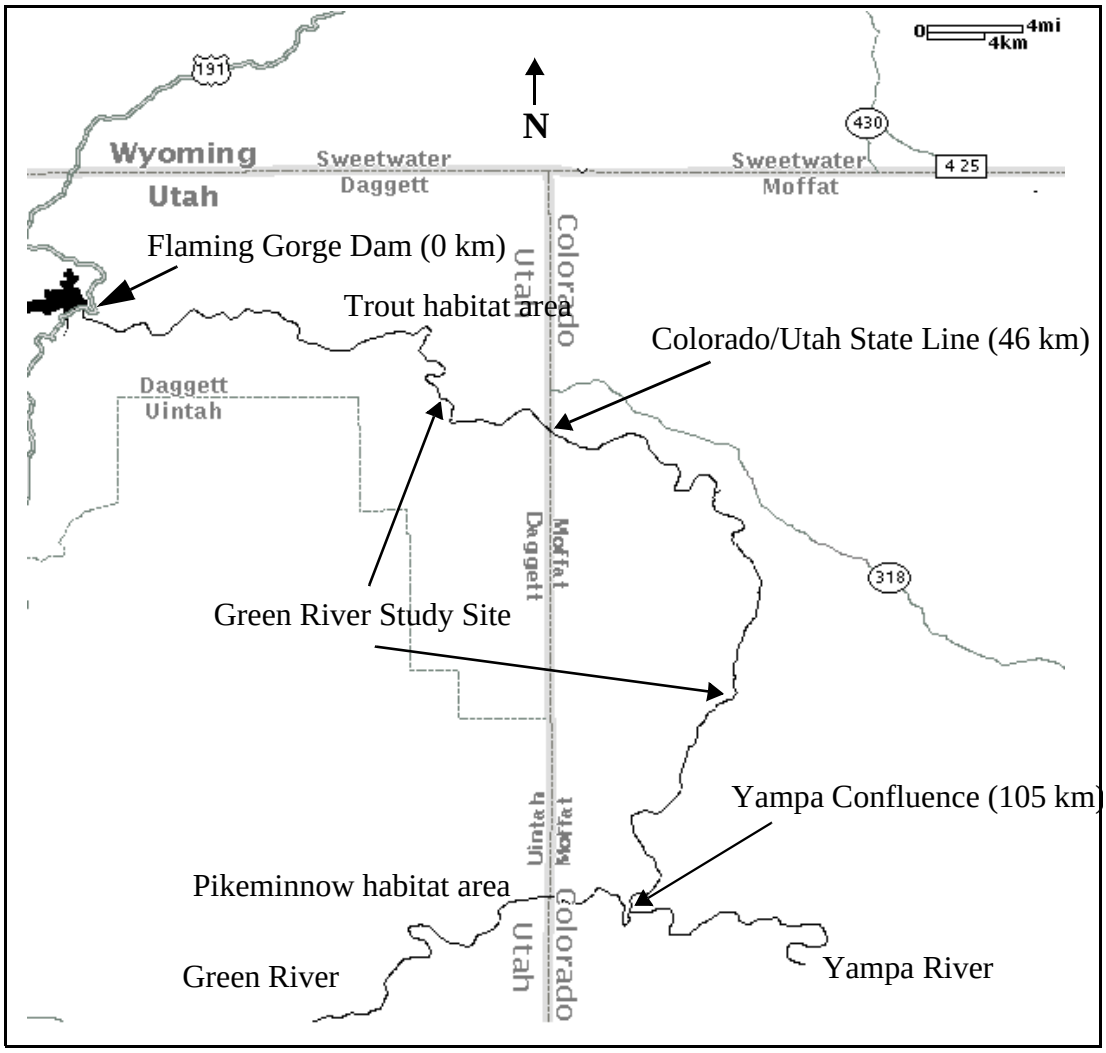

Figure 4.1: Green River and Flaming Gorge Dam.

ian communities downstream. The Colorado Pikeminnow is federally listed as an endangered species. It once flourished in the Green River through much of its length. Changes in stream flow and temperature resulting from dam operations have severely reduced the occurrence of this species in the upper Green River. Pre-dam average monthly temperatures varied from 0 ^{o}C during winter to nearly 21 ^{o}C in summer. The temperature of water released from the dam is limited to the range 4 - 15°C annually, and is further constrained depending on rate of thermal stratification from spring into summer.

The channel geometry can be reasonably approximated as a wide-rectangular channel with the following characteristics: bed slope = 0.00164, channel width = 50m, Manning's n = 0.04. These data were estimated from topographic maps, from field surveys in 1998, and through communications with various members of the Flaming Gorge Operations Workgroup (Brayton, 1998; Crist, 1998). In order to model streambed heat flux terms, estimates of the active bed thickness and thermal diffusivity are required. Streambed temperatures were collected during September and early October 1998 at Brown's Park National Wildlife Refuge. These data include streambed temperatures from 5, 15 and 40 cm. below the bed surface recorded every 15 minutes over a 5 week period. Stream temperatures were also monitored at the site during this period. Analysis of the data indicates that there is no diurnal heat flux in the bed below a depth of 0.5 meters. This value is in agreement with previous work (Jobson, 1977), and is the depth used for the no-flux boundary in the streambed heat flux computations. An average bed thermal diffusivity value of 1.8×10^{-6} m^2/s computed from the observations is similar to previously reported values (Jobson, 1977; Kim, 1993).

The model was calibrated using historical stream temperature and atmospheric data collected during the summer of 1994. Stream temperature data collected at numerous sites in the Green River were obtained from Mark Vinson of Utah State University. The stream temperature readings were taken every 3-4 hours using an Onset Inc. Hobo temperature recorder. Release data for Flaming Gorge were obtained from the United States Bureau of Reclamation, and included hourly average flow and daily average release temperatures.

Atmospheric data were gathered from two weather stations within 2 km of the river, one at Flaming Gorge Dam, the other at the Brown's Park National Wildlife Refuge headquarters approximately 55 river kilometers downstream from the dam. These data included daily minimum and maximum air temperatures, dry and wet bulb

temperatures, and average daily windspeed. Cloud cover data for the period could not be obtained, so rainfall data were used as a surrogate to eliminate potentially cloudy days from the test periods.

One difficulty in calibrating the model was a lack of flow data between Flaming Gorge Dam and the Yampa Confluence. The lack of flow data forced us to calibrate the unsteady flow component of the model against an existing model previously calibrated for the Green River (U.S. Bureau of Reclamation, 1992). That model, the Streamflow Synthesis and Reservoir Regulation (SSARR) model, uses the Muskingum routing algorithm. Parameters for Manning's n and the momentum diffusion coefficient were adjusted to replicate the SSARR model output for a synthetic reservoir release. The calibration point is just above the confluence with the Yampa River, at approximately 95 km below Flaming Gorge Dam (Figure 4.2).

Calibration of the temperature model was achieved by adjusting the shading coefficients to reflect the three distinct physiographic regions of the study reach. The regions roughly split the reach into thirds; an east-west trending canyon up to 300 m deep, followed by an east-west trending valley between 3-6 km wide, and a narrow north-south trending canyon up to 800 m deep. The shading coefficients are assigned values between 0 and 1, and serve to reduce direct solar radiation based on approximations of the physiographic and riparian obstacles. Data from the period 23-26 August 1994 are used for calibration, and from the period 30 August - 2 September 1994 for validation (Figure 4.3). The calibrated values for the shading coefficients are 0.8 for the upper and lower river segments, and 0.9 for the middle segment. We suspect that the noticeable discrepancy between the simulated and observed temperature in Figure 4.3 at approximately 42 hours is due to cloud cover - and hence reduced incident solar radiation - at the study site.

This pattern of lower observed daily maximum water temperatures is seen in the historical records on days which recorded measurable precipitation. The release

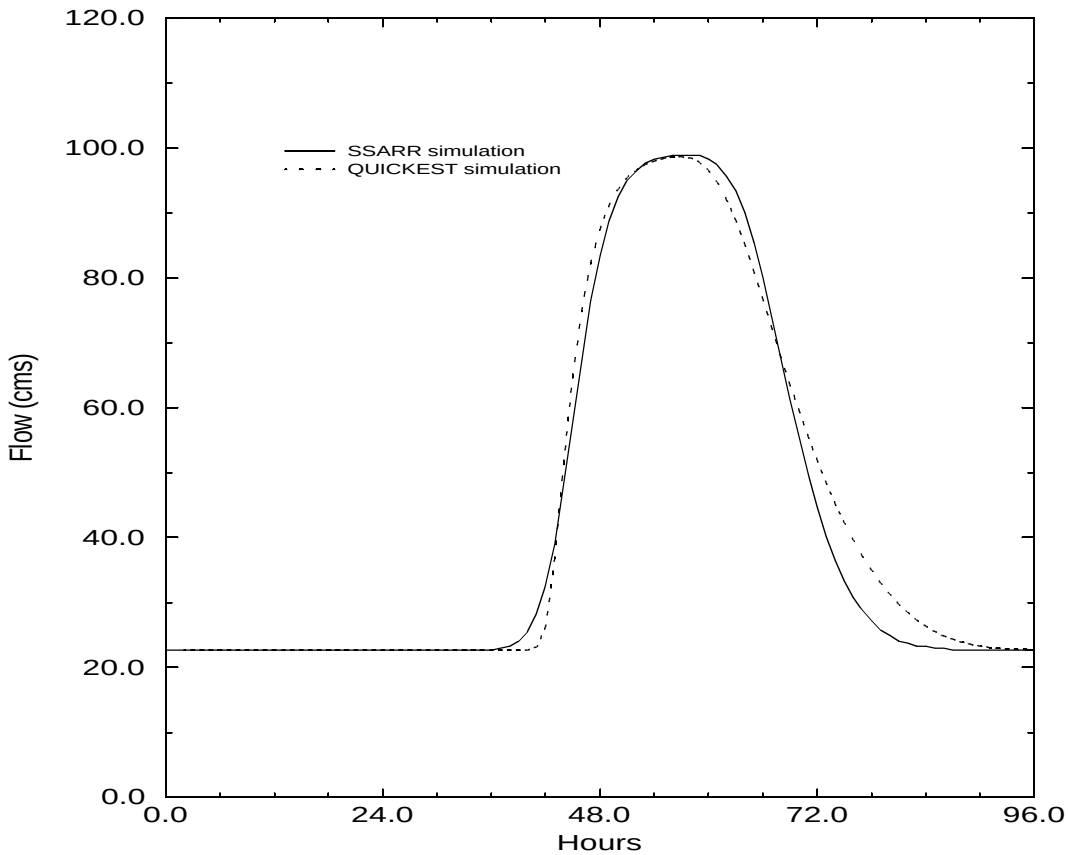

Figure 4.2: Calibration of QUICKEST model to SSARR model of Green River.

pattern during this period was characterized by a high flow period during late afternoon, as illustrated by Figure 4.4. This release pattern is typical for Flaming Gorge Dam when it is used for peaking hydropower generation.

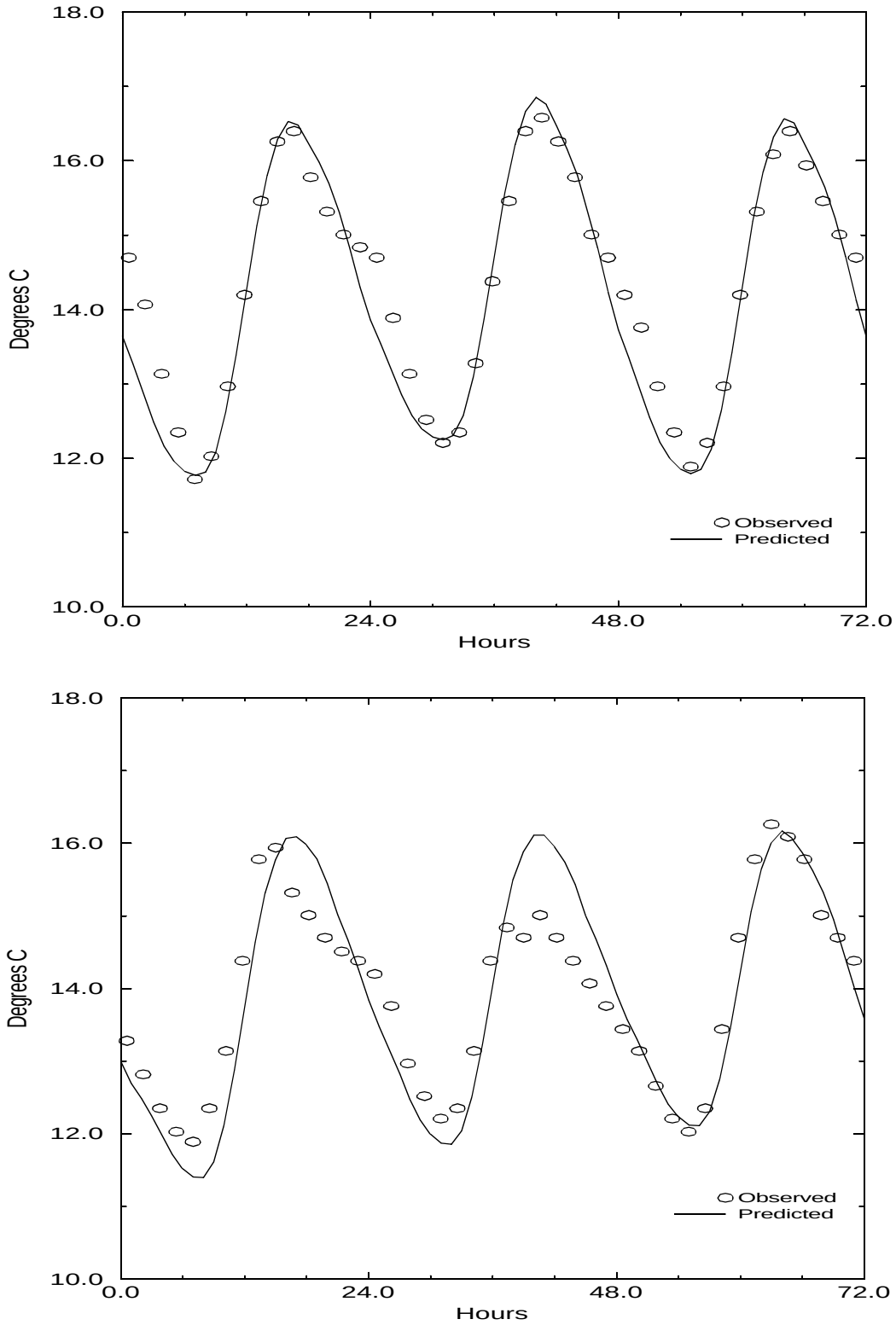

Figure 4.3: Calibration (top) and verification (bottom) of Green River temperature model. Data are from 22-26 August and 30 August - 2 September 1994 at Lower Swallow boat ramp, approximately 43 km below Flaming Gorge Dam.

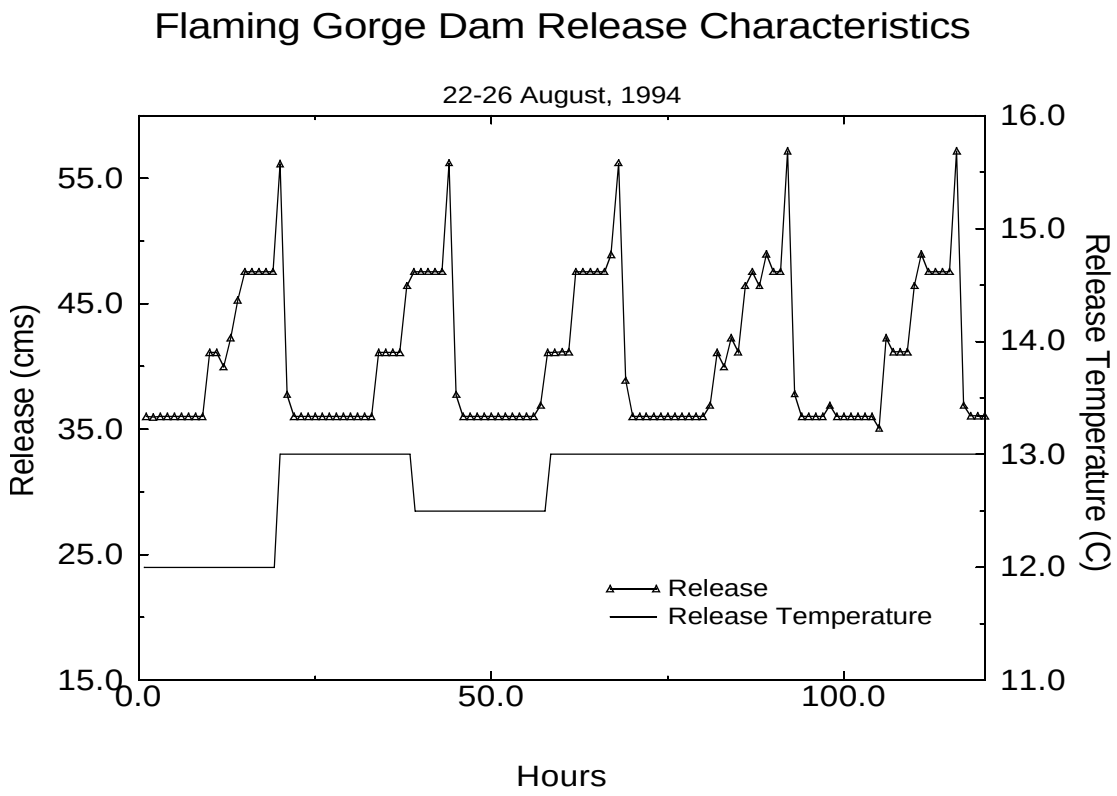

Figure 4.4: Flaming Gorge releases during the model calibration period.

4.2 INFLUENCE OF SHORT-TERM FLOW FLUCTUATIONS AND PROSPECTS FOR TEMPERATURE CONTROL

Even under steady flow, there are significant diurnal temperature fluctuations in rivers resulting from the diurnal atmospheric heating cycle (Sinokrot and Stefan, 1993; Polehn and Kinsel, 1997). Under transient flow conditions, the spatial and temporal variations in river temperatures are quite complex. An increase in flow rate leads to an increase in river depth, which in turn leads to a higher heat capacity within the reach. The result is that the rate of heating by atmospheric forcing is reduced. Increased flow rate also results in an increased flow velocity, which reduces travel time to downstream locations, and hence reduces the duration of atmospheric heating. Knowing that atmospheric conditions exhibit distinct diurnal cycles, one approach to

more efficiently reducing river temperatures would be to ensure large flow depths in the vicinity of constraint locations during the afternoon, when heating rates are highest. Conversely, water may be conserved if flows are reduced during periods when atmospheric heating is at a minimum. This suggests that the magnitude and timing of reservoir releases can be adjusted to control river temperatures. In doing so, it is necessary to take into account the travel time from control point to constraint location, and the effects of wave damping. In certain cases, control of release temperatures is also possible. Reservoirs which have selective withdrawal structures can release water from different depths. If a reservoir is thermally stratified, selective withdrawal provides release temperature as another control available for regulating river temperatures. Selective withdrawal can be particularly useful for managing river temperatures when there is little or no flexibility in the *amount* of water being released. In this section, we present some examples to illustrate the potential use of short-term transients to control river temperatures.

Flow Transients in the Green River

As noted above, the timing of transient releases will determine the downstream location where impacts of the release appear. Figure 4.5 and Figure 4.6 show the impact of two hypothetical flow transients on stream temperatures at two locations (20 km and 65 km) downstream of Flaming Gorge Dam. Stream temperatures under steady flow conditions are also shown for comparison. The modified hydrographs have 6 hour periods of reduced flows (28 cms vs. 85 cms) which occur between midnight and 6 am, and between noon and 6 pm. Atmospheric conditions from the model validation period (23-25 August, 1994) were used in this simulation. The figures clearly show the influence of flow transients on water temperatures at two different locations. At 20 km below Flaming Gorge Dam, the temperatures corresponding to an afternoon reduction of flow are approximately 2 ^{o}C higher than the temperatures

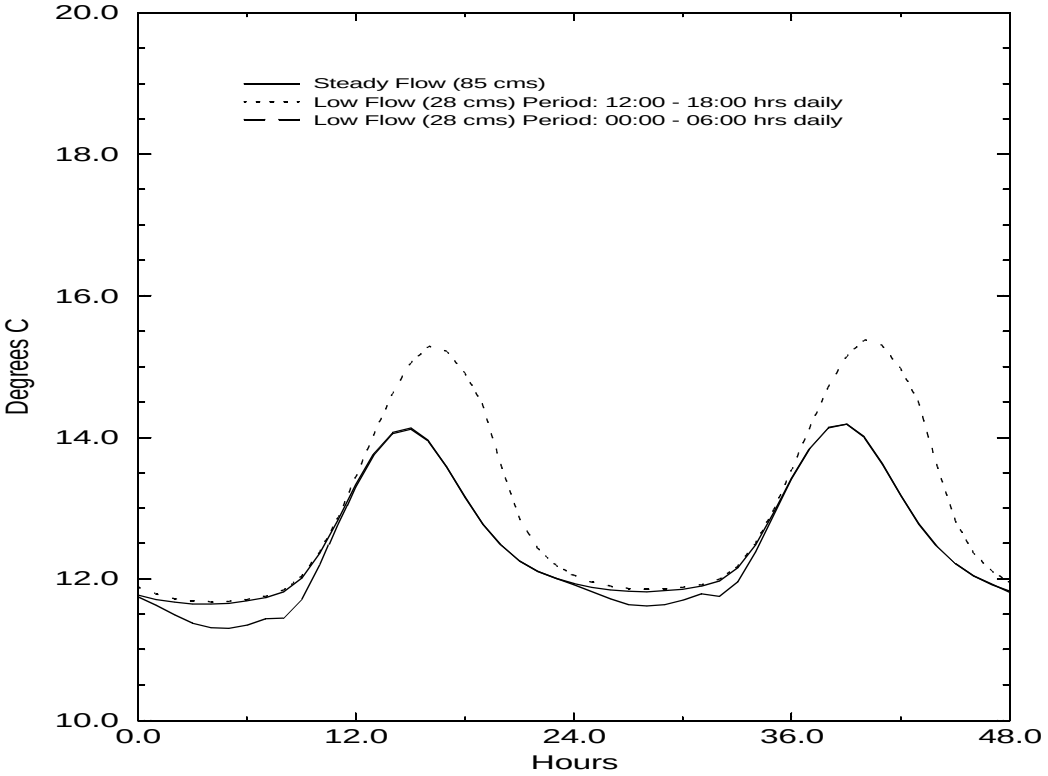

Figure 4.5: Impacts of transient releases on stream temperatures of Green River, 20 kilometers below Flaming Gorge Dam. The noon to 6 p.m. low flows produce increased water temperatures in the reaches immediately below the dam. These reduced flows have little impact on temperatures farther downstream (Figure 4.6).

resulting from a steady 85 cms release. Water released from Flaming Gorge at 28 cms has a velocity of approximately 4 km/hour. Thus, the reduced afternoon flows reach the 20 km point having been exposed to a high level of radiative heating over several hours. Conversely, the thermograph corresponding to the low flow period from midnight to 6 am shows no change in daily maximum temperature, since the flows during the period of maximum heating remain at 85 cms. Figure 4.6, however, shows opposite results. The thermograph corresponding to an early morning reduced flow exhibits warmer maximum temperatures, while the impact of the reduced flows in the afternoon shows a very small increase in daily maximum temperature. As in Figure 4.5, the timing of the transient and its exposure to atmospheric heating impacts the downstream location at which the temperature variation is observed.

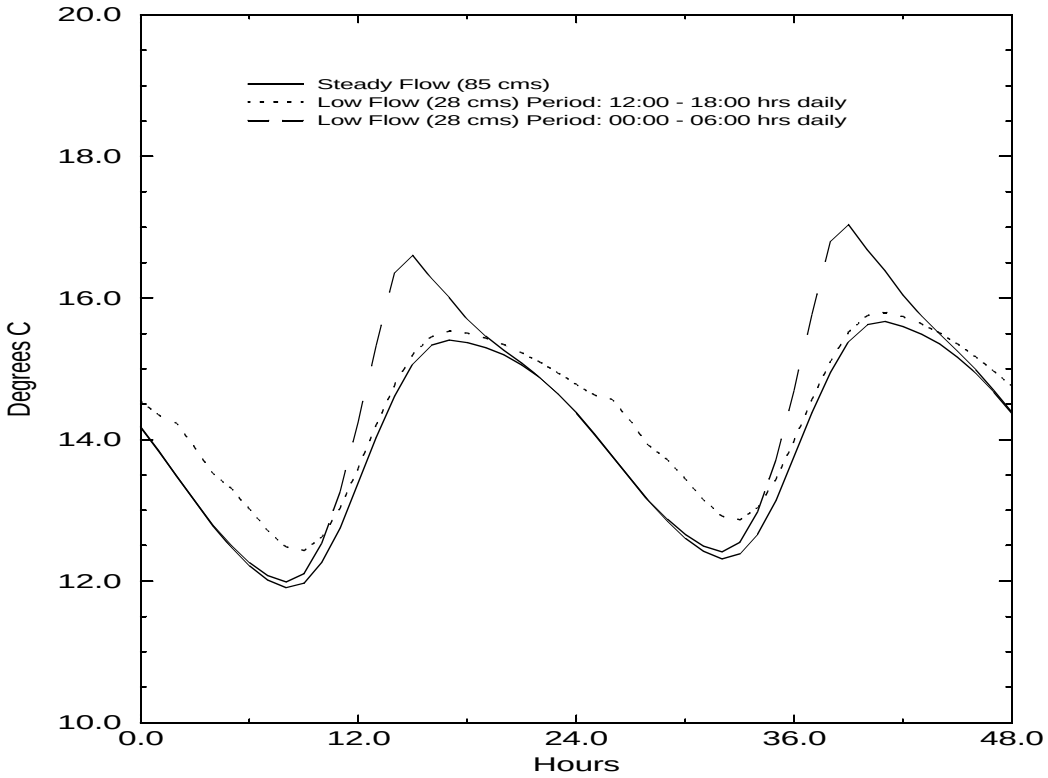

Figure 4.6: Impacts of transient releases on stream temperatures of Green River, 65 kilometers below Flaming Gorge Dam. The low flow period from midnight to 6 a.m. causes rapid warming around noon 65 kilometers downstream.

Temperature Control on the Stanislaus River

The Middle Fork of the Stanislaus River, in Tuolumne County, California is regulated in its lower reaches by Beardsley Reservoir and Sand Bar Reservoir. Flows at Sand Bar Reservoir are diverted for hydroelectric generation at the Stanislaus Powerhouse, located about 24 km downstream of the diversion point, and about 3 km below the confluence of the Middle and North Forks of the Stanislaus. Water used for hydropower generation re-enters the Stanislaus at this location. Previous works (Woodward Clyde, 1986; Railsback, 1997) have examined the impacts of steady flows on temperatures in the reach between Sand Bar Reservoir and the powerhouse after-

bay. Using data from the Woodward Clyde study, Railsback developed a regression equation relating water temperature at the confluence to air temperature and flow. A minimum flow of 3.4 cms was derived from this model using air temperatures representative of historical extreme atmospheric conditions for August. Railsback then showed that a reduction in the minimum flow did not lead to violation of temperature constraints at the confluence over long periods when atmospheric conditions were not at historical maxima.

We revisit this example to demonstrate how even at extreme atmospheric conditions, a reduction in flow can be achieved without violating temperature constraints. Using data on reach characteristics from the Woodward Clyde study, we simulated stream temperatures in the Middle Fork of the Stanislaus down to its confluence with the North Fork. Figure 4.7 shows the results for 5 different release patterns. One release pattern assumes a steady flow of 3.4 cms, as designated by Railsback (1997). The other four release patterns each contain a 6 hour period of reduced flows, as outlined in the figure. The flows during this period are 0.85 cms, which approximates the lowest minimum flow rate considered viable for the fishery. The results serve to illustrate the point that timing of transient flows is critical to achieving temperature management objectives. Stream temperatures for the release with a low-flow period from 8 pm to 2 am show close correspondence with the steady flow solution. Perhaps more interestingly, the thermograph resulting from a low-flow period between 2 - 8 pm shows significant (up to 4 ^{o}C) deviation from the steady flow solution over much of the reach, and yet deviates from the steady flow solution at the constraint location by less than 1 ^{o}C. Thus, this release pattern may be acceptable if the constraint is specified at a single location, but may not be acceptable if the temperature corresponding to a steady 3.4 cms flow must be met over the entire reach. These results clearly show how the timing of transient release patterns may impact temperatures in very different ways at various locations. Use of any of these cyclic release patterns reduces the total

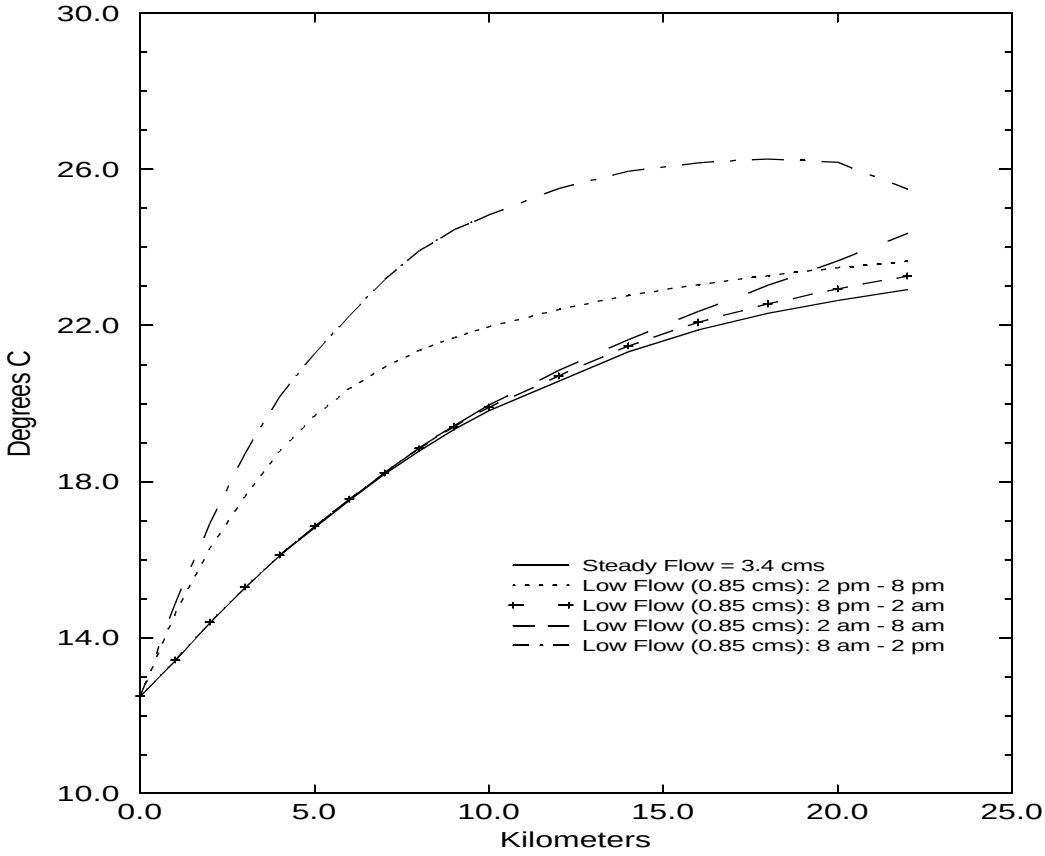

Figure 4.7: Comparison of daily maximum stream temperatures in the Stanislaus River below Sand Bar Diversion, under various release patterns. A steady flow of 3.4 cms is compared to release patterns in which the flow rate is reduced for a 6 hour period, as indicated in the legend.

release volume by 25%. Perhaps even larger savings can be realized by increasing low flow durations. The optimal duration of low flow periods can be determined based on additional studies.

Multiple Temperature Constraints on the Green River

Returning to the Green River, we now examine the prospects for meeting temperature constraints at more than one downstream location. The reaches immediately below Flaming Gorge Dam are home to an extremely productive trout fishery. The trout thrive in the cold release waters and provide a valuable economic resource to the

local tourism industry. The most important reaches where lower water temperatures need to be maintained for the trout habitat are from 0 to 45 km below the dam. At the confluence with the Yampa there is an ongoing rehabilitation program for the native warm-water Colorado Pikeminnow. Water released from Flaming Gorge is often cooler than the ideal temperature for the Pikeminnow (18 - 24 ^{o}C) when it reaches the Green / Yampa confluence. It is desirable, then, to design release patterns which can benefit both species. To illustrate how transient flows can achieve this, we consider the following objectives:

- For trout fishery habitat: daily maximum temperatures 45 km below Flaming Gorge Dam should not exceed 17 ^{o}C.
- For Colorado Pikeminnow restoration program: increase water temperatures at the Green / Yampa confluence (105 km) such that daily maximums are greater than 20 ^{o}C.

Figure 4.8 shows the daily maximum temperatures along the reach for six different release patterns. Two steady flow scenarios of 28 cms and 71 cms are considered, along with four release patterns which incorporate a baseflow of 28 cms and a 6 hour period of increased (71 cms) flows. The flow rate of 28 cms is close to the minimum instream flow of 23 cms, and has been suggested as a flow rate which would benefit the Pikeminnow habitat during spawning, which takes place in summer after the major snowmelt runoff events have occurred (Brayton, 1998). A flow of 71 cms is approximately 50% of the maximum flow which can be released through the turbines to generate electricity. The high-flow periods for the four transient patterns are midnight to 6 am, 6 am to noon, noon to 6 pm, and 6 pm to midnight. The results clearly show that a properly timed high-flow release leads to temperatures which benefit both fisheries at their respective locations. Of the four transient releases, the 6 am - noon high flow period gives the most favorable results. It meets the trout fishery requirement (T_{max} < 16 ^{o}C) at the 45 km location, and provides the warmest water at the con-

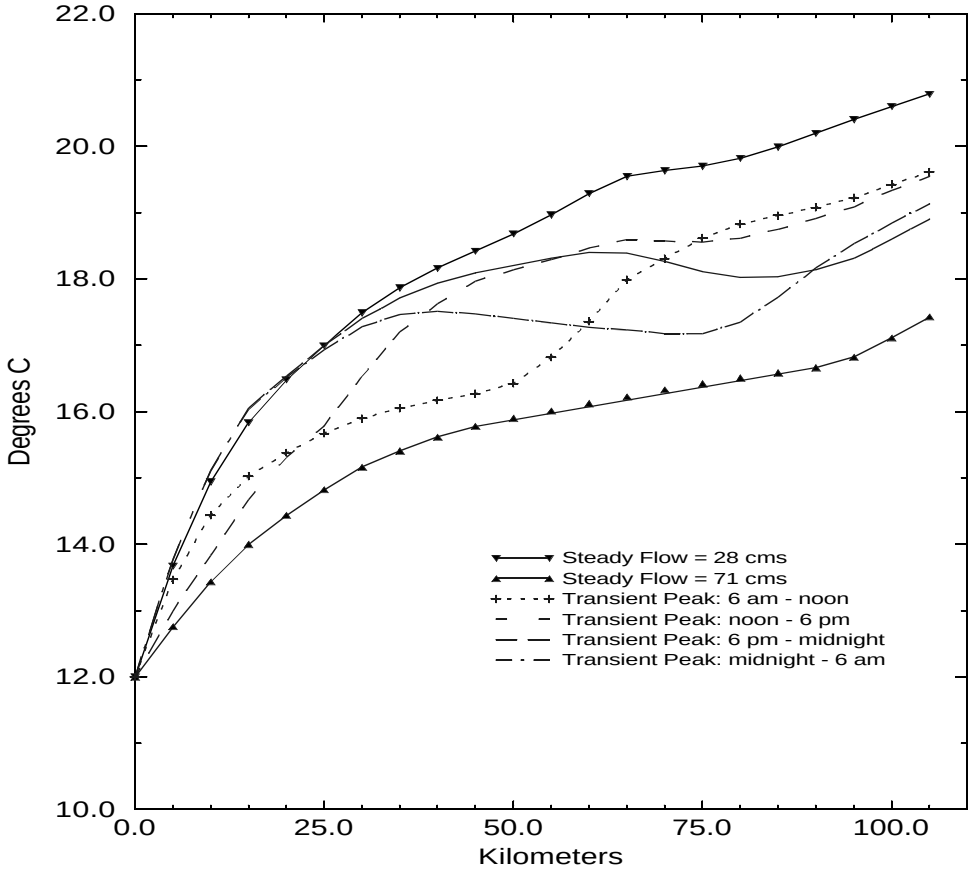

Figure 4.8: Comparison of daily maximum stream temperatures in the Green River below Flaming Gorge Dam, under various flow regimes using average June atmospheric conditions. The transient peaks are 6 hour periods of increased flow (71 cms) for the periods indicated in the legend. The impact of release timing on downstream temperatures is clearly visible.

fluence, although is slightly below the 20 ^{o}C target temperature at that location. The other three transient releases also provide fairly warm water at the confluence, but violate the maximum temperature objective at 45 km. It is also worth noting that neither of the steady flow solutions meets both temperature objectives. Thus, in this example, the use of transient flows appears to be essential for achieving the stated objectives. The timing of the transients in this example were chosen somewhat arbitrarily. However, it is clear that refinement of the timing and magnitude of the transient flows would lead to even better results. For instance, optimization techniques may be devel-

oped to achieve site-specific objectives while minimizing total release volume.

4.3 FACTORS LIMITING TEMPERATURE CONTROL IN REGULATED RIVERS

We have seen in the previous section that we can use cyclic release patterns to conserve water without significantly changing the temperature regime observed under steady flows. We might now want to examine the limitations on our ability to meet specific temperature objectives. The greatest factor influencing the ability to control stream temperatures will be variations in atmospheric conditions, since they are the primary heat source for river heating. Constraints on reservoir releases and release temperatures, and channel characteristics, will play secondary, but significant, roles. As an example of the bounds which atmospheric conditions place on temperature control, we consider sets of historical atmospheric conditions in the Green River in combination with a range of potential release temperatures. Figure 4.9 shows the results of simulations used to determine control limits resulting from various atmospheric conditions.

All the results shown represent daily maximum water temperatures along the river reach from Flaming Gorge Dam to the Yampa River confluence. The upper and lower solid lines represent high (38 ^{o}C) and low (18 ^{o}C) daily maximum air temperatures based on historical records for the months of July and August, and corresponding extremes in release temperatures (4 - 13 ^{o}C) and flows (23 - 125 cms). For example, the highest potential water temperatures occur when release temperatures are 13 ^{o}C, release is 23 cms, and atmospheric conditions are at historical highs. The thinner solid lines represent the potential range of stream temperatures based on actual atmospheric conditions of 22-24 August 1994, the actual release temperature over those days (12 ^{o}C), and hypothetical steady flows of 23 and 125 cms. The ability to control temperatures is limited in this case by the existing weather conditions and pre-specified release

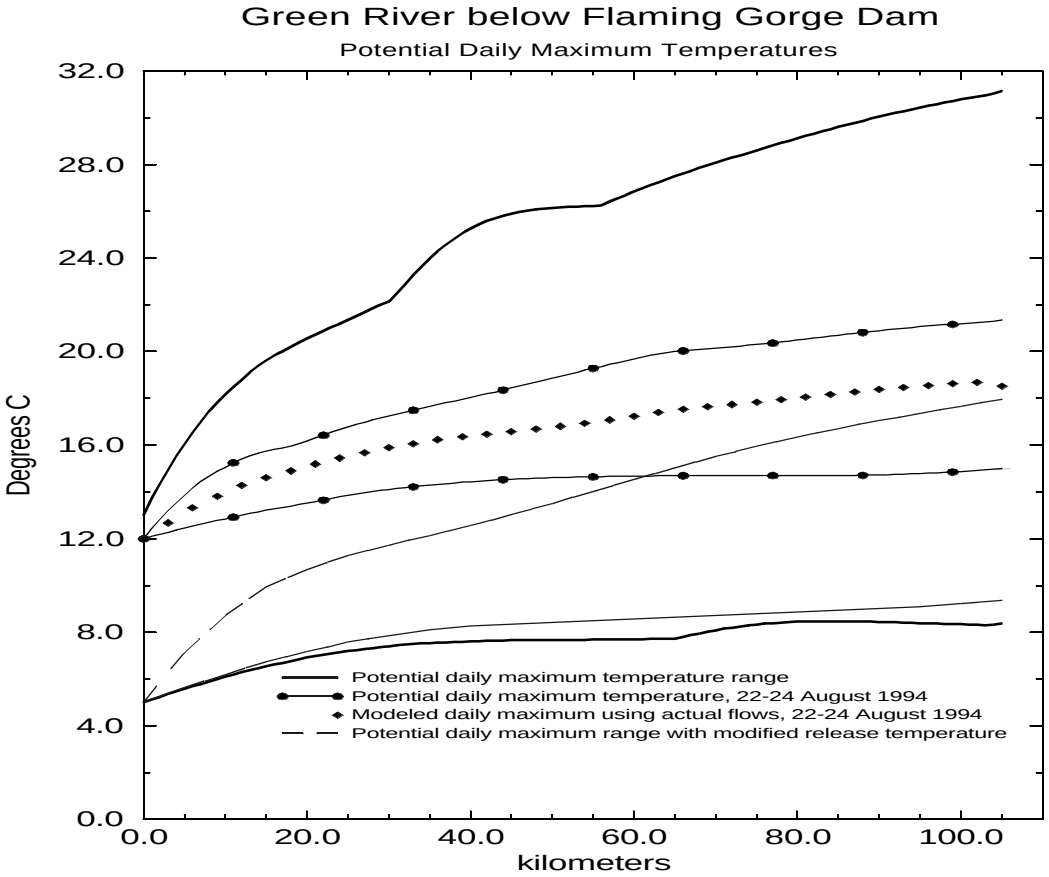

Figure 4.9: Impacts of atmospheric conditions and release temperatures on stream temperatures in the Green River. Atmospheric conditions and release temperatures significantly limit the range of attainable water temperatures.

temperature. Temperature control may be achieved by varying the release rate. However, it would not be possible to achieve a temperature greater than about 20 ^{o}C at the confluence with the Yampa unless operational constraints are violated (i.e., flow < 23 cms) or the release temperature is increased. The dashed line which falls in this range corresponds to the daily maximum temperatures shown in the calibration simulation (Figure 4.3) using the actual reservoir releases (which varied from approximately 34 to 57 cms, Figure 4.4). Finally, the dotted lines show how a change in release temperature using the selective withdrawal structure would have changed the potential temperature range over the 3 day period. These results show that it may not be possible to

meet specific temperature targets all the time, but by using selective withdrawal and transient releases we can certainly expect to influence the stream temperatures and try to minimize the deviations from those target temperatures.

It is clear from the above results that the spatial and temporal character of temperature objectives will dictate to a large degree the ability to realize a savings through reduced release volumes. This variability also has implications for how temperature objectives in regulated rivers are defined and monitored. In the Green River example, if the location of the objectives for the two fisheries were reversed (i.e., requiring warmer water at 45 km and cooler water at 105 km), meeting both objectives would be essentially impossible during the summer.

The ability to manage downstream temperatures must be considered within the context of other operational constraints. Issues such as flood control, hydropower generation, delivery obligations, and recreation, may be of equal or greater priority as management objectives. We might then ask whether or not there are existing operational guidelines which either positively or negatively impact downstream temperatures. For example, Flaming Gorge Dam is sometimes operated as a peaking hydropower plant. This might occur during extreme weather conditions, or when there are outages at other generating facilities. We have already seen that transient releases will slow downstream warming at specific locations. It is logical then to ask what impact peaking power generation will have on downstream temperatures, and where those impacts will occur. The most common time for peaking hydropower generation to occur is in late afternoon and early evening. These peaking power releases can easily double the daily mean flow from the reservoir. Referring back to Figure 4.8, peaking power production may be assumed to correspond to a high flow transient between noon and 6 pm. This particular release pattern is seen to be beneficial to the Pikeminnow, but somewhat detrimental to the trout fishery beyond 30 kilometers, where the daily maximum exceeds 16 ^{o}C.

Several factors will ultimately determine our ability to manage temperatures in regulated rivers. The Green River is somewhat unique in that from Flaming Gorge to the Yampa Confluence it flows through an uninhabited area with almost no tributary inflow. This characteristic makes temperature management more clear-cut, if not always achievable, because considerations such as urban/industrial effluent, diversions, etc. may be ignored. However, in general, the influence of diversions, return flows, tributary inflows, and other effluents should also be considered. To illustrate these influences further, we consider the historical temperature characteristics for 4 regulated rivers in the United States: the Green and Stanislaus discussed previously, the Chattahoochee (Jobson and Keefer, 1979), and the Tualatin (Risley, 1997). We compare the behavior of these rivers using a non-dimensional measure of stream temperature, the ratio $(T_{water} - T_0)/(T_{air} - T_0)$, where T_0 is the stream temperature at the release point (Figure 4.10). Steady flow conditions are considered for simplicity.

The use of this non-dimensional measure to some extent eliminates the diurnal temperature variations, since both T_{air} and T_{water} experience diurnal variations. The month of August is considered, since is represents typical summer weather conditions. In the absence of any diversions or uncontrolled inflows, the non-dimensional stream temperature would be expected to approach a constant value at large travel times from the release point. The actual value of the non-dimensional stream temperature will depend on the flow rate. Indeed, the Green River exhibits the aforementioned behavior. However, the Chattahoochee and Stanislaus both show sharp changes in stream temperatures, due to significant diversion and return flows in the case of the Stanislaus, and urban effluent from Atlanta in the case of the Chattahoochee. The Tualatin also experiences significant tributary inflow and urban effluent, and is impacted in its lower reaches by a low-head diversion dam. Nevertheless, it warms relatively slowly; a characteristic which might be attributed to a smaller surface area to depth ratio (increased heat capacity) and relatively small difference between water and air temper-

CHAPTER 5

CONTROL AND OPTIMIZATION THEORY

5.1 INTRODUCTION

The previous chapters have shown that it is possible to strongly influence downstream temperatures by using fluctuating reservoir releases. The question then arises as to whether or not we can use fluctuating releases to meet a specific set of temperature objectives. This chapter provides a brief review of optimization methods, and then outlines the theoretical framework for bound-constrained optimization techniques used in this thesis. We then discuss the details of our implementation of the methods, including formulation of objective functions and constraints.

5.2 OVERVIEW OF OPTIMIZATION OF NONLINEAR SYSTEMS.

The general form of the problem for which we seek a solution contains two parts: an objective function to be minimized (or maximized), and a set of constraints which limit the domain of the system controls and other variables. If the problem is linear in both its objective function and constraint definitions, then the problem falls under the category of *linear programming.* If, for example, only the constraints are nonlinear, the problem is one of *linear programming with nonlinear constraints.* If both the objective function and constraints contain nonlinear components, the problem becomes one of *nonlinear programming*. Many specialized areas of research within

the arena of nonlinear programming can be identified. These are based largely on specific characteristics of the objective function or constraints. For example, problems with linear constraints fall under the heading of *linearly constrained optimization*; problems which additionally have an objective function which is at most quadratic are termed *quadratic programming* problems. The class of problems we examine in this work can be solved using *bound-constrained optimization* techniques. These problems are (potentially) nonlinear in the objective function, and are constrained only by simple bounds (upper and lower limits) on some or all of the variables. This representation of the problem is preferable to one which includes inequality or equality type constraints, as it would then require techniques used for *nonlinear programming*, which are generally more computationally expensive and complex to formulate. For an overview of various optimization techniques for nonlinear systems and constraints, see Fletcher (1987), Nemhauser et. al. (1989), or Gill et al. (1981).

5.3 THEORY OF BOUND-CONSTRAINED OPTIMIZATION

The bound-constrained optimization problem can be represented by (NEOS, 1996)

$$min\ \{f(\boldsymbol{x}): \boldsymbol{l} \le \boldsymbol{x} \le \boldsymbol{u}\} \tag{5.1}$$

where *f()* is the objective function to be minimized, $\boldsymbol{x}$ is the set of control variables, and $\boldsymbol{l}$, $\boldsymbol{u}$ are lower and upper bounds (some possibly infinite) of $\boldsymbol{x}$. First order necessary conditions for $\boldsymbol{x}^*$ to be a local minima of f can be expressed as

$$\begin{gathered} B(\boldsymbol{x}^*) = \{i: x_i^* = l_i, \partial_i f(\boldsymbol{x}^*) \ge 0\} \cup \{i: x_i^* = u_i, \partial_i f(\boldsymbol{x}^*) \le 0\} \\ \partial_i f(\boldsymbol{x}^*) = 0, i \notin B(\boldsymbol{x}^*) \end{gathered} \tag{5.2}$$

where $B(x^*)$ is known as the *binding* set. This condition essentially requires all partial derivatives of f with respect to x_i which are not at their upper or lower bounds to be

zero, and those partial derivatives with respect to x_i which are at a bound to be greater than zero at the lower bound and less than zero at the upper. Second order sufficiency conditions require the first-order conditions to hold, plus

$$\boldsymbol{w}^T \nabla^2 f(\boldsymbol{x}^*)\boldsymbol{w} > 0$$
$$\text{for all vectors } \boldsymbol{w}, \boldsymbol{w} \neq 0, w_i = 0, i \in B_s(\boldsymbol{x}^*) \tag{5.3}$$

where the strictly binding set $B_s(\boldsymbol{x}^*)$ is defined as

$$B_s(\boldsymbol{x}^*) = B(\boldsymbol{x}^*) \cap \{i\colon \partial_i f(\boldsymbol{x}^*) \neq 0\} \tag{5.4}$$

Equations 5.2 - 5.4 are known as the Kuhn-Tucker conditions for constrained optimization problems.

The most commonly used techniques for solving bound-constrained optimization problems are based on Newton, quasi-Newton, or gradient-projection methods. These methods typically operate by identifying the free variables (variables which are not at one of their bounds) and using this reduced set and its gradient to compute a new estimate of the optimal $\boldsymbol{x}$.

5.4 QUASI-NEWTON SOLUTION FOR BOUND-CONSTRAINED OPTIMIZATION

Let us turn to an example problem which will demonstrate the quasi-Newton method we use to solve the bound-constrained optimization problem described above. We use an objective function and constraints which correspond to the stream temperature problems addressed in the next chapter. The objective function f can be written for a general water temperature control problem as:

$$f(\boldsymbol{U}) = \int_0^{\tau}\int_0^{L} G(\boldsymbol{U}, \boldsymbol{T})\, dL\, d\tau \tag{5.5}$$

Where $\boldsymbol{U}$ = the control vector, $\boldsymbol{T}$ = a vector of stream temperatures at some target location(s) downstream, G = a function designed to measure the deviation of the existing system states from some desired target states. We will discuss the specific functional forms which G can assume in the applications of the following chapter. The control vector $\boldsymbol{U}$ is typically a set of release values over some pre-defined control intervals. It may also include a value or values representing release temperatures, which are available as control variables in reservoirs with selective withdrawal mechanisms. The vector $\boldsymbol{T}$ can take on many forms. It may be location specific, or cover part or all of the spatial domain of the system. It may be either a maximal value (e.g., daily maximum temperature at a location) or an average temperature at a point or over a region.

Our problem is now one of finding the set of controls $\boldsymbol{U}$ such that the objective function f is minimized. One common approach to this problem is to examine variations of the function f resulting from perturbations in the control vector $\boldsymbol{U}$. These so-called variational approaches use objective function gradient information in an iterative fashion to identify optimal controls. There are two commonly used methods for developing the required gradient information. The first is to differentiate the governing equations and objective functions with respect to the control variables, and evaluate the gradients analytically. This approach is cumbersome for complex systems, as the gradient vector and Hessian matrix must be computed (and in the case of the Hessian, inverted) analytically at each iteration. Additionally, because our objective function involves system responses which are computed by numerical solution of the governing equations, it is impossible to evaluate the gradient information analytically. A second approach is to perturb each of the control variables, one at a time, and compute a localized linear gradient approximation based on a difference equation centered on the current estimate of the optimal control.

This work uses the second of these approaches. It is appropriate here for a

number of reasons. First, the physical nature of reservoir release control is such that there is a relatively small, finite number of controls which need to be evaluated. Second, the local curvature of the governing equations and objective functions with respect to the controls is not highly nonlinear, and so a perturbation approximation to the gradient does not result in unacceptable errors. Additionally, we use a root finding algorithm based on the well-known BFGS scheme which uses successive gradient values to approximate the Hessian without actually computing the second-derivative values analytically. The BFGS scheme has been shown to be effective in reducing solution time of nonlinear optimization problems compared to simpler root finding algorithms such as steepest descent, etc. (Zhu et. al., 1997). An iterative solution to the problem is achieved through use of an updating scheme for the control vector, as follows (Piasecki and Katapodes, 1997(b); Katapodes et al., 1990)

$$\boldsymbol{U}^{i+1} = \boldsymbol{U}^{i} - \alpha^{i}\boldsymbol{R}^{i}\boldsymbol{g}^{i} \tag{5.6}$$

Where $\boldsymbol{g} = \dfrac{\partial f}{\partial \boldsymbol{U}}$ is the gradient of the objective function with respect to the control vector, α is a weighting coefficient which controls the step size along the projected gradient direction. $\boldsymbol{R}$ is a matrix which modifies the gradient projection, and i denotes the iteration number. Different definitions of $\boldsymbol{R}$ result in different techniques for traversing the functional space towards its minimum value (see Press et. al., 1988). In its simplest form, $\boldsymbol{R} = \boldsymbol{I}$, the identity matrix, which results in the (rather inefficient) method of steepest descent. A much more efficient approach is to use

$$\boldsymbol{R} = \boldsymbol{H}^{-1} = \left[\frac{\partial^2 f}{\partial U_j \partial U_k}\right]^{-1} \tag{5.7}$$

This is the commonly used Newton-Raphson method, in which **H** is the inverse Hessian matrix of f with respect to the control vector. The Newton Raphson method takes advantage of the concept of conjugate directions to reduce the number of local

minimization procedures. If f is a quadratic function, this approach reaches the functional minimum in N updates of the control vector $\boldsymbol{U}$, where N is the number of discrete control intervals. If f is not quadratic, the method does not converge to the minimum in N updates, but still converges quadratically with repeated cycles of the minimization routine (Press et. al., 1988). Unfortunately, this approach requires computation of $\boldsymbol{H}$, which is often prohibitively difficult, or computationally expensive.

Fortunately, there exist a class of methods known as quasi-Newton, or variable-metric, techniques which provide a means for developing an approximation to the Hessian matrix $\boldsymbol{H}$ without analytical derivation of the second derivatives. These methods include the well-known Broyden-Fletcher-Goldfarb-Shanno (BFGS) method used here, and the Davidon-Fletcher-Powell (DFP) method. We provide a general derivation of these methods, drawing significantly from Katopodes (1990), Press et al (1988), and Piasecki and Katapodes (1997(b)). Readers interested in the original derivations of the BFGS scheme are directed to Broyden (1967), Fletcher (1970), Goldfarb (1970), and Shanno (1970).

The basic idea of the quasi-Newton methods is to approximate the second derivatives of the Hessian through use of the gradient information computed (and saved) from repeated computations of the gradient vector $\boldsymbol{g}$. First, let

$$\boldsymbol{d} = -\boldsymbol{H}^{-1}\boldsymbol{g} \tag{5.8}$$

be the vector defining the correction to the current control set $\boldsymbol{U}$, and define

$$\Delta\boldsymbol{g} = \boldsymbol{g}^{i+1} - \boldsymbol{g}^{i} \qquad \Delta\boldsymbol{U} = \boldsymbol{U}^{i+1} - \boldsymbol{U}^{i} \tag{5.9}$$

Eq. 5.6 can thus be rewritten as

$$\Delta\boldsymbol{U} = \alpha^{i}\boldsymbol{d}^{i} \tag{5.10}$$

Multiplying Eq. 5.10 by $\boldsymbol{H}^{-1}$ and using Eq. 5.9 leads to

$$\boldsymbol{H}^{-1(i+1)}\boldsymbol{U}^{i+1} = \boldsymbol{H}^{-1(i+1)}(\boldsymbol{U} + \alpha\boldsymbol{d})^{i} \tag{5.11}$$

Now, the Hessian matrix is derived from a Taylor series expansion of the functional, truncated after the quadratic term:

$$f(\boldsymbol{U})^{i+1} = f(\boldsymbol{U})^{i} + \sum_{j}\left[\frac{\partial f}{\partial U_j}U_j\right]^{i} + \sum_{j,k}\left[\frac{\partial^2 f}{\partial U_j \partial U_k}U_j U_k\right]^{i} + \ldots \tag{5.12}$$

The partial derivatives of the control vector $\boldsymbol{U}$ are indexed by j and k. Recall that $\boldsymbol{g} = \frac{\partial f}{\partial \boldsymbol{U}}$. From Eq. 5.12, the following relationship between ΔU and Δg is developed:

$$\Delta\boldsymbol{U} = \boldsymbol{H}^{-1(i+1)}\Delta\boldsymbol{g} \tag{5.13}$$

Substitution of Eq. 5.13 into Eq. 5.11 yields

$$\boldsymbol{H}^{-1(i+1)}\Delta\boldsymbol{g} = \alpha\boldsymbol{d}^{i} \tag{5.14}$$

The Hessian is now approximated by taking the derivative of $\boldsymbol{g}$ with respect to $\boldsymbol{U}$:

$$\boldsymbol{A}^{i+1} = \left(\frac{\partial \boldsymbol{g}}{\partial \boldsymbol{U}}\right)^{i+1} \tag{5.15}$$

Using Eq. 5.13 and substituting $\boldsymbol{A}$ for $\boldsymbol{H}^{-1}$ results in

$$\Delta\boldsymbol{g} = \boldsymbol{A}^{i+1}\alpha^{i}\boldsymbol{d}^{i} - \delta_{*} \tag{5.16}$$

The DFP and BFGS methods are identical to this point. They differ in the algorithm used to update the approximate Hessian matrix $\boldsymbol{A}$ at each iteration. The BFGS update scheme is given by

$$\boldsymbol{A}^{i+1} = \boldsymbol{A}^{i} - \left(\frac{\boldsymbol{A}\Delta\boldsymbol{g}\Delta\boldsymbol{U}^{T} + \Delta\boldsymbol{U}\Delta\boldsymbol{g}^{T}\boldsymbol{A}}{\Delta\boldsymbol{U}^{T}\Delta\boldsymbol{g}}\right)^{i} + \left[\left(1 + \frac{\Delta\boldsymbol{g}^{T}\boldsymbol{A}\Delta\boldsymbol{g}}{\Delta\boldsymbol{U}^{T}\Delta\boldsymbol{g}}\right)\frac{\Delta\boldsymbol{U}\Delta\boldsymbol{U}^{T}}{\Delta\boldsymbol{U}^{T}\Delta\boldsymbol{g}}\right]^{i} \tag{5.17}$$

Equations Eq. 5.6 and Eq. 5.17, plus evaluation of the functional I and gradient vector

g provide the basis for finding the optimal control ***U***. In this thesis, we employ the optimization library L-BFGS-B (Zhu et. al., 1997), which solves the nonlinear minimization subject to bound constraints on the control vector. Gradient information can be computed either by analytical differentiation of the functional and governing equations with respect to the control variables, or by using a perturbation approach. The perturbation approach only works well for situations in which there is a relatively small number of discrete controls to vary; a large number of controls result in a heavy computational burden. We use perturbation here because it is preferable to analytical differentiation. We discuss the issue of discretization of the control variable(s) in the next chapter. Suffice it to say for now that the number of discrete controls in our case study does not make our approach prohibitively expensive.

The solution of the optimal control problem can be summarized as follows:

1. Using an initial set of potentially optimal controls, generate system states (simulation), and evaluate objective function *f*.
2. Perturb individual controls one at a time, and re-run simulation model. Evaluation of objective function for each perturbed control set yields a difference approximation of the functional gradient.
3. Input objective function and gradient values to L-BFGS-B library. The L-BFGS-B routine performs the following functions (Byrd et. al., 1994):
    - 3(a). An updated Hessian matrix is generated based generally on the procedure outlined in Eq. 5.8-Eq. 5.17 above.
    - 3(b). The Hessian is used to define a quadratic approximation to the objective function centered on the current control set.
    - 3(c). A search direction is computed using gradient projection to identify active variables (variables which are held at their bounds), and the quadratic model is used to minimize the free variables.
    - 3(d). Lastly, a line search is executed along the search direction, defined to be the vector from the current control vector to the newly generated functional minimizer.
    - 3(e). The L-BFGS-B routine returns a new set of controls to be evaluated.
4. Convergence tests determine whether the optimization loop is terminated. If not, return to 1 and continue.

Verification of Solutions

One of the less desirable characteristics of the L-BFGS-B algorithm is that it converges slowly in the vicinity of the optimal solution (Zhu et. al., 1997). We avoid overly expensive computations by terminating the BFGS scheme at a lower tolerance level than prescribed by its authors, and using a quadratic minimization function to identify the local minima of the objective. This is done as a final check of the optimal solution, and is implemented by generating two perturbed solutions for each control. A quadratic function fit to the functional value resulting from the simulations is used to generate a final control vector. The quadratic minimization scheme is also used for simpler single control optimization problems, particularly when selecting a single release temperature value given a pre-defined set of reservoir releases.

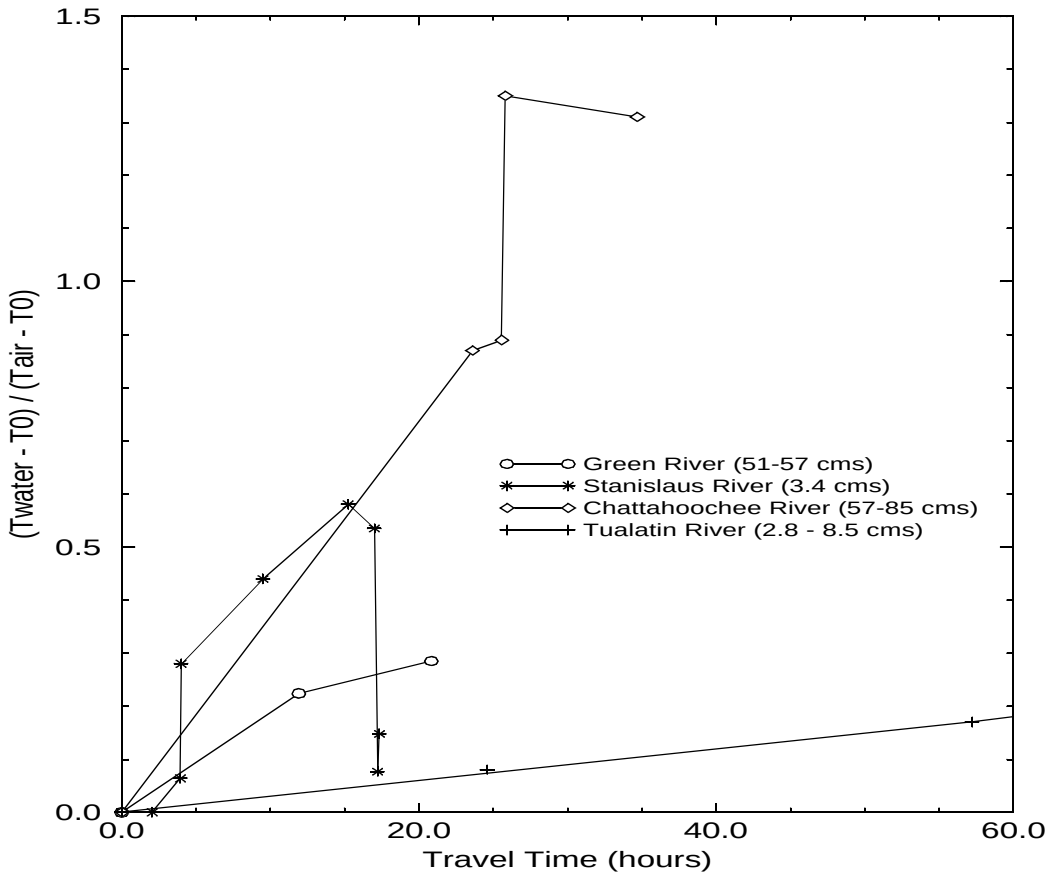

Figure 4.10: Non-dimensional comparison of heating rates for 4 rivers using average August meteorological conditions. The sharp changes in water temperatures on the Stanislaus are caused by diversion to, and return flow from, a hydroelectric facility, and on the Chattahoochee by urban effluent.

atures at the upstream boundaries of the reach. From this comparison it is clear that although temperature management is feasible, factors such as urban effluent, diversions, and return flows can significantly limit our ability to control stream temperatures.

CHAPTER 6

OPTIMAL CONTROL OF RESERVOIR OPERATIONS

6.1 INTRODUCTION

Let us turn now to the application of the previously discussed optimization techniques to temperature management problems. Large reservoirs have significant impacts on downstream water quality and aquatic habitat. Changes in numerous characteristics, including temperature, water chemistry, bed-load movement, and suspended solids, can cause adverse impacts to the ecosystem. As management objectives such as fisheries habitat and recreation are considered together with the more traditional goals of flood control, water delivery, and hydropower generation, reservoir operators are faced with increasingly complex management problems. Among the more important of these is modification to stream temperature. Stream temperatures are known to significantly impact aquatic environments (Ward and Stanford, 1979; Lillehammer and Saltveit, 1982). Minimum flow requirements are often imposed in an effort to reduce negative impacts of high water temperatures on aquatic species. Usually, minimum flow constraints are imposed based on worst-case scenarios of atmospheric heating. This may result in inefficient allocation of water during periods in which atmospheric conditions would allow a further reduction in flow while still meeting temperature constraints.

Railsback (1997) noted that a long-term reduction of water usage on the order

of 20% could be realized by adjusting flows over periods of several days to reflect short-term prediction of atmospheric conditions. He also noted that based on stream ecosystem models, these lower flows would have a negligible impact on fisheries biomass. Results from Chapter 4 indicate that even shorter-term flow modifications could be used successfully to reduce water usage while maintaining temperatures at acceptable levels. We also saw that release temperature can have a significant impact on the ability to control downstream temperatures. Using the theories introduced in Chapter 5, we develop optimal release strategies for these problems.

The primary goal of developing optimal release patterns for Flaming Gorge Dam is to enhance the native fisheries habitat in the Green River near its confluence with the Yampa River, in Dinosaur National Monument. This will ideally be achieved without causing any negative impact to the existing trout fishery immediately below Flaming Gorge Dam. One of the few remaining populations of the endangered Colorado Pikeminnow is found in the Green River below Dinosaur National Monument. The Pikeminnow spawn in the Yampa River sometime in June or July, depending on the timing and magnitude of spring snowmelt runoff. These fish then migrate downstream of the confluence, where they are thought to spend most of their adult lives. It is believed that dramatic changes in flow and temperature resulting from operations of Flaming Gorge dam have a negative impact on the fishery (Crist, 1998). We have shown in Chapter 4 that it is possible to influence temperatures at the confluence of the Green and Yampa. Meeting these temperature targets, however, is not the only objective for which the reservoir is operated. Release targets, in terms of daily average flows, will typically be defined based on the hydrologic state of the basin. Typically, The reservoir operators will have year-end reservoir pool elevation targets to meet in preparation for the spring snowmelt runoff period. There may also be delivery requirements based on the Colorado River Compact or other obligations to irrigators, municipalities, etc. Based on current reservoir elevation, and predicted inflow, a target release

value will be set for one to several months into the future. For example, daily average flows of 57 - 71 cms are typical in hydrologically “wet” years. In below average years, the average release target may be as low as 22.6 - 28 cms through late summer and fall. Meeting temperature targets through the use of reduced flows during such years may be difficult to achieve without violating the daily flow target.

6.2 FORMULATION OF OBJECTIVE FUNCTION

Recall from the previous chapter the general form of the objective function *f(**U**):*

$$f(\boldsymbol{U}) = \int_0^{\tau}\int_0^{L} G(\boldsymbol{U}, \boldsymbol{T})\, dL\, d\tau \qquad \textbf{(6.1)}$$

Where $\boldsymbol{U}$ = the control vector, $\boldsymbol{T}$ = a vector of stream temperatures at some target node(s) downstream, G = a function designed to measure the deviation of the existing system states from some desired target states. Let us examine the form that these functions and variables can take in more detail.

The control vector $\boldsymbol{U}$ is comprised of a set of discrete reservoir release values, plus (possibly) a reservoir release temperature value. The release values may in theory be discretized to any time increment desired. In practice, it is uncommon for reservoir operators to vary release rates more than a few times daily. For reservoirs with selective withdrawal structures, release temperature can also be controlled. However, these structures typically do not allow diurnal changes in release temperature. Rather, a single release temperature may be selected for periods of one to several days at a time. Both release rate and temperature are subject to operating constraints. For flow, the constraints will include minimum and maximum release rates (as a function of both institutional constraints and the physical capabilities of the reservoir release structures), and may include restrictions on total daily fluctuations and ramping rates.

Release temperature will be constrained primarily by the degree of thermal stratification in the reservoir in the area of the selective withdrawal structure. Annual cycles of heating in the reservoir will modify the range of potential release temperatures from month to month.

The function G in Eq. 6.1 reflects the deviation of the system states from a set of target states. In general, G may be evaluated over the entire space-time domain, or at site-specific and time-specific locales. As such, it is really the sum of one or more functions describing the "penalties" incurred for each optimization variable's deviation from its target value. The functional forms which G may take on vary greatly (see, for examples, Gill et. al., 1981; Nemhauser et. al., 1989, Bazaraa et. al., 1993). In this work we use three:

$$
\begin{aligned}
Quadratic: \int_0^{\tau}\int_0^{L} G(\boldsymbol{U}, \boldsymbol{T})\,dL\,d\tau &= \sum_{l=1}^{n} \alpha_l (T^l_{max} - T^l_{opt})^2 + \sum_{c=1}^{m} \beta_c (U^c - U^c_{opt})^2 \\
Linear: \int_0^{\tau}\int_0^{L} G(\boldsymbol{U}, \boldsymbol{T})\,dL\,d\tau &= \sum_{l=1}^{n} \alpha_l (T^l_{max} - T^l_{opt}) + \sum_{c=1}^{m} \beta_c (U^c - U^c_{opt}) \\
Exponential: \int_0^{\tau}\int_0^{L} G(\boldsymbol{U}, \boldsymbol{T})\,dL\,d\tau &= \sum_{l=1}^{n} \alpha_l \frac{1}{Exp(T^l_{max} - T^l_{opt})} + \\
&\quad \sum_{c=1}^{m} \beta_c \frac{1}{Exp(U^c - U^c_{opt})}
\end{aligned}
\tag{6.2}
$$

where the index l is a specific location in the spatial domain L, and the index c indicates a specific control interval in the time domain t. $\boldsymbol{T}^l_{opt}$ and $\boldsymbol{U}^c_{opt}$ are target temperature and control vectors towards which the system states will be driven. The target temperatures in this work are those deemed necessary to maintain the two fisheries. Target controls are the reservoir release values which have been identified as necessary to meet the reservoir's long-term water delivery and flood control obligations. The coefficients α_l and β_c act to weight the relative value of the objectives. Each of these

objective function forms will drive the system toward its target in different ways (Figure 6.1). The quadratic form penalizes deviations from the optimum (in this exam-

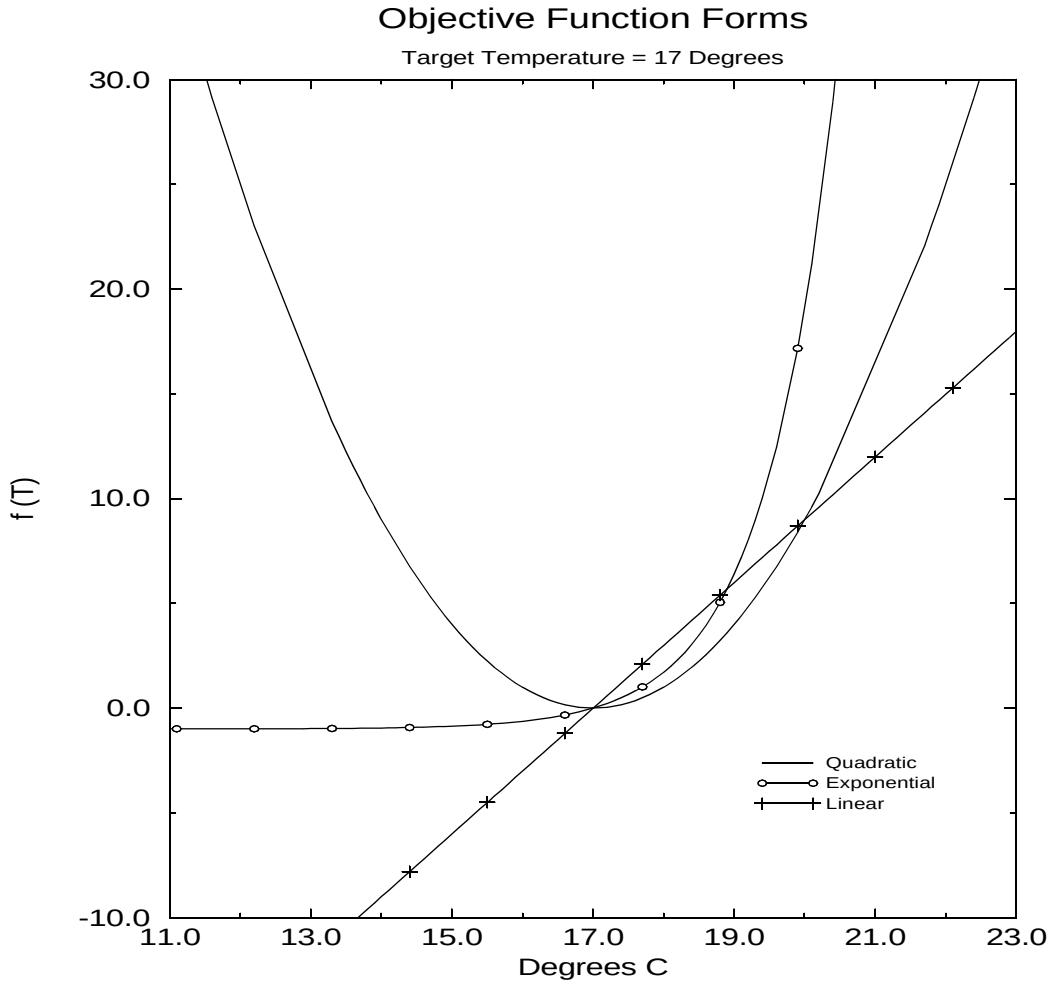

Figure 6.1: Graphical depiction of objective function forms.

ple, a target temperature of 17 ^{o}C) equally on either side of the optimum. Thus temperatures below 17 ^{o}C are penalized with the same magnitude as those above. The exponential form penalizes stream temperature values on one side of the optimum more heavily than those on the other. This is akin to saying there is no penalty (or more accurately, a very small gain in benefit) for values less than 17 ^{o}C, but the penalty for exceeding the target temperature is significant. Finally, the linear function will push

the solution to the lowest possible value (where large negative values become “best”). Notice that in the case of a linear objective function, definition of the target is somewhat unnecessary; the optimization scheme will try to achieve the lowest or highest possible temperature. However, definition of the target allows us to evaluate whether or not the solution is in compliance with the specified target (i.e., if the objective function is less than zero). These objective function forms can be combined within a single problem, as will be shown later.

6.3 FEASIBLE SOLUTIONS USING UNSTEADY RELEASES

The first problem we address is that of using reservoir releases to meet downstream temperature targets. These examples have a single target temperature at one downstream location, and no constraints or target values for reservoir releases. A linear objective function of the following form is defined:

$$min\ f(U) = \sum_{l=1}^{n} max(0, \alpha(T_{max}^{l} - T_{opt}^{l})) \tag{6.3}$$

In its simplest form, the use of a linear objective function for target temperatures with no additional objectives will yield a feasible solution to the temperature control problem. We call the solution here feasible as opposed to optimal because the optimization scheme in this case will terminate with an answer as soon as the value of the objective function reaches zero. This indicates that the current control set satisfies the target temperature objectives. Notice that defining α=(-1) generates solutions in which the optimal temperature is greater than the target, while defining α=1 generates solutions in which the optimal temperature is less than the target. In many situations, there will be multiple feasible solutions to this type of problem.

Atmospheric forcings and boundary conditions for this and all of the following optimization examples are based on observed historical data from the Green River.

Historical mean and maximum atmospheric conditions were generated based on approximately 10 years of daily meteorological observations from the Brown's Park National Wildlife Refuge weather station. These data include minimum and maximum daily air temperatures, dewpoint temperature, precipitation, and average windspeed. Channel characteristics are given in the calibration section of Chapter 4. Unless otherwise noted, the shortwave radiation inputs are based on solar altitudes observed during mid-July. Specific examples which use data other than these are explicitly outlined in the problem description.

Feasible Solution for Pikeminnow Habitat Objective

The objective function for the Pikeminnow, specified at 105 km below Flaming Gorge Dam, is given by

$$min\ f(U) \ = \ max(0, \alpha(T_{max}^{105} - T_{opt}^{105})) \tag{6.4}$$

where T_{opt}^{105} = 22 ^{o}C, and α = (-1). From previous discussions, we know intuitively that low-flow solutions are required to meet this objective. We saw in Chapter 4 that low flows are necessary to meet this temperature objective. To demonstrate progression of the controller to a feasible solution, we start the optimization scheme using a high steady flow of 71 cms. Release temperatures are 12 ^{o}C, which has been the average August release temperature over the past several years (Brayton, 1998). The optimal (feasible) control sequence generated using four 6 hour control intervals is shown in Figure 6.2. The optimal controller generates a feasible solution after 9 iterations, as shown in Figure 6.3. The linear relationship between temperature at the constraint location and the value of the objective function is clear from that figure.

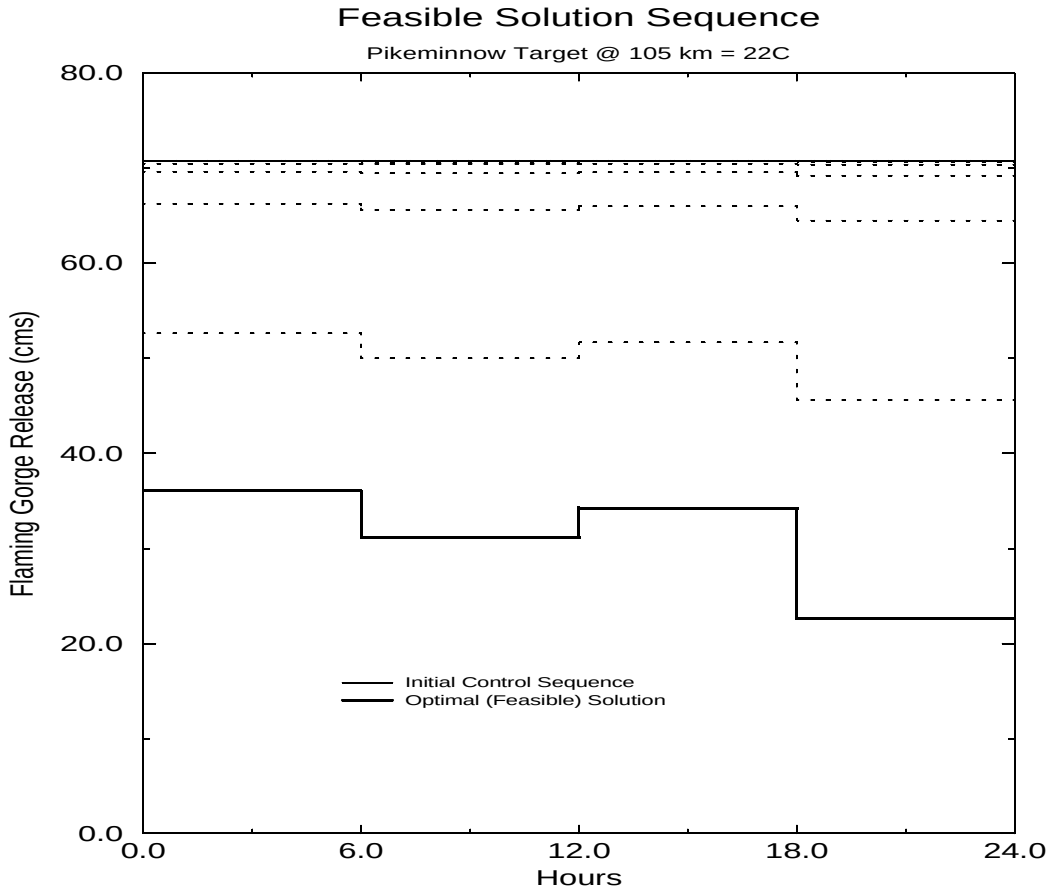

Figure 6.2: Feasible control solution for Pikeminnow objective.

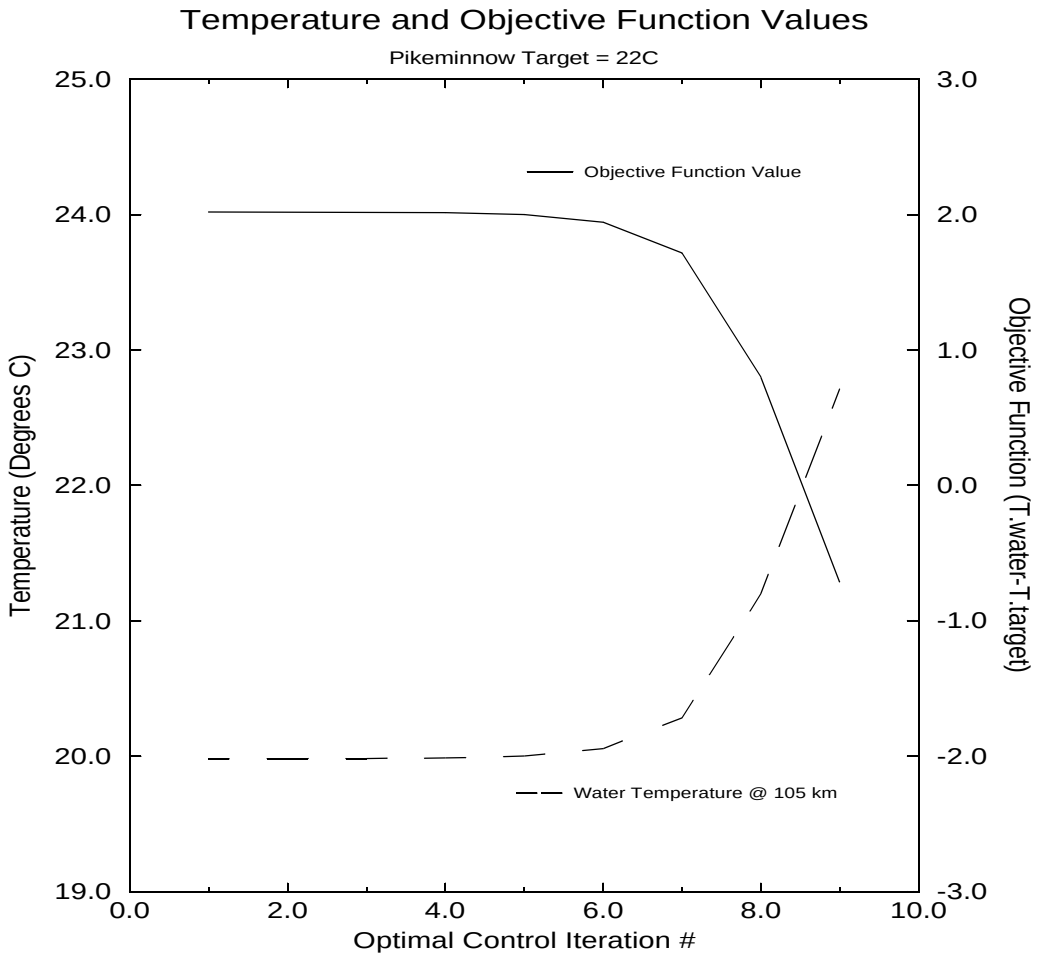

Figure 6.3: Temperature and objective function values for Pikeminnow objective.

Feasible Solution for Trout Habitat Objective

The objective function for trout habitat in the Green River is given by

$$min\ f(U) \ = \ max(0, \alpha(T_{max}^{46} - T_{opt}^{46})) \tag{6.5}$$

where T_{opt}^{46} = 17 ^{o}C, and α = (1). We start the optimization scheme using a steady flow of 22.6 cms, which we know from experience is well below the flow required to meet the objective. Release temperatures are again assumed to be 12 ^{o}C. Figure 6.4 shows the optimal (feasible) control sequence for the trout habitat. The feasible solution was obtained after 103 iterations. The values for the maximum daily stream temperature at the target location, and the corresponding objective function values, are shown in Figure 6.5. The optimal controller is particularly inefficient for this problem. This

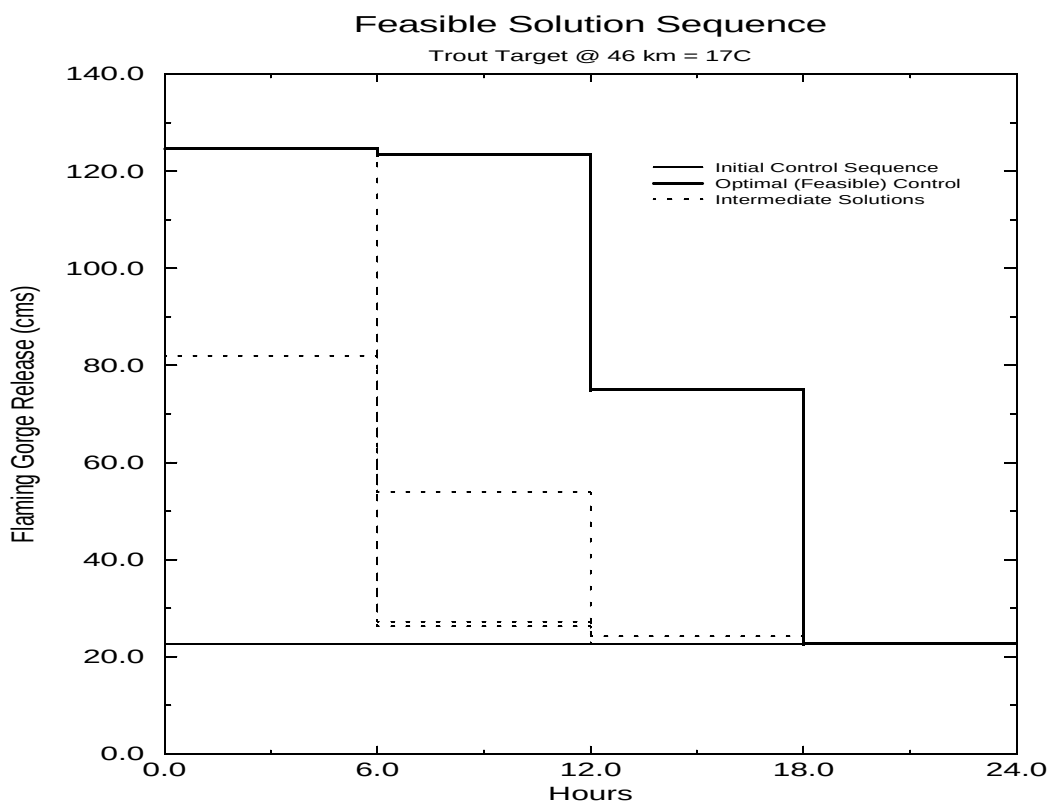

Figure 6.4: Feasible control solution for trout habitat objective.

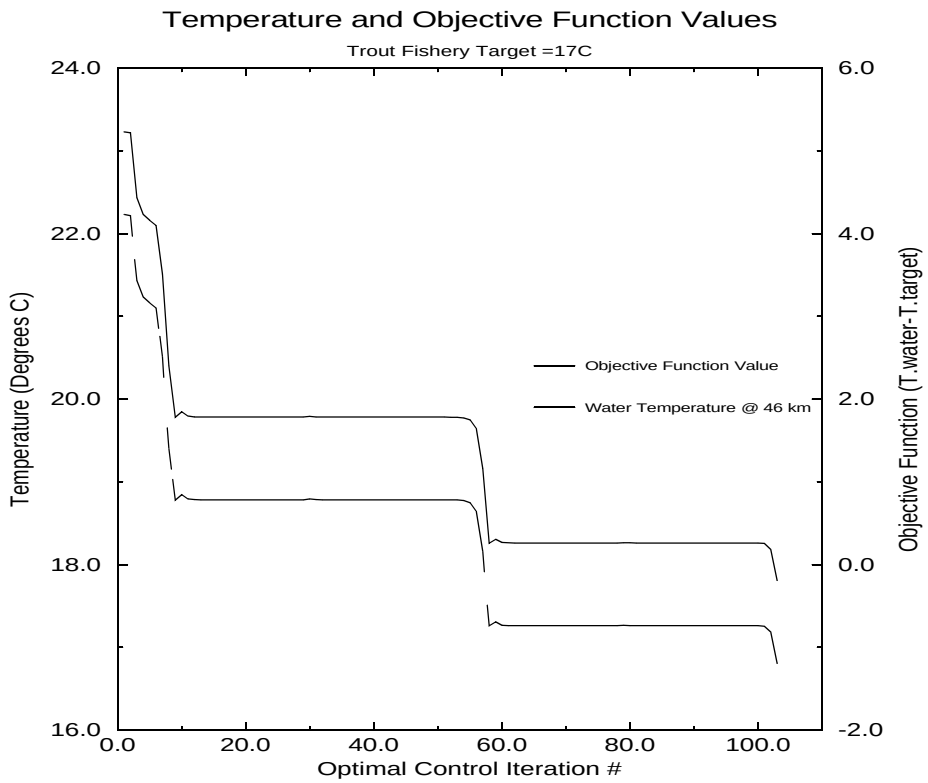

Figure 6.5: Temperature and objective function values for trout objective.

inefficiency is due in large part to a poor initial guess for the optimal control sequence.

These examples, while quite simple, provide some insight into the behavior of the optimal controller. For the trout habitat problem, the controller initially tries a flow which is quite large during the early hours of the day. This occurs because at lower flows, the releases occurring between midnight and 6 a.m. have an impact on daily maximum temperatures at the constraint location. However, as the controller increases the flow in this interval, the flow velocity increases, and eventually moves through the reach so quickly as to eliminate its usefulness at the constraint location. The controller then starts increasing flows during the second 6 hour period, which has a more significant impact on daily maximum temperatures at higher flows. Compare the results obtained for this problem to those obtained below for the same problem when additional objectives are included to minimize total release volume.

6.4 Optimal Solution for Pikeminnow and Trout Habitat Objectives

We turn to a slightly more difficult problem, that of meeting both the trout and Pikeminnow objectives. We use an exponential objective function for each objective. Additionally, we want to minimize the total volume of water used to meet the objectives. The resulting objective function takes the following form:

$$min\ f(U) = \frac{1}{Exp(T_{opt}^{46} - T_{max}^{46})} + \frac{1}{Exp(T_{max}^{105} - T_{opt}^{105})} + \beta \sum_{c=1}^{m} (U^{c}) \tag{6.6}$$

where β is a coefficient weighting the relative value of reducing total flow to that of meeting the temperature objectives. A control sequence of 28.3 cms steady flow is used as the initial condition for the optimization model. The release temperature is 12 ^{o}C, and a weighting coefficient of 0.005 is used. The small value for β results in solutions which are weighted heavily toward satisfying the target temperatures. It will nevertheless serve to drive the controls to a minimum value when there is flexibility in the control. Two sets of optimal solutions are developed, one using historical maximal air temperatures, and the second using historical average air temperatures.

Results for Maximum Air Temperatures

Figure 6.6 shows the optimal control sequence for the problem, using the historical maximum air temperatures, and 6 hour control intervals. The BFGS algorithm converged on an optimal solution after about 75 iterations. Figure 6.7 shows the progression of stream temperatures at the constraint locations through the iterative solution process. The target temperatures of 17 and 22 ^{o}C are shown in grey. Recall from the discussion of the optimization techniques in the previous chapter that the BFGS methods become inefficient as they approach the optimal solution. A solution to this problem is to terminate the BFGS solver at a lower tolerance level (i.e., farther from

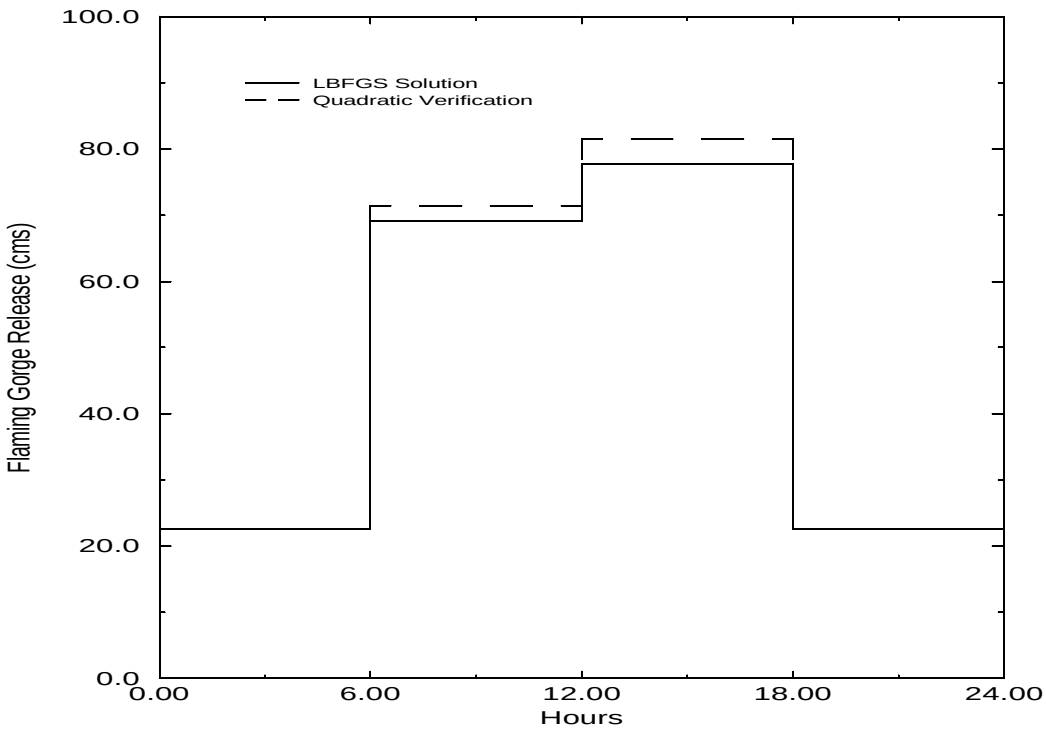

Figure 6.6: Optimal reservoir releases for problem described by Eq. 6.6. Historical maximal air temperatures.

the true optimum), and use another approach to verify the optimal values. This second approach, which is essentially a single quadratic programming type step, based on small perturbations of the control, provides the final optimal control sequence, as well as a check on the validity of the BFGS solution. The use of this technique assumes that in the immediate vicinity of the optimal solution, the objective function can be reasonably approximated by a quadratic function. The optimal control sequence derived using the quadratic programming technique is also shown in Figure 6.6 along with the BFGS solution. The solutions at each control interval are within 5% of each other. The stream temperatures at the objective locations resulting from the quadratic control is also shown in Figure 6.7. The quadratic solution is seen to yield slightly lower temperature values, and in fact brings the temperature at 46 km exactly into compliance with the 17 ^{o}C maximum. The objective function values for this problem are shown in

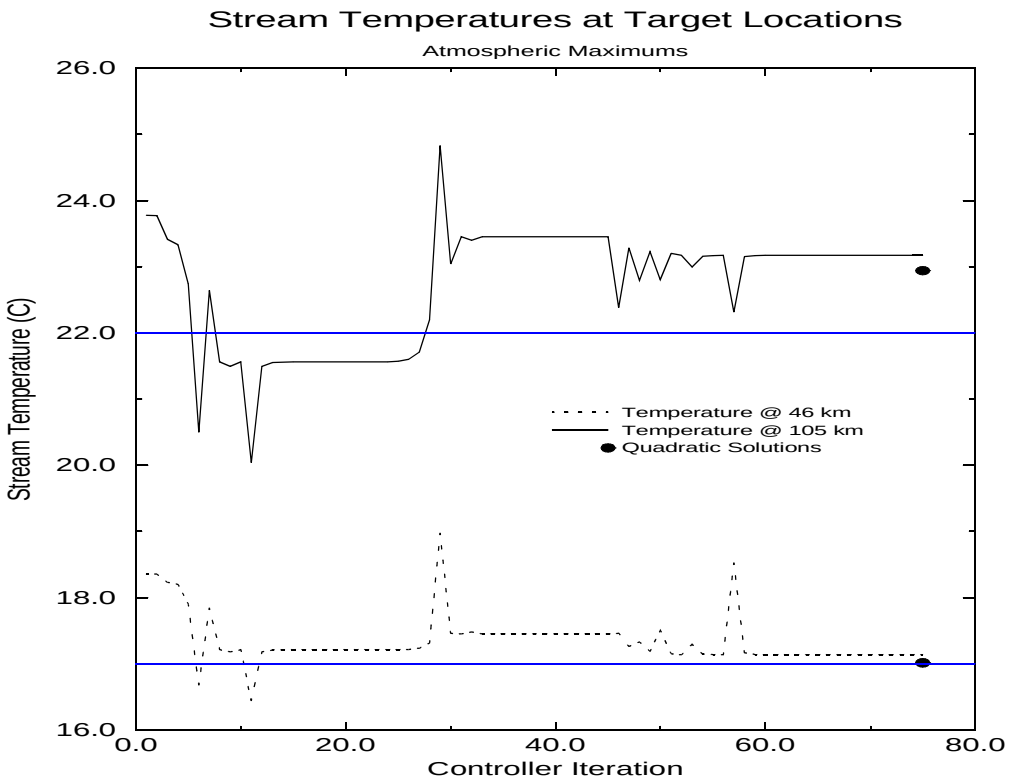

Figure 6.7: Progression of stream temperature values at the objective locations.

Figure 6.8. The objective function value derived using the quadratic approximation is shown as well. The quadratic solution improves the final value for the objective function by 3.4%.

Results for Average Air Temperatures

Results for the same problem using historic atmospheric averages are shown in Figure 6.9 - Figure 6.11. As one would expect, the optimal release pattern is similar in shape to the solution for the maximal atmospheric heating. The peak flows needed to meet the temperature objective at 46 km are somewhat less, particularly during the period 12:00 - 18:00 hours. This is explained by the timing of maximum solar radiation and air temperature values during the day. The maximum and average atmospheric conditions reflect significant differences in air temperatures (daily maximums of 38 ^{o}C and 30 ^{o}C, respectively). The maximum daily air temperature occurs later in

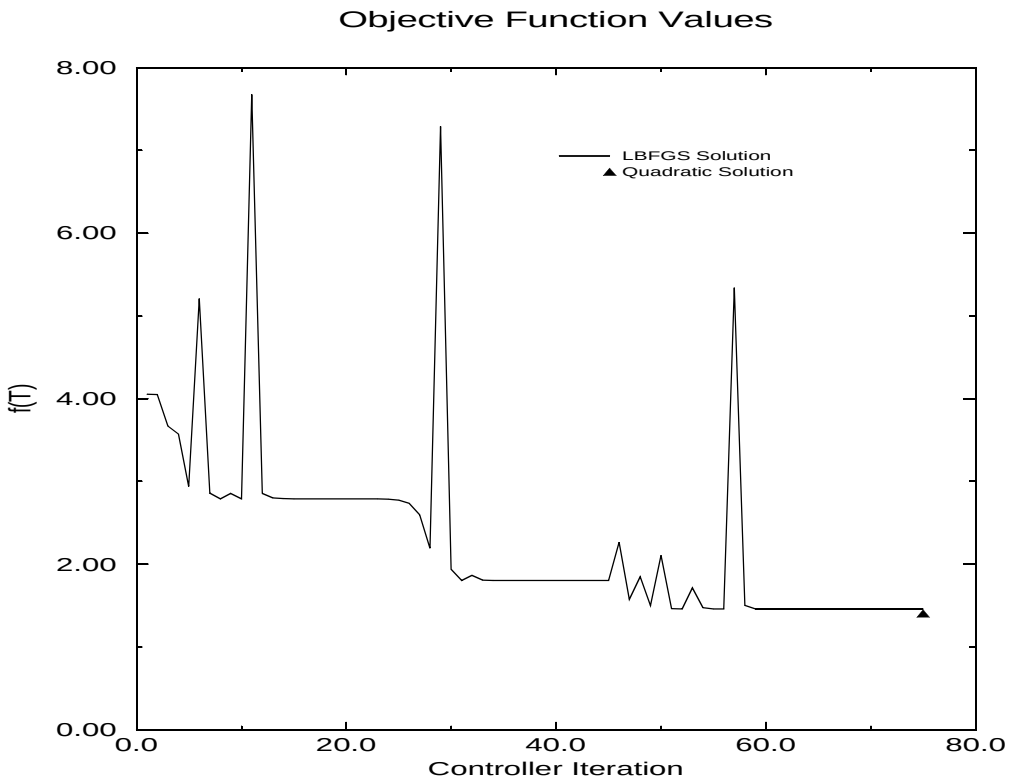

Figure 6.8: Objective function values for exponential objective function of Eq. 6.6.

the day than the maximum incident solar radiation. The result is that for the optimal control for the average meteorology problem, the reduced maximum air temperature, and hence reduced heat flux into the stream, allows for a reduced release during the afternoon period. Additionally, because the release during the previous control interval (6:00 - 12:00) is reduced, it will travel past the objective location more slowly. As a result, it will influence the temperature at that location over a longer period of time. Resulting stream temperatures at the objective locations and the objective function values are shown, respectively, in Figure 6.10 and Figure 6.11. The solutions were again verified using the quadratic programming algorithm. Variations in the release (control) values were between 0 - 4%. The quadratic programming solution yields values for stream temperatures within 0.2 ^{o}C of the LBFGS solution, and a final objective function value of 1.913, versus 1.937 for the LBFGS solution. The results of both examples

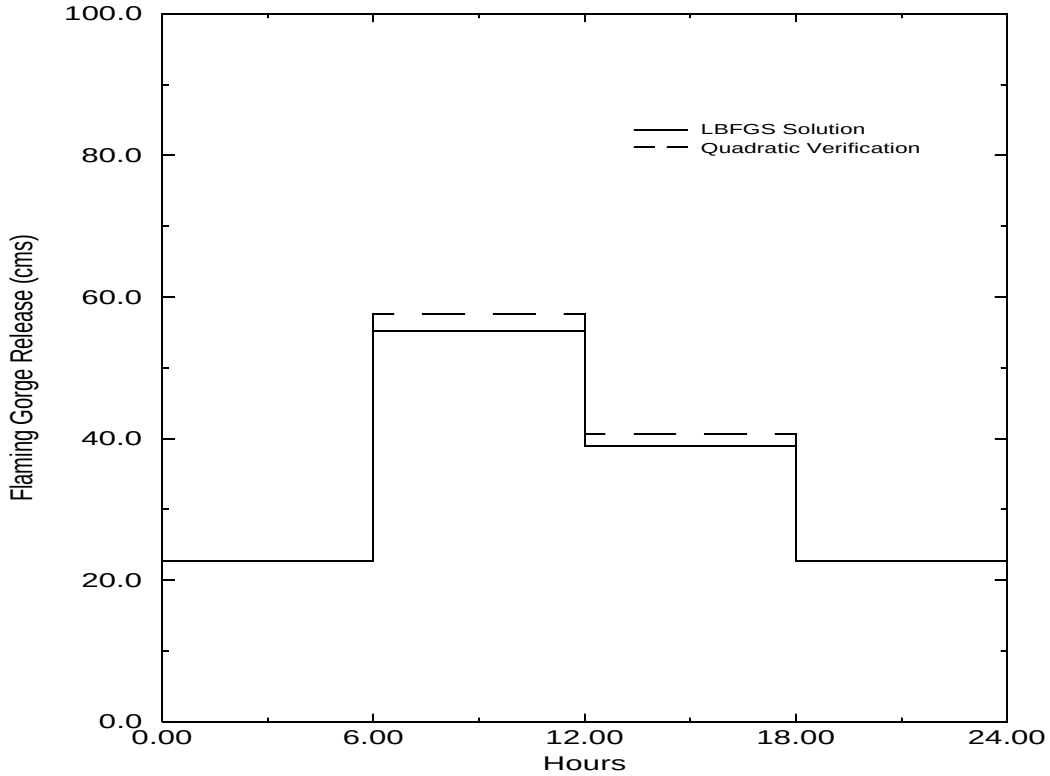

Figure 6.9: Optimal reservoir releases for problem described by Eq. 6.6. Historical average air temperatures.

indicate that the LBFGS solver is useful for identifying near-optimal solutions from rough estimates of the initial control sequence. The quadratic controller allows us to terminate the LBFGS scheme at a lower tolerance level - at a significant savings in computation time - and generate a final optimal solution.

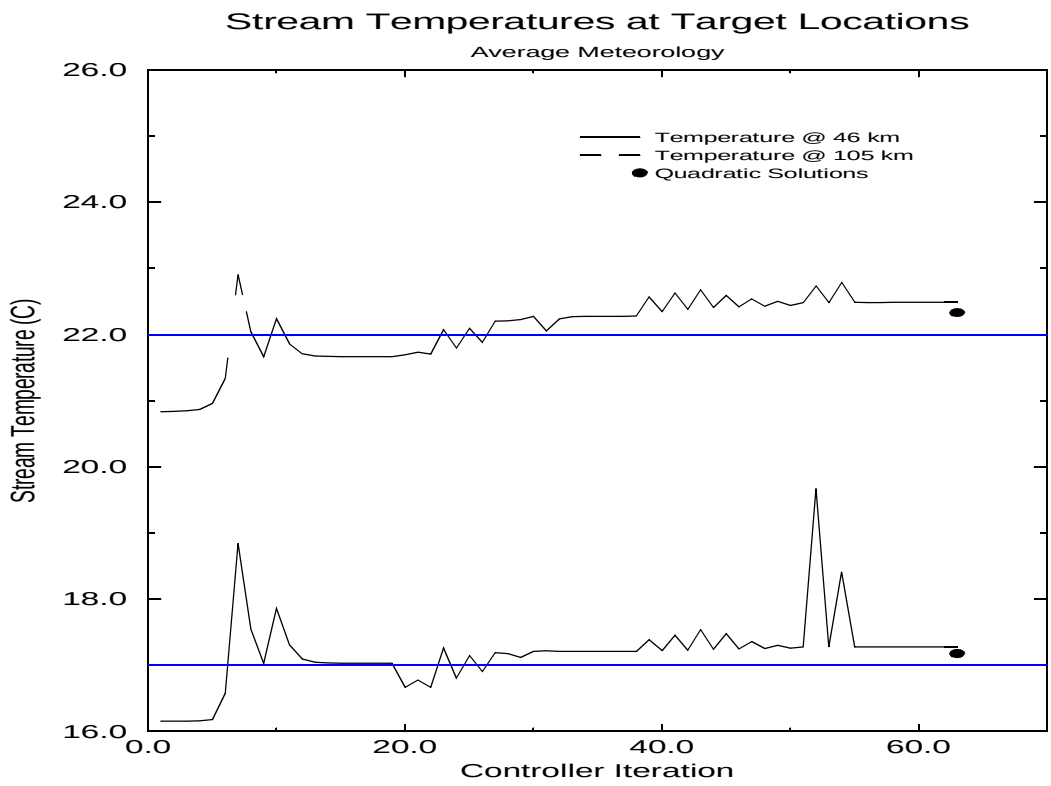

Figure 6.10: Progression of stream temperature values at the objective locations.

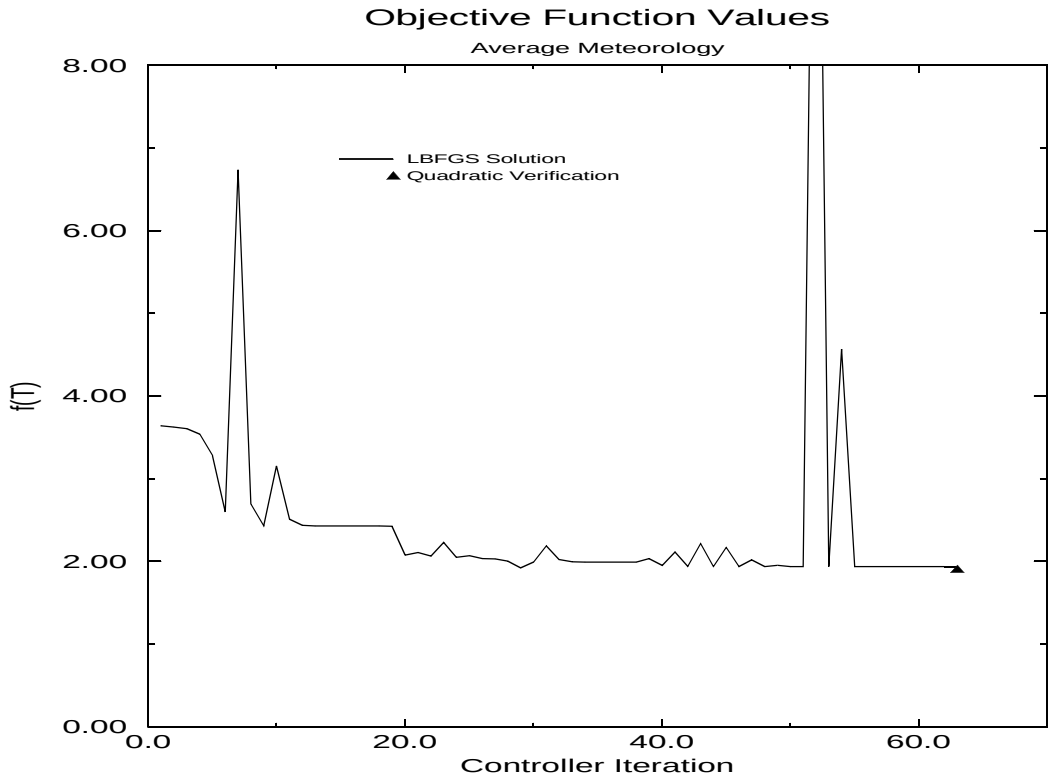

Figure 6.11: Objective function values for exponential objective function of Eq. 6.6

6.5 OPTIMIZATION USING SELECTIVE WITHDRAWAL

For reservoirs which have selective withdrawal mechanisms, the question arises as to whether it is more desirable to use variable flows, or fixed flows with a modified release temperature, to meet downstream temperature objectives. Usefulness of selective withdrawal structures is largely dependent on the degree of thermal stratification in the reservoir at the location of the withdrawal structure. It is further limited by the pool elevation of the water in the reservoir, and its relation to the selective withdrawal structures. For reservoirs which have significant restrictions on their flows - for flood control, water delivery, etc. - selective withdrawal structures may be the only feasible approach to modifying stream temperatures. Associated with the use of selective withdrawal structures are other significant water quality considerations. Releasing water from different depths may cause adverse changes to other water quality constituents. For example, water released from great depths may be oxygen poor, while warm water released through spillways may become supersaturated (Lillehammer and Saltveit, 1982). Either can be toxic to fish. These factors may in some cases negate any potential benefits gained by releasing water at a specific temperature.

To demonstrate the potential usefulness of the selective withdrawal structure on Flaming Gorge Dam, we revisit the problem of meeting two temperature objectives simultaneously. However, we now seek solutions using a single control variable: the release temperature. The objective function for this problem is given by

$$min\ f(U) = (T_{opt}^{46} - T_{max}^{46})^2 + (T_{opt}^{105} - T_{max}^{105})^2 \tag{6.7}$$

where the control vector U is now a single value ($T_{release}$) representing the reservoir release temperature. We use a quadratic objective function for this problem because in general, it is not possible to meet both the objectives using a steady release. The quadratic form will ensure that the deviations from the two objectives are roughly equal. Average flows from Flaming Gorge Dam during the summer months are in the range

22.6 - 79 cms. Target release values are determined based on current and predicted hydrologic conditions. In extremely wet hydrologic years, summer flows in excess of 79 cms are possible. The maximum flow which can be released through the hydro-power turbines is approximately 125 cms. We examine flows ranging from 22.6 - 113 cms for this example. During the early summer, Flaming Gorge Reservoir stratifies thermally. Based on historical data of reservoir temperatures and pool elevations, release temperatures can range from 5 - 15 ^{o}C in late summer. We use these values as the bounds on release temperature used in this work.

In this problem, a quadratic programming algorithm is employed. It is identical to the method used to verify the BFGS scheme in the previous example. An initial guess of the optimal release temperature is provided to the solver. Two perturbations of the release temperature, plus the initial guess, are simulated and the results used to develop a quadratic approximation to the objective function. The root (first derivative minimum) of this approximation is found, and that temperature value is used as the next optimal temperature estimate. The procedure iterates until a specified tolerance (0.1 ^{o}C) is reached. The method converges on the optimal value in 5 iterations or less in all cases examined.

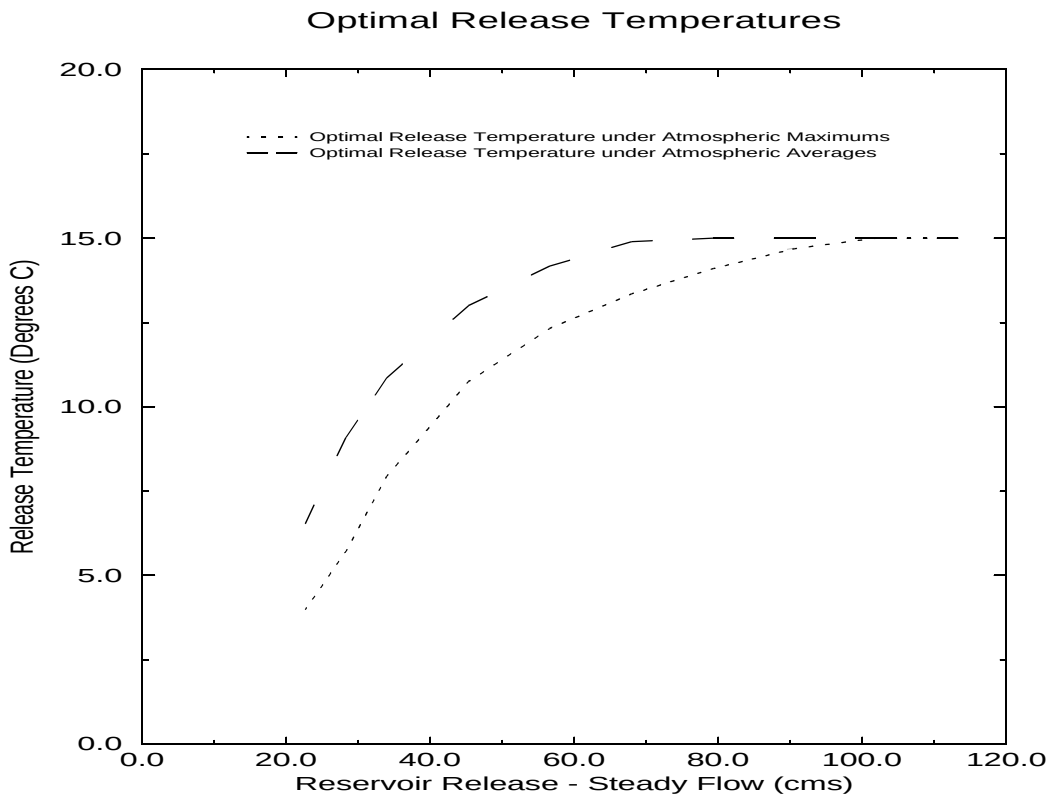

Figure 6.12: Optimal release temperatures for steady reservoir releases.

Figure 6.12 shows the optimal release temperature curves for various steady flow releases, under both average and extreme atmospheric conditions. At high steady flow values, the optimal solution is to increase release temperatures as much as possible. For steady releases greater than 68 cms in the case of average air temperatures, and 99 cms for maximum air temperatures, the optimal release temperature is constrained at its upper bound of 15 ^{o}C. The value of the objective function at the optimal release temperatures for the range of flows is given in Figure 6.14. The results indicate that as atmospheric temperatures move from below average to above average, a higher steady flow and selective withdrawal combination result in better adherence to the objectives. Finally, Figure 6.13 shows the actual stream temperatures at the constraint locations under the optimal releases shown in Figure 6.12. From Figure 6.13 it is clear

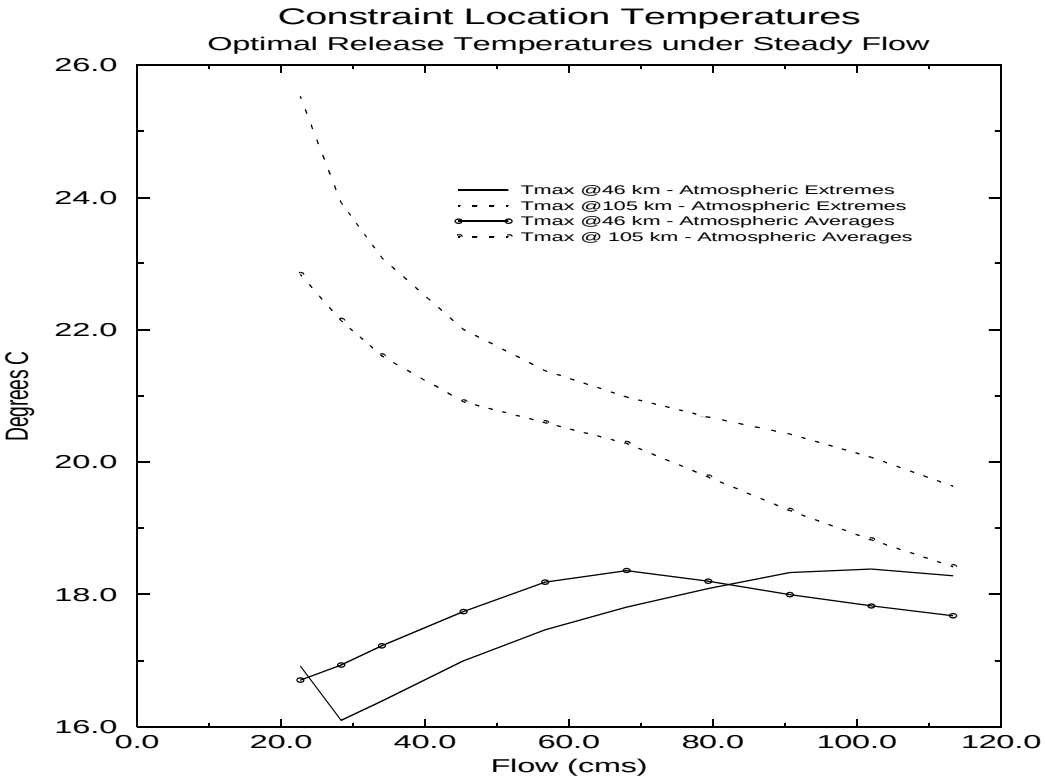

Figure 6.13: Stream temperatures at constraint locations under steady flows with optimized release temperatures.

that meeting the stream temperature objective at 105 km becomes increasingly difficult as flows increase. In fact, under “normal” atmospheric conditions, any steady flow over approximately 34 cms will not warm to the desired 22 ^{o}C. The trout habitat objective, however, exceeds its target temperature by less than 1.5 ^{o}C over the entire range of steady flow solutions.

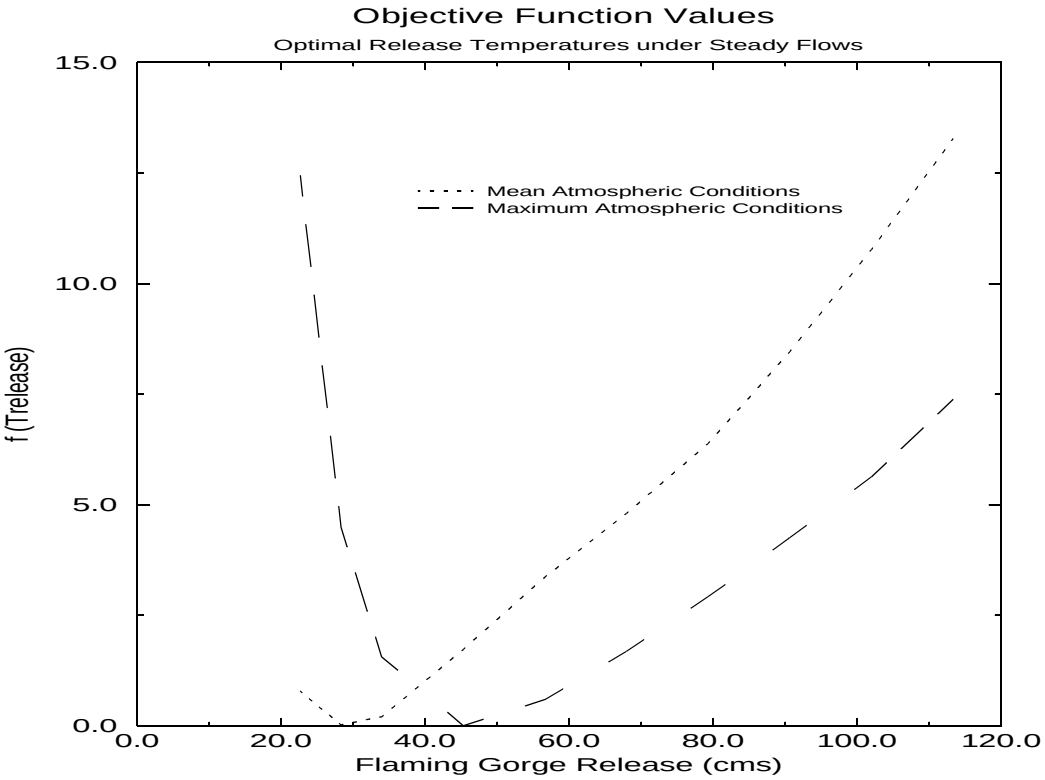

Figure 6.14: Objective function values for optimal release temperatures.

Optimal Release Temperature for Hydropower Operations

There may be situations when reservoir releases are not subject to control, and are not necessarily steady, as in the case of peaking hydropower operations. Under these conditions, it is still desirable to identify the optimal release temperature. As is the case with most steady reservoir releases, it is impossible to satisfy both temperature objectives using only the selective withdrawal mechanism. Thus, we seek a solution which minimizes the deviation from the target temperatures without modifying the release pattern. Recall from Chapter 4 that the simulation model was calibrated using data from 1994 (Figure 4.4). Flaming Gorge Dam was at that time being used to generate peaking hydropower during the late afternoon and evening hours. The release temperature during this period was 12°C. Using these original data as inputs, as well

as the observed atmospheric data from that period, daily maximum stream temperature values were 16.47 ^{o}C at 46 km and 18.77 ^{o}C at 105 km. This corresponds to an objective function value (Eq. 6.7) of 10.71. Using the optimization scheme for release temperature described above, with the objective function described by Eq. 6.7, an optimal release temperature of 15 ^{o}C is identified. Simulation of the period 22-24 August 1994 using a release temperature of 15 ^{o}C results in an objective function value of 5.01 with stream temperatures of 18.77 ^{o}C and 20.63 ^{o}C at 46 km and 105 km respectively. Figure 6.15 shows the daily maximum temperatures along the study reach for the

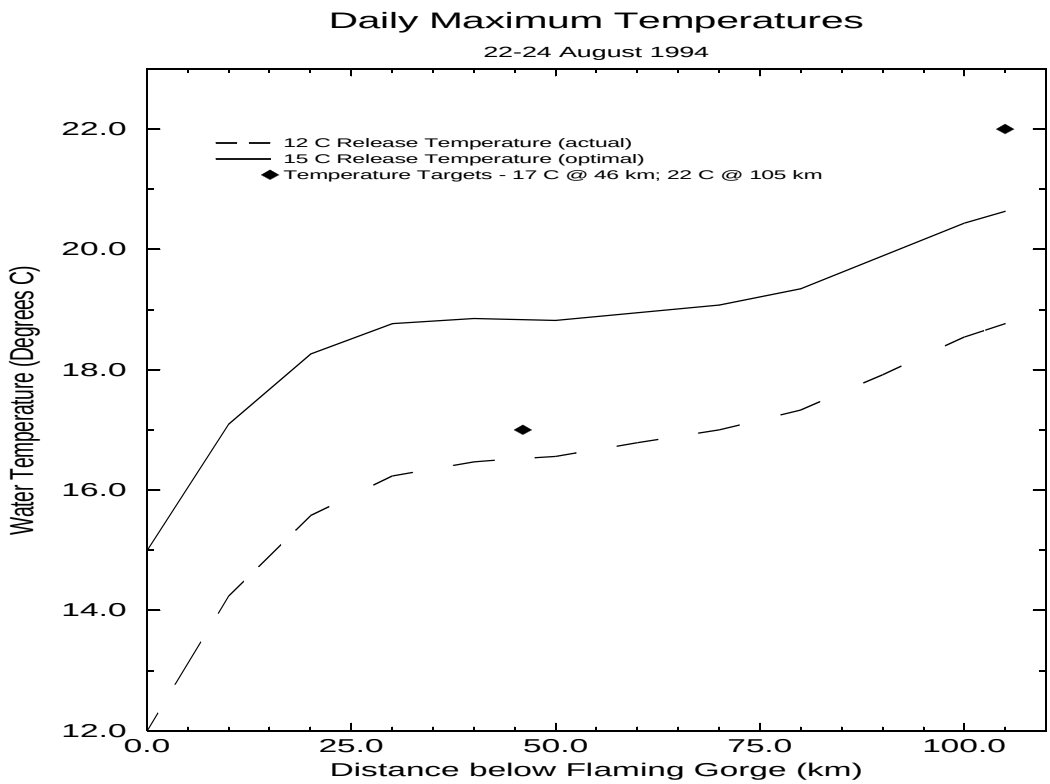

Figure 6.15: Daily maximum stream temperatures below Flaming Gorge Dam, using actual and optimal release temperatures with data from 22-24 August, 1994.

period 22-24 August, 1994 using the actual (12 ^{o}C) and optimal (15 ^{o}C) release temperatures. Notice that the temperature objective at 46 km was being achieved with the actual release temperature. The optimal release temperature results in both objectives

being violated, but because the objective function is quadratic, the total penalty is minimized.

6.6 Optimization using both Unsteady Releases and Selective Withdrawal

In the previous sections we saw that diurnally varying flows and release temperature modification can lead to optimal solutions to the temperature control problem. To this point, we have assumed either a fixed release while optimizing release temperature, or a fixed release temperature while optimizing release. We now look at what benefits may be gained by modifying both release rate and temperature to meet the previously defined objectives. To demonstrate, we begin by looking at stream temperatures resulting from a steady flow of 56.6 cms, with a release temperature of 12 ^{o}C, and average meteorological conditions for mid-July. We know from previous sections that these inputs will not result in optimal stream temperature conditions. The flow and release temperature values correspond to the expected release during a moderately wet hydrologic year, and the typical historical summer release temperature. The objective function for this problem is:

$$min\ f(U) = \frac{1}{Exp(T_{opt}^{46} - T_{max}^{46})} + \frac{1}{Exp(T_{max}^{105} - T_{opt}^{105})} + \beta \sum_{c=1}^{m} (U^{c} - U_{opt}) \qquad \textbf{(6.8)}$$

with $\beta = 0.005$, $U_{opt} = 56.6$ cms. Temperatures at the target locations and objective function values for the example are shown in Table 6.1. From the previous section, we saw that the optimal release temperature at a steady flow of 56.6 cms was 14.2 ^{o}C. Use of the optimal release temperature with a steady 56.6 cms release improves the objective function value by about 8% (column 2). If we use the original 12 ^{o}C release temperature and allow the flows to vary, an improvement of 38% is realized (column 3). Finally, using the optimal release temperature for the steady flow solution, and then

generating a set of optimal controls, a reduction of over 70% is realized (column 4). Notice, however, that the final two solutions from Table 6.1 result in fairly significant flow fluctuations (though certainly no larger than seen during peaking hydropower operations), as shown by the values in the final row. They also result in slight violations (< 10%) of the 56.6 cms average flow target.

Table 6.1: Comparison of solutions for combined flow and temperature control.
*These values for *f*(T) reflect temperature deviations plus deviations from the target flow of 56.6 cms.

	Steady Flow 12 ^{o}C	**Steady Flow 14.2 ^{o}C**	**6 hr Controls 12 ^{o}C**	**6 hr Controls 14.2 ^{o}C**
Temperature @ 46 km	16.6 **^{o}C**	18.2 **^{o}C**	16.5 **^{o}C**	17.8 ^{o}C
Temperature @ 105 km	19.3 **^{o}C**	20.6 **^{o}C**	19.8 **^{o}C**	21.3 ^{o}C
f(T)	15.55	14.34	9.63 10.81*	4.54 5.00*
Flow Fluctuation	none	none	~37 cms	~37 cms

6.7 INFLUENCE OF DIFFERENT CONTROL INTERVALS ON OPTIMAL SOLUTIONS

To this point, we have used control intervals of 6 hours to develop optimal release schedules. Four flow modifications per day is not uncommon for reservoirs that are being operated for generation of electricity. We might reasonably ask if it is possible to conserve water - or obtain a better solution - by using a shorter control interval. We return to the problem of meeting the downstream temperature objectives discussed in Section 6.4. We now employ eight 3-hour control intervals to developing the optimal solution. The resulting optimal control is shown in Figure 6.16. Maximum

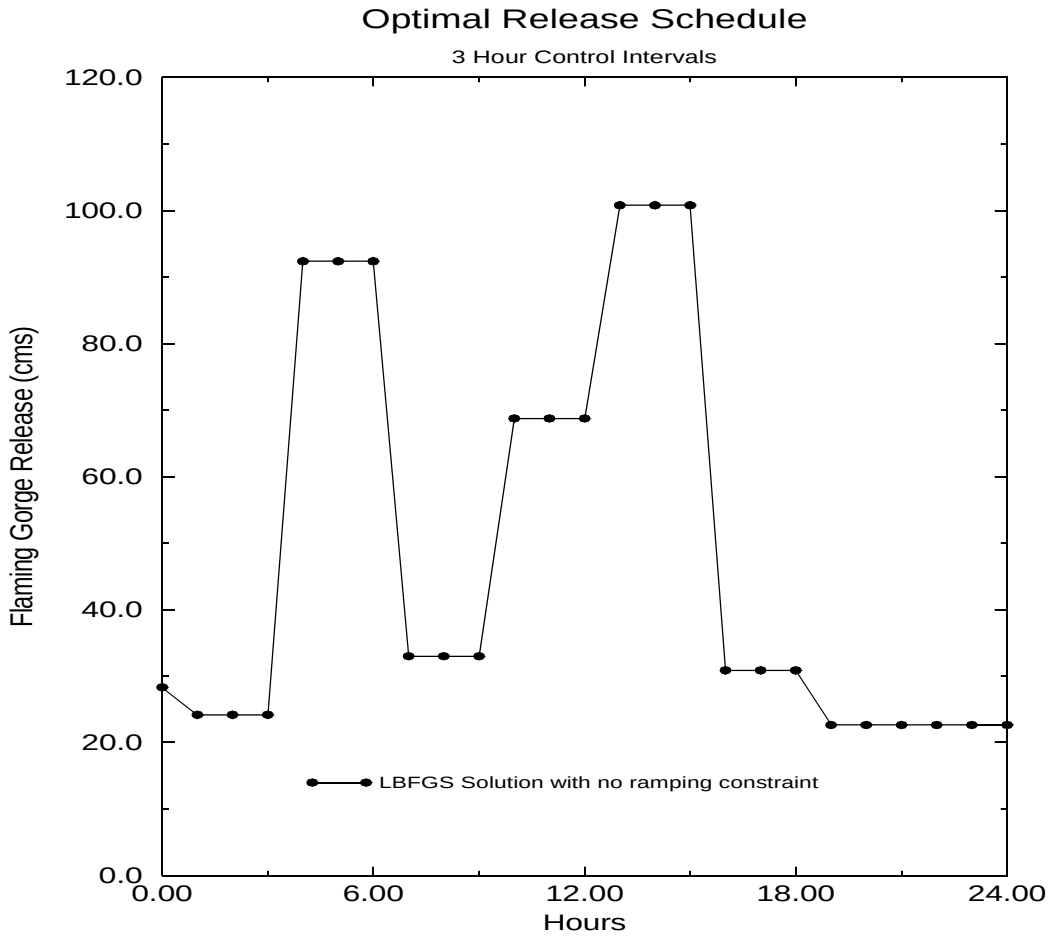

Figure 6.16: Optimal control sequence using 3-hour control intervals.

temperature values at the target locations for this solution are 17.0 ^{o}C at 46 km and 22.7 ^{o}C at 105 km. Although both target temperature values have been achieved, the optimization model has generated a release pattern that is not desirable. Generally, reservoir operators will try to minimize both the number and magnitude of fluctuations in releases over the course of a day. We can encourage the optimal controller to generate a more “friendly” solution by adding a ramping constraint to our original objective function (Eq. 6.6):

$$min\ f(U) = \frac{1}{Exp(T_{opt}^{46} - T_{max}^{46})} + \frac{1}{Exp(T_{max}^{105} - T_{opt}^{105})} + \beta \sum_{c=1}^{m} (U^c) + \beta_2 \sum_{c=1}^{m} (U^c - U^{c-1})^2 \quad (6.9)$$

where the last term on the RHS minimizes the difference between successive control values. As with the choice of β, the user must take care when choosing β_2. If too large a value is chosen for the coefficient, the solution will tend to a steady flow without attempting to meet the temperature objectives. We are only concerned here with reducing the large fluctuations seen in Figure 6.16. A value of $\beta_2 = 0.0001$ is adequate to eliminate the fluctuations, while ensuring the temperature objective are met. Using this new objective function, the optimal controller generates the release sequence shown in Figure 6.17. The temperature values at the target locations for this solution are 17.2 ^{o}C at 46 km and 23.0 ^{o}C at 105 km. We again use the quadratic solver to check the BFGS solution. The control sequence it generates is quite similar to the BFGS solution (Figure 6.17). A comparison of three optimal solutions for this problem is shown in Table 6.2. The 3 hour solution with ramping constraints slightly exceeds the 46 km temperature objective. Use of the 3 hour control interval with ramping constraints results in a reduction of the daily average flow of about 2.1 cms, or roughly 4%.

Table 6.2: Comparison of solutions for 3 and 6 hour control intervals.

Variable	**6 hour**	**3 hour**	**3 hour + ramp constraint**
Average Flow	48.1 cms	49.6 cms	45.9 cms
Temperature @ 46 km (max)	17.0 ^{o}C	17.0 ^{o}C	17.2 ^{o}C
Temperature @ 105 km (max)	22.9 ^{o}C	22.7 ^{o}C	23.0 ^{o}C

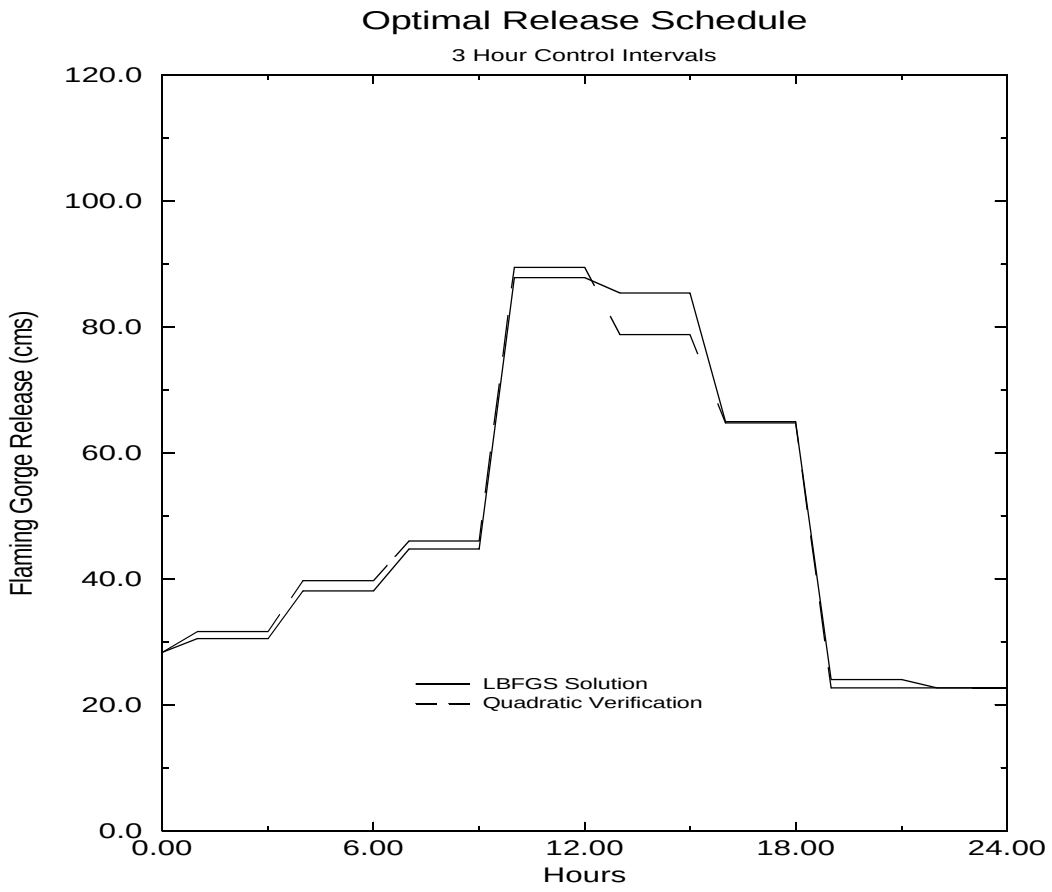

Figure 6.17: Optimal control sequence using 3-hour control intervals plus a ramping objective to minimize fluctuations.

6.8 STRATEGIES FOR MEETING TEMPERATURE OBJECTIVES

The examples demonstrate the ability of diurnally varying flows to meet multiple temperature objectives on the Green River. When possible, the use of the selective withdrawal mechanism produces more efficient temperature modifications downstream, as compared to the use of transient flows, with their potentially large fluctuations. Clearly, though, selective withdrawal cannot usually be used exclusively to meet the temperature targets.

The inclusion of additional objectives, such as targets for average releases,

complicate the optimization process. The value of slightly violating the temperature targets must be weighed against violation of average flow targets and ramping constraints. There is a significant long term implication of this problem. Average flow targets typically reflect average flows needed to meet monthly or seasonal release volume objectives. Thus, short-term violations of these targets to meet stream temperature objectives should not pose serious management problems. Long periods of extreme atmospheric conditions could however result in violation of the long-term release targets. Periods of “favorable” atmospheric conditions can be utilized to balance periods when either lower or higher flows than the target are required.

CHAPTER 7

IMPACTS OF UNCERTAIN ATMOSPHERIC FORCINGS AND STREAM DEPTH ON TEMPERATURE PREDICTION

7.1 INTRODUCTION

Uncertainty manifests itself in multiple ways in complex models of hydrologic systems. Errors in data observations, in model parameters, and as a result of discretization of continuous systems all point to the need to quantify the amount of uncertainty carried through the modeling process. It is not enough to understand the magnitude of the uncertainties. We need to be able to predict how uncertainties propagate through the system, and how sensitive the system is to errors in model parameters and inputs.

In this work, we are particularly interested in identifying potential sources of error involved in predicting stream temperatures. Previous works by Webb and Walling (1993), Sinokrot and Stefan (1994) and Evans et. al. (1998), evaluate the impact of atmospheric and stream-bed heat flux on water temperatures. Sinokrot and Stefan conclude that air temperature and solar radiation have nearly an order of magnitude greater influence on water temperatures when compared to relative humidity, cloud cover, and wind speed. Their sensitivity analysis also confirmed earlier results (Sinokrot and Stefan, 1993) showing that streambed heat flux is particularly important in predicting diurnal water temperatures in shallow streams. Evans et al. (1998) note that on average, approximately 15% of the diurnal energy flux occurred at the streambed.

They further note that the streambed acts on average as a heat sink during the summer, and as a heat source during winter.

In this chapter we develop the equations for propagating variance and covariances of temperature errors. The method employed is similar to those developed previously for water quality modeling by Hoybye (1996) and for atmospheric forcings for water temperature by Sinokrot and Stefan (1994). The methods are applied to the Green River case study previously developed. The goal is to identify sources of error and develop a quantitative measure of how reliable our stream temperature predictions are. The results can provide a basis for relaxation or tightening of the objective functions, and may indicate specific improvements in data observation to improve stream temperature forecasts.

Throughout this work, we have used ground-based data observations to calibrate and test the temperature model. In an operational setting, we need to specify reservoir controls which reflect predicted stream temperatures one or two days into the future based on forecasts of future atmospheric conditions. In most cases, forecast data will only be available at a regional scale. As a result, we would expect to observe errors between these forecasts and locally observed ground data. If we assume that the ground data - to which the models have been calibrated - represent the “true” atmospheric conditions at the study site, then we can develop statistical relationships between the forecast data and the ground “truth”. These statistics form the basis for the variance and covariance forcings which are used to drive the uncertainty equations developed in this chapter. For meteorological forecasts, we utilize forecast data generated by the National Weather Service using their Eta mesoscale climate model. The ground-based data is taken from the Brown’s Park National Wildlife Refuge meteorological station. The results quantify the uncertainty in stream temperature predictions resulting from the use of regional meteorological forecasts.

7.2 UNCERTAINTY PROPAGATION

When modeling complex natural systems, it is reasonable to expect that there will be errors in parameter values, forcing functions, and observed data. Development of uncertainty equations for every model parameter and input is quite complex and, based on the results of the works outlined above, unnecessary. We develop uncertainty propagation equations for water temperature using stream depth, air temperatures, and solar radiation as uncertain inputs. Sinokrot and Stefan (1994) showed that solar radiation and air temperature were much more important than other atmospheric variables when predicting stream temperature.

Mathematically, the variable uncertainty, or errors, can be represented by defining the "true" value of model states or parameters as the sum of the model estimate for the variable plus some unknown error (Gelb, 1974). For example, taking the stream temperature T_w, we have:

$$T_w = \hat{T}_w + \delta T_w \tag{7.1}$$

where the left hand side (LHS) is the true (but unknown) value, and the right hand side (RHS) contains the model estimate (^) and the unknown model error (δ). Because we can never actually know the value of the errors in the model, we rely on estimates of their statistical properties to compute variance and covariance values. Predicted and unknown error values for stream depth, air temperature, and solar radiation are similarly represented:

$$\begin{aligned} y &= \hat{y} + \delta y \\ T_a &= \hat{T}_a + \delta T_a \\ R &= \hat{R} + \delta R \end{aligned} \tag{7.2}$$

where y is depth, T_a air temperature and R solar radiation. Replacing each of these variables in the governing equation for heat transport (Eq. 2.7) with their uncertain

equivalent, and retaining only the error terms, yields:

$$\frac{\partial}{\partial t}(\delta T_w) + v\frac{\partial}{\partial x}(\delta T_w) = \frac{\partial}{\partial T_w}\left(\frac{\Delta\hat{H}}{\rho C_p \hat{y}}\right)\delta T_w + \frac{\partial}{\partial T_a}\left(\frac{\Delta\hat{H}}{\rho C_p \hat{y}}\right)\delta T_a + \frac{\partial}{\partial y}\left(\frac{\Delta\hat{H}}{\rho C_p \hat{y}}\right)\delta y + \frac{\partial}{\partial R}\left(\frac{\Delta\hat{H}}{\rho C_p \hat{y}}\right)\delta R \tag{7.3}$$

Notice that the atmospheric forcing function has been linearized about each of the uncertain variables. To develop the variance propagation equation for water temperature, we multiply Eq. 7.3 by δT_w, which gives

$$\frac{1}{2}\frac{\partial}{\partial t}(\sigma^2_{T_w}) + \frac{v}{2}\frac{\partial}{\partial x}(\sigma^2_{T_w}) = \frac{\partial}{\partial T_w}\left(\frac{\Delta\hat{H}}{\rho C_p \hat{y}}\right)\sigma^2_{T_w} + \frac{\partial}{\partial T_a}\left(\frac{\Delta\hat{H}}{\rho C_p \hat{y}}\right)\sigma_{T_w T_a} + \frac{\partial}{\partial y}\left(\frac{\Delta\hat{H}}{\rho C_p \hat{y}}\right)\sigma_{T_w y} + \frac{\partial}{\partial R}\left(\frac{\Delta\hat{H}}{\rho C_p \hat{y}}\right)\sigma_{T_w R} \tag{7.4}$$

where, for example,

$$\sigma_{T_w T_a} = E\{\delta T_w \delta T_a\} \tag{7.5}$$

and *E{}* is the expectation operator. Eq. 7.4 is the governing equation for the variance of stream temperature. From the RHS of this equation, it is clear that we need to develop governing equations for the error covariances $\sigma_{T_w T_a}$, $\sigma_{T_w y}$, and $\sigma_{T_w R}$. Applying the procedure used to develop Eq. 7.4, we obtain similar equations for the covariances:

$$\frac{\partial}{\partial t}(\sigma_{T_w T_a}) - \delta T_w \frac{\partial}{\partial t}(\delta T_a) + v\frac{\partial}{\partial x}(\sigma_{T_w T_a}) - v\delta T_w \frac{\partial}{\partial x}(\delta T_a) \;=$$

$$\frac{\partial}{\partial T_w}\left(\frac{\Delta\hat{H}}{\rho C_p \hat{y}}\right)\sigma_{T_w T_a} + \frac{\partial}{\partial T_a}\left(\frac{\Delta\hat{H}}{\rho C_p \hat{y}}\right)\sigma^2_{T_a} + \frac{\partial}{\partial y}\left(\frac{\Delta\hat{H}}{\rho C_p \hat{y}}\right)\sigma_{T_a y} + \frac{\partial}{\partial R}\left(\frac{\Delta\hat{H}}{\rho C_p \hat{y}}\right)\sigma_{T_a R}$$

$$\frac{\partial}{\partial t}(\sigma_{T_w R}) - \delta T_w \frac{\partial}{\partial t}(\delta R) + v\frac{\partial}{\partial x}(\sigma_{T_w R}) - v\delta T_w \frac{\partial}{\partial x}(\delta R) \;=$$

$$\frac{\partial}{\partial T_w}\left(\frac{\Delta\hat{H}}{\rho C_p \hat{y}}\right)\sigma_{T_w R} + \frac{\partial}{\partial T_a}\left(\frac{\Delta\hat{H}}{\rho C_p \hat{y}}\right)\sigma_{T_a R} + \frac{\partial}{\partial y}\left(\frac{\Delta\hat{H}}{\rho C_p \hat{y}}\right)\sigma_{R y} + \frac{\partial}{\partial R}\left(\frac{\Delta\hat{H}}{\rho C_p \hat{y}}\right)\sigma^2_{R} \qquad \textbf{(7.6)}$$

$$\frac{\partial}{\partial t}(\sigma_{T_w y}) - \delta T_w \frac{\partial}{\partial t}(\delta y) + v\frac{\partial}{\partial x}(\sigma_{T_w y}) - v\delta T_w \frac{\partial}{\partial x}(\delta y) \;=$$

$$\frac{\partial}{\partial T_w}\left(\frac{\Delta\hat{H}}{\rho C_p \hat{y}}\right)\sigma_{T_w y} + \frac{\partial}{\partial T_a}\left(\frac{\Delta\hat{H}}{\rho C_p \hat{y}}\right)\sigma_{T_a y} + \frac{\partial}{\partial y}\left(\frac{\Delta\hat{H}}{\rho C_p \hat{y}}\right)\sigma^2_{y} + \frac{\partial}{\partial R}\left(\frac{\Delta\hat{H}}{\rho C_p \hat{y}}\right)\sigma_{R y}$$

The second and fourth terms on the LHS of Eq. 7.6 represent the partial derivatives of the variable errors with respect to time and space (resulting from differentiation by parts). For long-term estimates of air temperatures, solar radiation, and stream depth, these values may be non-zero. However, because we are comparing predicted and observed data which is available once every 12 hours, the short-term errors between them can be assumed to be negligible in both time and space (i.e., $\delta T_w \frac{\partial}{\partial t}(\delta T_a) \approx 0$, $\delta T_w \frac{\partial}{\partial x}(\delta T_a) \approx 0$, etc.). This is further justified by examining the regression plots of Figure 7.2. The two regressions (one for 00:00 hours, the other for 12:00 hours) shown are quite similar, and we can reasonably state that there will not be significant changes in the magnitude of the errors between the forecast periods (i.e., if the Eta model is overpredicting air temperatures during one forecast period, it can reasonably be expected to overpredict in the following period). These simplifications result in:

$$
\begin{aligned}
&\frac{\partial}{\partial t}(\sigma_{T_w T_a}) + v\frac{\partial}{\partial x}(\sigma_{T_w T_a}) = \\
&\qquad \frac{\partial}{\partial T_w}\left(\frac{\Delta\hat{H}}{\rho C_p \hat{y}}\right)\sigma_{T_w T_a} + \frac{\partial}{\partial T_a}\left(\frac{\Delta\hat{H}}{\rho C_p \hat{y}}\right)\sigma^2_{T_a} + \frac{\partial}{\partial y}\left(\frac{\Delta\hat{H}}{\rho C_p \hat{y}}\right)\sigma_{T_a y} + \frac{\partial}{\partial R}\left(\frac{\Delta\hat{H}}{\rho C_p \hat{y}}\right)\sigma_{T_a R} \\
&\frac{\partial}{\partial t}(\sigma_{T_w R}) + v\frac{\partial}{\partial x}(\sigma_{T_w R}) = \\
&\qquad \frac{\partial}{\partial T_w}\left(\frac{\Delta\hat{H}}{\rho C_p \hat{y}}\right)\sigma_{T_w R} + \frac{\partial}{\partial T_a}\left(\frac{\Delta\hat{H}}{\rho C_p \hat{y}}\right)\sigma_{T_a R} + \frac{\partial}{\partial y}\left(\frac{\Delta\hat{H}}{\rho C_p \hat{y}}\right)\sigma_{R y} + \frac{\partial}{\partial R}\left(\frac{\Delta\hat{H}}{\rho C_p \hat{y}}\right)\sigma^2_{R} \\
&\frac{\partial}{\partial t}(\sigma_{T_w y}) + v\frac{\partial}{\partial x}(\sigma_{T_w y}) = \\
&\qquad \frac{\partial}{\partial T_w}\left(\frac{\Delta\hat{H}}{\rho C_p \hat{y}}\right)\sigma_{T_w y} + \frac{\partial}{\partial T_a}\left(\frac{\Delta\hat{H}}{\rho C_p \hat{y}}\right)\sigma_{T_a y} + \frac{\partial}{\partial y}\left(\frac{\Delta\hat{H}}{\rho C_p \hat{y}}\right)\sigma^2_{y} + \frac{\partial}{\partial R}\left(\frac{\Delta\hat{H}}{\rho C_p \hat{y}}\right)\sigma_{R y}
\end{aligned}
\tag{7.7}
$$

These four equations (Eq. 7.4 and Eq. 7.7) are modeled using the same QUICKEST method used to propagate the mean values for flow and temperature. In addition to the four governing equations, there are six additional error variance and covariance values to define. The error variances for *y*, T_a and *R*, (σ^2_y, $\sigma^2_{T_a}$, and σ^2_R) and the error covariance $\sigma_{T_a R}$ are user defined values (model inputs). The error covariances $\sigma_{T_a y}$ and σ_{Ry} are assumed to be zero, as there is clearly no correlation between errors in air temperature and stream depth or solar radiation and stream depth. Development of values used for the independent uncertain forcing values is discussed in the following section.

7.3 ESTIMATION OF PARAMETER ERRORS

Having developed simulation and optimization methods which allow us to predict and control water temperatures in regulated rivers, we want to now quantify the degree to which errors in forecast data and stream channel characteristics could impact these results. The data used to calibrate and test the simulation and optimization models was based on observations made from various sites within the Green River basin. In an operational setting, these models would rely on forecasts of atmospheric conditions

as inputs. Depending on flow, forecasts of up to two days into the future would be needed to predict stream temperatures at the Yampa River confluence.

We obtained 4 months of forecast data generated during the summer of 1998 by the Hydrometeorological Prediction Center of the National Weather Service, using their Eta mesoscale climate model. The model predicts conditions up to 36 hours into the future, on 6 hour intervals. Data are generated from the model on 1600 km^2 grid cells. Three of these cells cover the Green River study site used in this work. Model forecasts are published daily at 00:00 and 12:00 hours Greenwich Mean time. Surface air temperature and incident solar radiation data were extracted from these historical forecasts. The Eta model surface air temperature data were compared to the observed air temperature data taken over the same period at the Brown's Park National Wildlife Refuge meteorology station. Eta model predictions of incident solar radiation were compared to the predicted solar radiation values developed from the physically-based algorithm within our heat flux model. Regression analysis of these data sets allowed us to develop a relationship between the Eta model forecasts, and the data used to calibrate the model. The (co)variance estimates are thus really an estimate of the expected differences between Eta model forecasts and our (assumed) true data. Thus we are evaluating a situation where the Eta model forecasts are used in an operational setting to predict stream temperatures, with the uncertainty model providing confidence bounds on these predictions. Standard deviation of the errors in the air temperature and solar radiation values were derived using a least-squares regression. Results of the regressions for solar radiation are shown in Figure 7.1, and for daily maximum and minimum air temperatures in Figure 7.2.

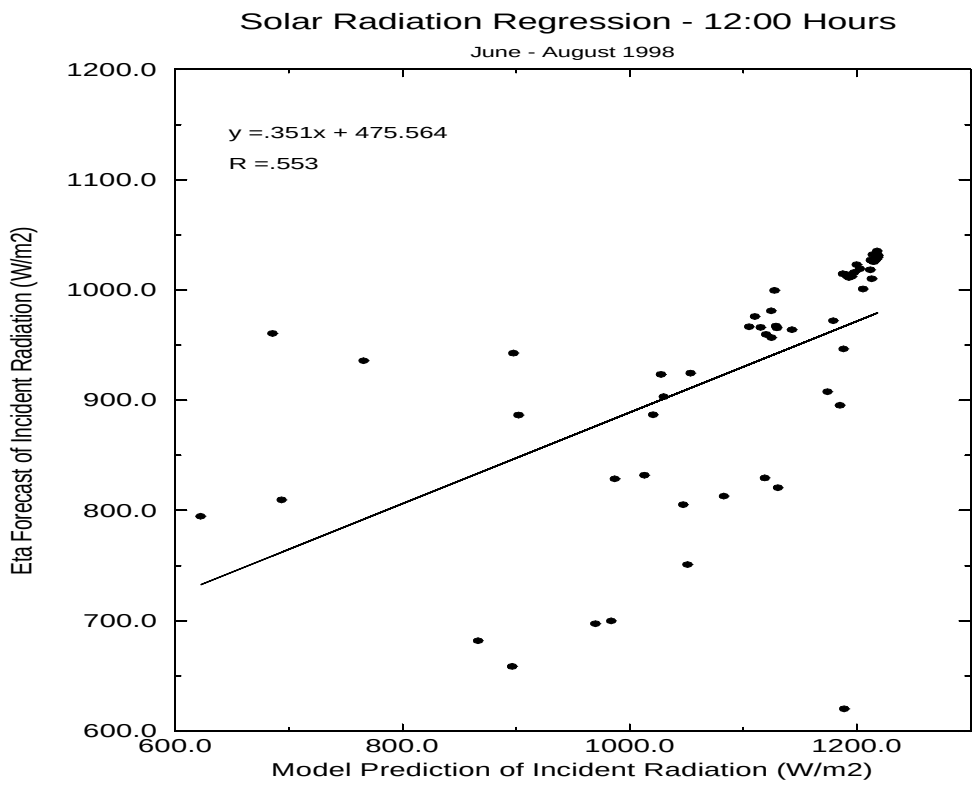

Figure 7.1: Regression of Eta model forecast incident solar radiation onto values predicted by the Green River model. Data are from the period June - August 1998.

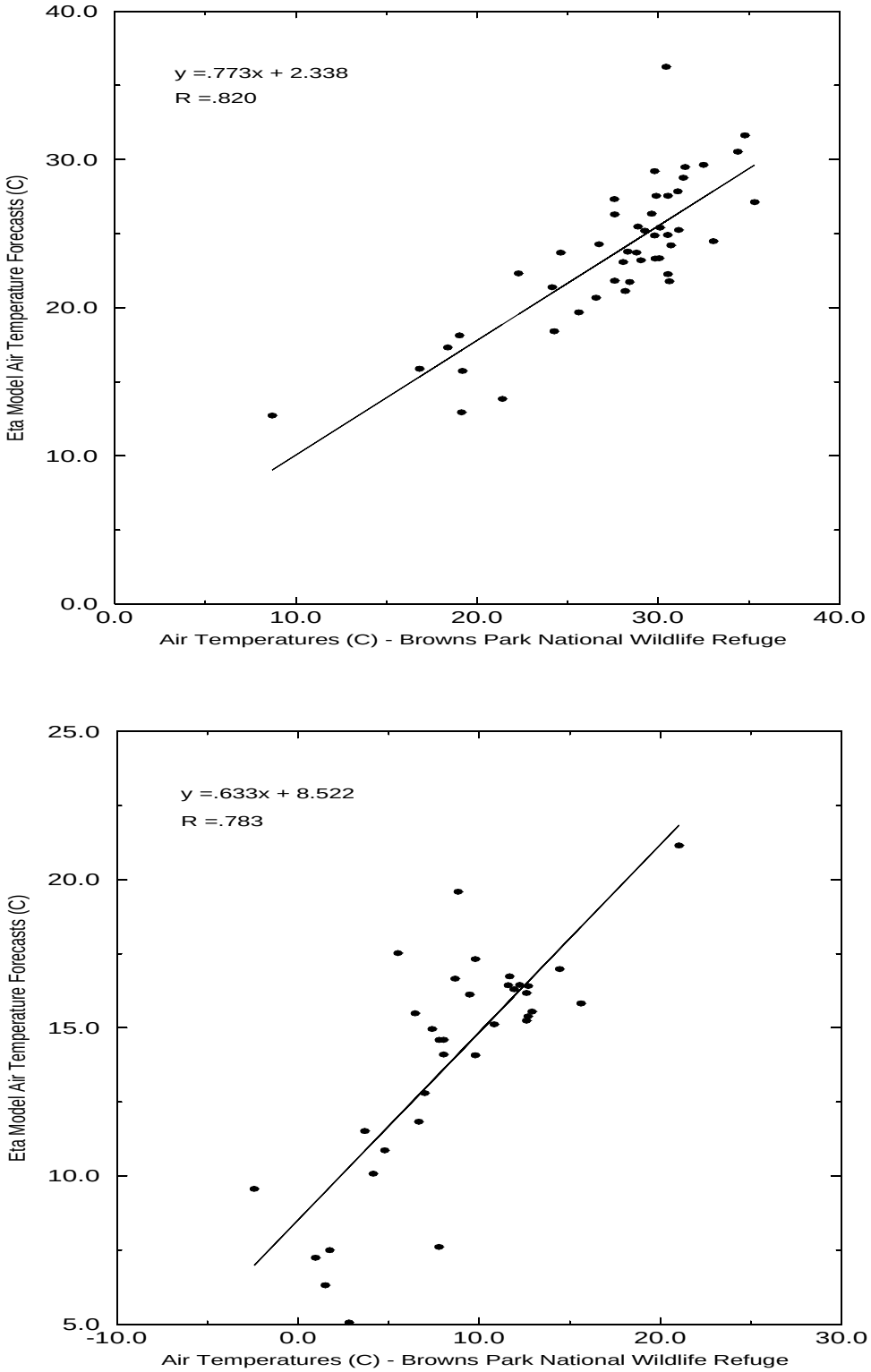

Figure 7.2: Regression of Eta model forecast air temperatures with observed data from Browns Park National Wildlife Refuge meteorological station. Top graph is 12:00 hours MST, bottom is 00:00 hours MST. June - August 1998.

The uncertainty model also requires as input a value for the covariance of the errors between air temperature and solar radiation. Using errors in the predicted (Eta) versus observed (model and ground observations) values for solar radiation and air temperatures, we generated Figure 7.3. The correlation coefficient from these data is 0.147. The value of the covariance between errors in air temperature and solar radiation in general is given by $\sigma_{T_aR}\rho_{T_aR}$ where ρ_{T_aR} is the cross-correlation coefficient. In the case where the errors are perfectly positively correlated, the correlation coefficient is one (1.0) and the covariance of the errors is simply the product of their standard deviations. Using a correlation coefficient of 1 yields a “worst-case” output. The value derived above (0.147), and the worst-case value of 1.0 are compared in the results. Data from the above regressions were used to compute standard deviation values (Table 7.1), which in turn are used to generate variance values for the uncertainty computations. It is assumed that the variance values do not change over time.

Values for the variance of stream depth were estimated based on information previously obtained about the channel geometry. For the range of flows considered here (22.6 - 125 cms), the change in river depth corresponding to a 20% increase in flow is between 10-12%. Depth variations were assumed to be uncorrelated with downstream distance and time. Based on this analysis, a value of 10% of the mean depth was used for the standard deviation of the depth error term.

Table 7.1: Modeled standard deviations of independent variables as a percentage of the mean value.

Solar Radiation	Air Temperature	Stream Depth
13.4%	15.4%	10%

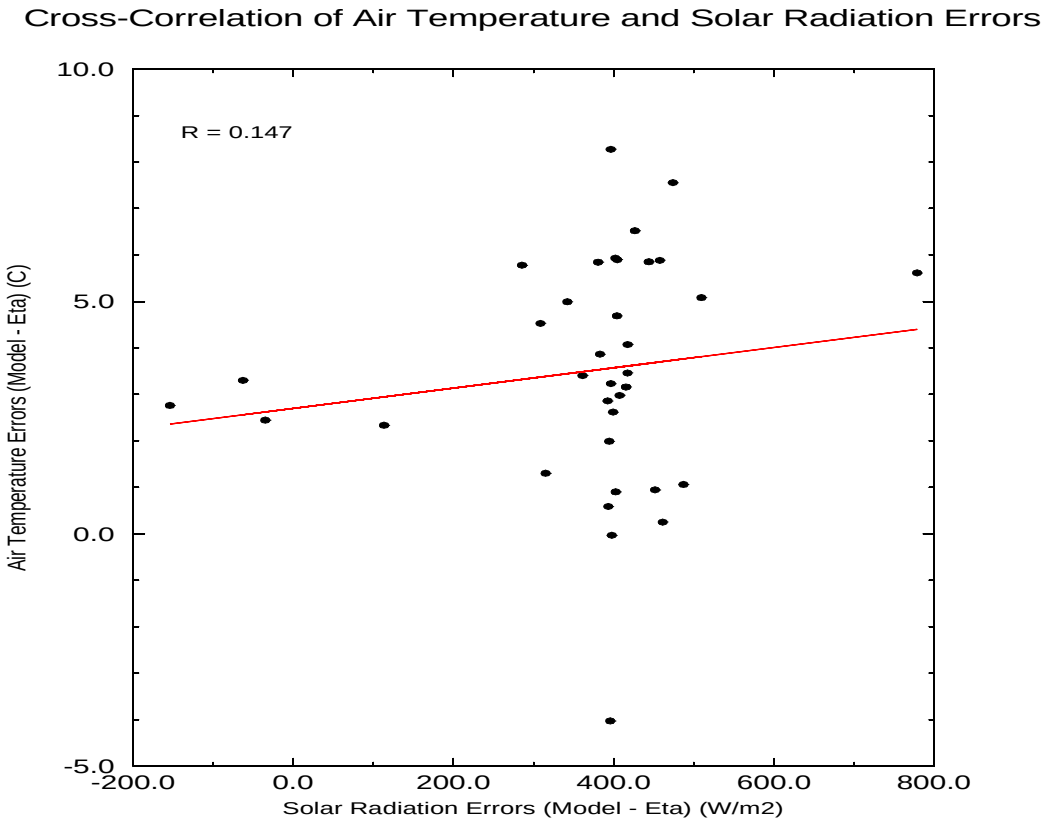

Figure 7.3: Correlation between Air Temperature and Solar Radiation errors. The least squares regression line is shown.

7.4 IMPACTS OF UNCERTAINTY ON STREAM TEMPERATURE PREDICTION

Simulations of various steady and unsteady flow scenarios were run with the previously derived error values as inputs. The impacts of the uncertain variables are examined both individually and jointly. In general, lower flows will result in greater uncertainty when predicting stream temperatures. There are two reasons for this. First, longer exposure to atmospheric conditions, resulting from slower stream velocity allows more time for errors to accumulate. Second, a smaller total heat capacity due to decreased flow depth magnifies the effects of errors in the heating terms. Also, the magnitude of the uncertainty increases with distance below Flaming Gorge, because the release temperature is precisely known (i.e., zero uncertainty at the release point). Figure 7.4 shows the maximum standard deviation values with distance below Flaming Gorge Dam, for three different steady flow values. Notice that the increase in error

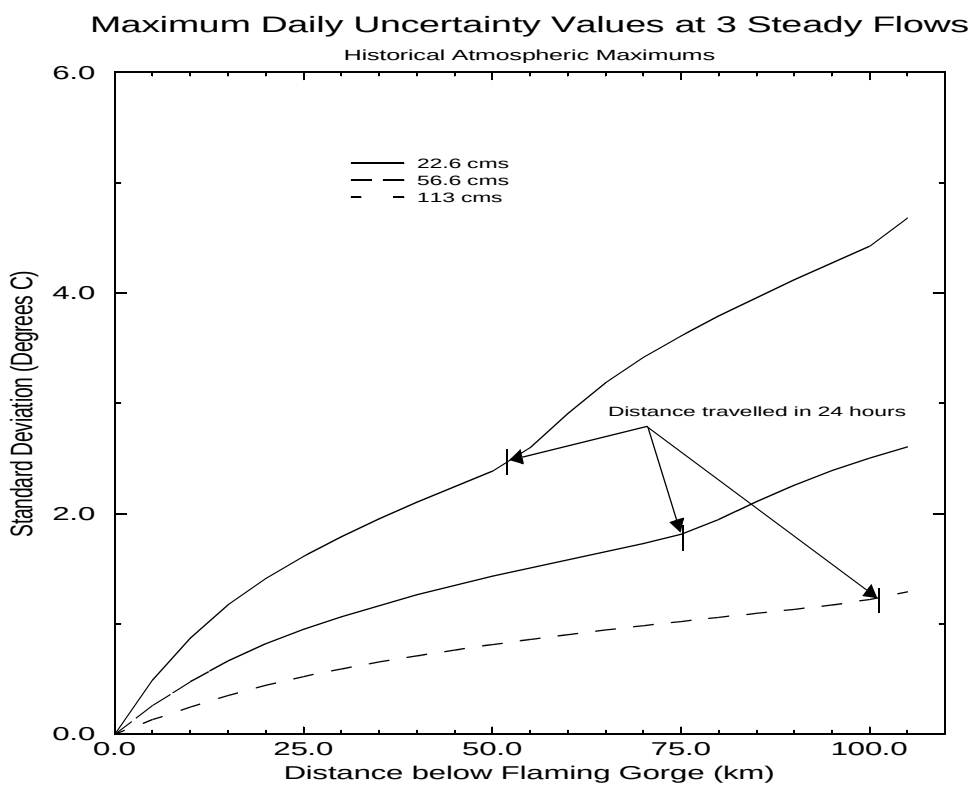

Figure 7.4: Maximum daily standard deviations below Flaming Gorge Dam.

with distance is not linear. Also notice that at a distance equal to 24 hour travel time for each flow, there is a slight reduction in the rate of error accumulation. This pattern of reduced variations at a distance equal to 24 hours travel time was noted by Pohlen and Kinsel (1997) in their examination of diurnal changes in stream temperatures. Figure 7.5. is useful in explaining this pattern. It shows the standard deviations of

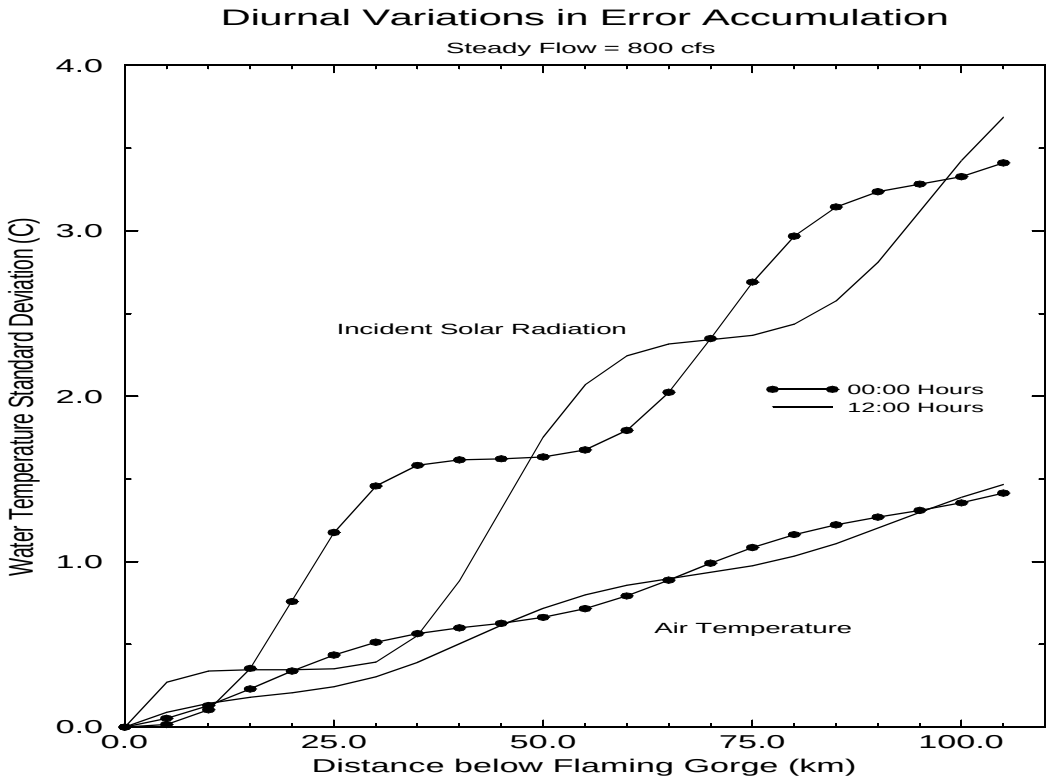

Figure 7.5: Accumulation of errors in stream temperature prediction resulting from uncertain solar radiation and air temperature data.

stream temperatures with distance below Flaming Gorge at two different times, resulting from errors in solar radiation and air temperatures. Both solar radiation and air temperature terms have a diurnally varying character, although that of the solar radiation term is quite pronounced. There is clearly no accumulation of errors due to solar radiation during the night (water released during the period of no solar influx shows no increase in standard deviation of temperature with distance).

Figure 7.6 shows the relative influence of the different uncertain parameters on the magnitude of the standard deviation at the two objective locations. The influence of errors in the solar radiation term can be seen to contribute about twice as much as the errors in the air temperature term. The assumed error of 10% in the depth term has nearly as much influence as the solar radiation error. As mentioned before, a 10% standard deviation in depth is equivalent to about a 20% change in the flow. This is a significant error, and again I feel it represents a worst-case estimate of the uncertainty. Figure 7.7 illustrates the relative magnitude of the computed standard deviation values to the change in stream temperatures resulting from a 20% increase in stream flow. The results indicate that the impact on stream temperature prediction of uncertainty in air temperature, solar radiation and depth is roughly equivalent to a 20% change in flow.

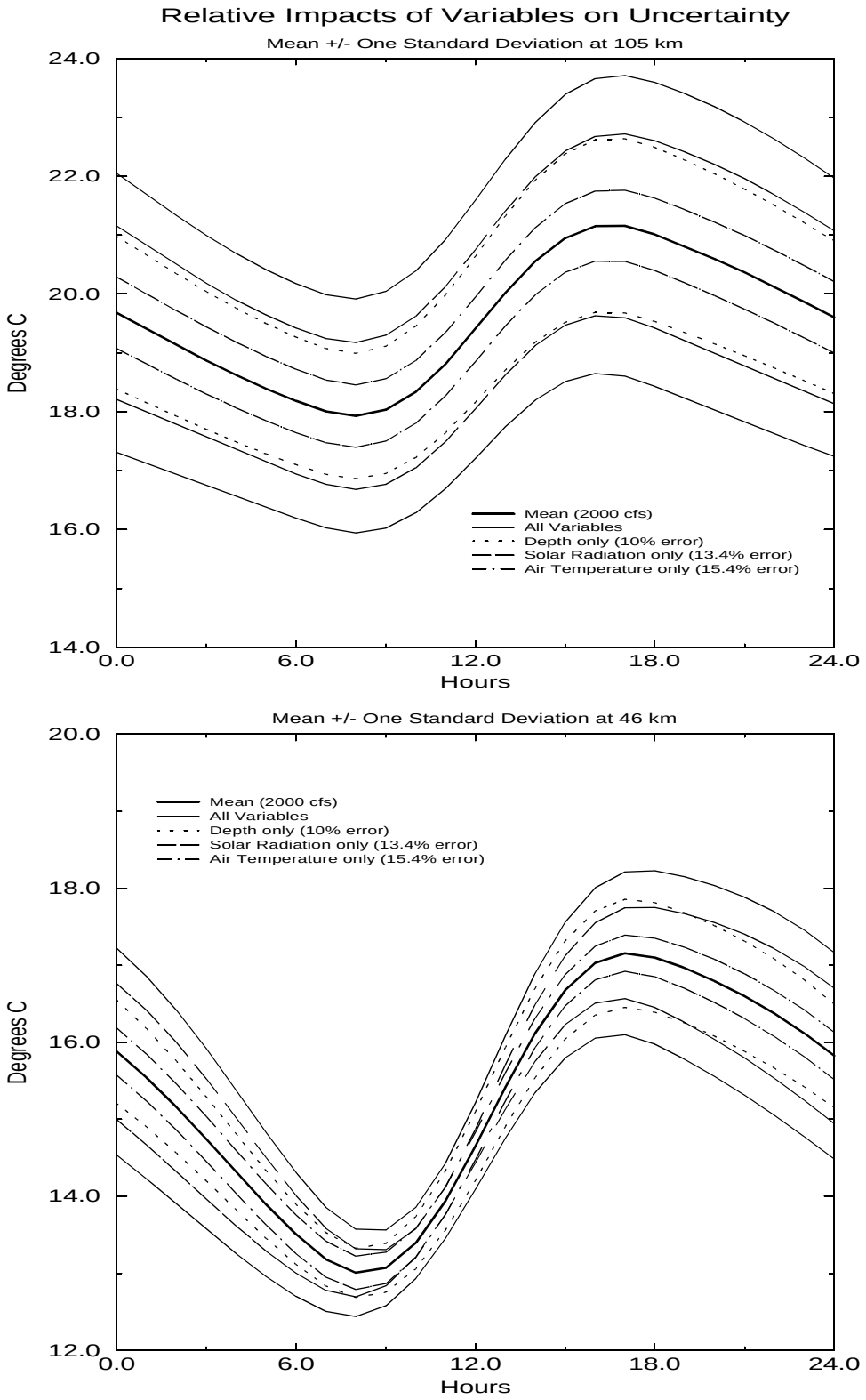

Figure 7.6: Relative Impacts of uncertain variables on standard deviations in stream temperature at 105 km (top) and 46 km (bottom) below Flaming Gorge Dam.

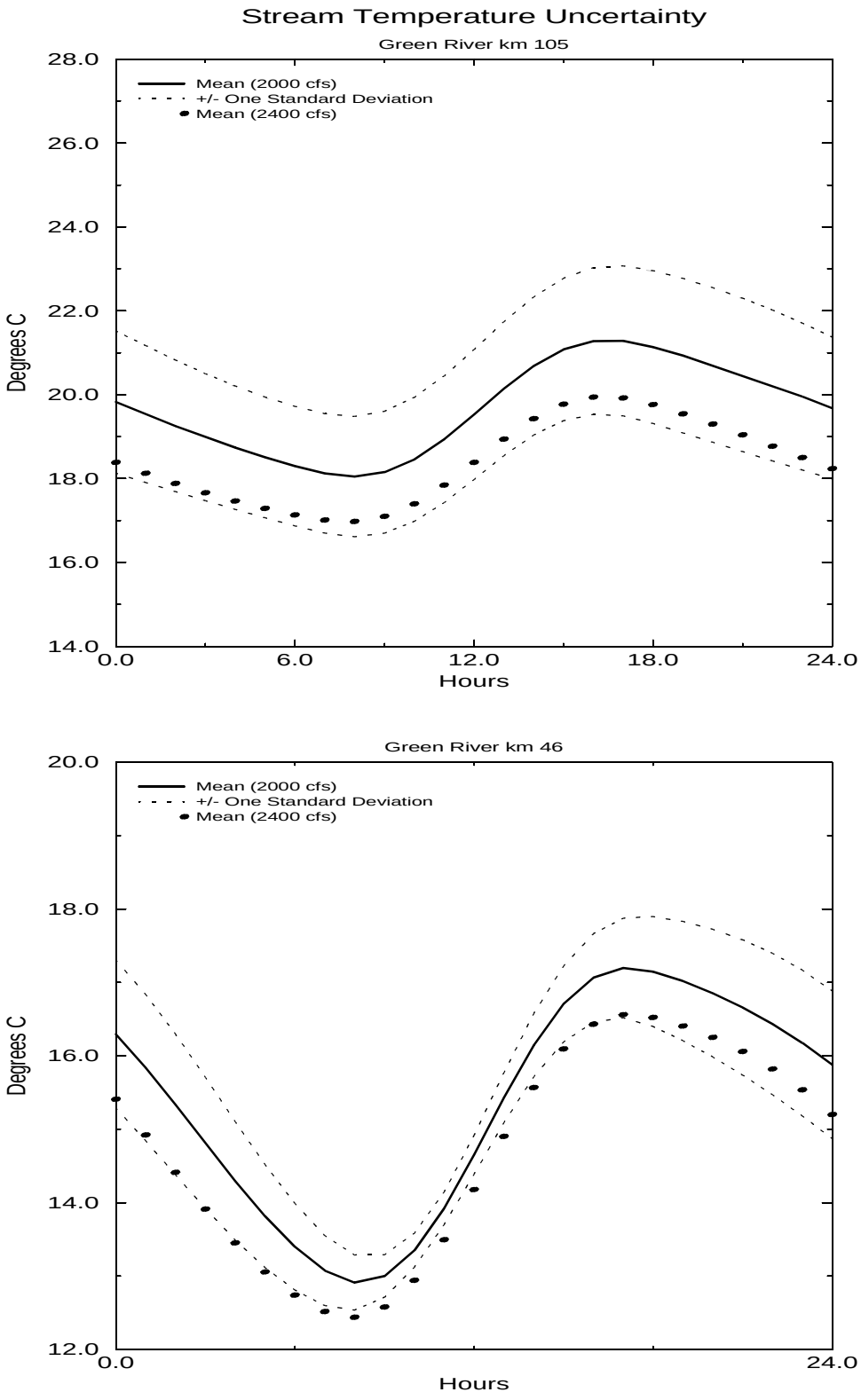

Figure 7.7: Comparison of total uncertainty (+/- one standard deviation) with the mean value resulting from a 20% increase in flow, 105 km (top) and 46 km (bottom).

Temperature Management Implications

The results of the uncertainty analysis indicate that the uncertainty in stream temperature prediction, at a value of 1 standard deviation, is roughly equivalent to a 20% change in reservoir release rate. This is well less than the magnitude of diurnal variations in flow which were shown to be necessary for temperature control in some of the examples of Chapter 6. In some cases, diurnal releases varied from 22.6 to nearly 113 cms over a 24 hour period (a roughly 100% change from the mean daily flow). More accurate predictions of atmospheric conditions, particularly in the lower part of the study reach (Lodore Canyon), could significantly reduce the variance at the confluence. Managers of Flaming Gorge Dam can use these data to refine their objective functions based on their aversion to the risk of exceeding specific target temperature values. For example, increasing the target temperature at the Yampa confluence by one standard deviation would be equivalent to asking that the optimal controller find solutions which meet the objective temperature (still 22 ^{o}C) with an ~83% probability as opposed to a 50% probability.

CHAPTER 8

SUMMARY AND CONCLUSIONS

This dissertation has examined the use of short-term (diurnal) modifications to reservoir releases for the purpose of controlling stream temperatures to meet water quality and habitat objectives. Computational studies employing the QUICKEST explicit finite-difference scheme to simulate coupled unsteady flow and heat transport were used to investigate the influence of flow rate, release temperature and atmospheric conditions on stream temperatures. The QUICKEST scheme was found to be quite robust for these types of systems; it exhibited the accuracy of more time-consuming approaches such as the finite element ELLAM scheme, while remaining efficient computationally.

The prospects for achieving temperature targets in the Green River, Utah and the Stanislaus River, California, were examined in detail. These rivers were also contrasted with two other rivers - the Chattahoochee in Georgia and the Tualatin in Oregon. In the Stanislaus and Green Rivers, our investigations suggest that significant savings in water can be realized by using diurnal variations in flow rates to attenuate atmospheric heating during the hottest part of a day. In the case of the Green River, where low temperatures are desirable in the first 45 km downstream of the Flaming Gorge reservoir and higher temperatures are desirable at the confluence with the Yampa, 105 km downstream, our results suggest that diurnal variations in flow rate are

essential for achieving both objectives under a range of atmospheric conditions.

Management of stream temperatures downstream from reservoirs is influenced by several factors, including atmospheric conditions, structural limitations of the outlet works, and institutional and legal constraints on reservoir operations. In systems where there is some flexibility in modifying release rates, the use of short-term flow transients can lead to a savings in water over traditionally imposed minimum flow designations, which involve constant release rates. It should also be noted that diurnal variations in reservoir release rates are quite common when reservoirs are used for hydropower generation.

An optimal control approach was implemented to identify releases which would meet a set of downstream temperature objectives. Additional objective functions were defined to limit ramping rates and for overall water usage. The results indicate that the control scheme is useful in identifying release patterns to meet specific temperature objectives. We also demonstrated the optimal use of selective withdrawal mechanisms with both steady and unsteady reservoir releases. Selective withdrawal was shown to be more efficient when used in tandem with varying release rates. The results also illustrate that care should be taken when defining additional operational objectives.

Finally, we developed an uncertainty propagation model to evaluate the impacts of forecast uncertainty on our ability to predict stream temperatures. The data indicate that standard deviations in stream temperatures resulting from forecast errors are of the same magnitude as the change in stream temperatures observed with a 20% change in flow. The First Order Second Moment approach was shown to be useful for developing confidence intervals around predicted stream temperatures.

The results of this dissertation have been provided to the Flaming Gorge Operations Workgroup. They are currently revising the operating policy for Flaming Gorge, and simulation results from this work have been incorporated in the planning process.

The methods described in this work are readily transferable to other regulated rivers. As dams continue to be retrofit with selective withdrawal structures, the ability to determine the optimal combination of flow and temperature will be in the forefront of reservoir operations problems.

REFERENCES

Auslander, D.M., Y. Takahashi, and M.J. Rabins. Introducing Systems and Control. McGraw-Hill Kogakusha. Tokyo.

Barnett, S. and R.G. Cameron. 1985. Introduction to Mathematical Control Theory. Clarendon Press. Oxford.

Bazaraa, M.S., H.D. Sherali, and C.M. Shetty. 1993. Nonlinear Programming: Theory and Algorithms. John Wiley and Sons, Inc. New York. 638 pages.

Bolke, E.L and K.M. Waddell. 1975. Chemical Quality and Temperature of Water in Flaming Gorge Reservoir, Wyoming and Utah, and the Effect of the Reservoir on the Green River. U.S.G.S. Water Supply Paper 2039-A. Washington, D.C.

Bowles, D.S., D.L. Fread, and W.J. Grenney. 1977. *Coupled Dynamic Streamflow-Temperature Models*. ASCE Journal of the Hydraulics Division, 103(HY5), 515-530.

Box, G.E.P., and G.E. Jenkins. 1970. Time Series Analysis: Forecasting and Control. Holden-Day. San Francisco.

Brady, D.K., W.L. Graves, and J.C. Geyer. 1969. Surface Heat Exchange at Power Plant Cooling Lakes. Cooling Water Discharge Project Report No. 5. Edison Electric Institute Publication No. 69-901. New York.

Bradley, A.A., F.M. Holly Jr., W.K. Walker, and S.A. Wright. 1998. *Estimation of Water Temperature Exceedance Probabilities using Thermo-Hydrodynamic Modeling*. Journal of the American Water Resources Association. 34(3) 467-480.

Bras, R.L. and I. Rodriguez-Iturbe. 1985. Random Functions and Hydrology. Addison-Wesley Publishing. Reading, Mass.

Bravo, H.R., W.F. Krajewski and F.M. Holly. 1993. *State-Space Model for River Temperature Prediction*. Water Resources Research. 29(5), 1457-1466.

Brayton, S. 1998. Personal Communications. Utah Division of Wildlife Resources, Flaming Gorge Operations Workgroup.

Brocard, D.N. and D.R.F. Harleman. *One-Dimensional Temperature Predictions in Unsteady Flows*. Journal of the Hydraulics Division, ASCE. 102(HY3), 227-240.

Brown, L.C. 1987. *Uncertainty Analysis in Water Quality Modeling Using QUAL2E*. In: Systems Analysis in Water Quality Management. Pergamon Press, New York. pages 309-319.

Broyden, C.G. 1967. *Quasi-Newton Methods and their Application to Functional Minimization.* Mathematics of Computation, 21, 368-381.

Byars, M.S. 1994. Modeling Variable Flow Water Quality and Quantity in Streams. Thesis, University of Colorado, Boulder.

Byrd, R.H., P. Lu, J. Nocedal, and C. Zhu. 1995. *A Limited Memory Algorithm for Bound Constrained Optimization*. SIAM Journal on Scientific Computing, 16(5), 1190-1208.

Cappelaere, B. 1997. Accurate Diffusion Wave Routing. Journal of Hydraulic Engineering, ASCE, 123(3), 174-181.

Cardwell, H., and H. Ellis. 1993. *Stochastic Dynamic Programming for Water Quality Management*. Water Resources Research. 29(4), 803-813.

Carslaw, H.S. and J.C. Jaeger. 1959. Conduction of Heat in Solids. Clarendon Press, Oxford.

Celia, M.A., I. Herrera, E. Bouloutas, and J.S. Kindred. 1989. *A New Numerical Approach for the Advective-Diffusive Transport Equation*. Numerical Methods for Partial Differential Equation. 5, 203-226.

Chapra, S.C. 1997. Surface Water Quality Modeling. WCB/McGraw-Hill. Boston.

Chavent, G., M. Dupuy, and P. Lemonnier. 1975. *History Matching by use of Optimal Control Theory.* Society of Petroleum Engineering Journal, 15(1), 74-86.

Cluis, D.A. 1972. *Relationship Between Stream Water Temperature and Ambient Air Temperature*. Nordic Hydrology, 3(2), 65-71.

Correia, P.B., and M.G. Andrade. 1988. *Optimal Operation of a Reservoir System with Network Flow Algorithm*. In: Computational Methods in Water Resources, Vol. 2: Numerical Methods for Transport and Hydrologic Processes. Elsevier, New York. pages 399-404.

Crist, L. 1998. Personal Communications. United States Bureau of Reclamation, Upper Colorado Region, Salt Lake City, Utah.

Dreyfus, S.E. 1965. Dynamic Programming and the Calculus of Variations. Academic Press. New York.

Edinger, J.E., D.K. Brady and W.L. Graves. 1968. *The Variation of Water Temperatures due to Steam Electric Cooling Operations*. Journal of the Water Pollution Control Federation, 40(9), 1632-1639.

Edinger, J.E., D.K. Brady and J.C. Geyer. 1974. Heat Exchange and Transport in the Environment. Cooling Water Discharge Research Project Report RP-49. Electric Power Research Institute. Palo Alto, CA.

Evans, E.C., G.R. McGregor, and G.E. Petts. 1998. *River Energy Budgets with Special Reference to River Bed Processes*. Hydrological Processes, 12, 575-595.

Faye, R.E., H.E. Jobson and L.F. Land. 1979. Impact of Flow Regulation and Powerplant Effluents on the Flow and Temperature Regimes of the Chattahoochee River-Atlanta to Whitesburg, Georgia. U.S.G.S. Professional Paper 1108. Washington, D.C.

Ferrick, M.G., J. Bilmes and S.E. Long. 1983. Analysis of a Diffusion Wave Flow Routing Model with Application to Flow in Tailwaters. Cold Regions Research and Engineering Laboratory Report 83-7. U.S. Army Corps of Engineers. Washington, D.C.

Finlayson, B.A. 1992. Numerical Methods for Problems with Moving Fronts. Ravenna Park Publishing, Inc. Seattle.

Fischer, H.B., E.J. List, R.C.Y. Koh, J. Imberger, and N.H. Brooks. 1979. Mixing in Inland and Coastal Waters. Academic Press, Inc. San Diego.

Fletcher, R. 1970. *A New Approach to Variable Metric Algorithms*. Computer Journal, 13, 317-322.

Fletcher, R. 1987. Practical Methods of Optimization. John Wiley & Sons, Inc. New York.

Fontane, D.G., J.W. Labadie, and B. Loftis. 1981. *Optimal Control of Reservoir Discharge Quality through Selective Withdrawal*. Water Resources Research. 17(6), 1594-1604.

Gelb, A. (Ed.). 1974. Applied Optimal Estimation. MIT Press. Cambridge, Mass.

Georgakakos, A.P. 1984. Real-Time Control of Reservoir Systems. Ph.D. Thesis, Mas-

sachusetts Institute of Technology. Cambridge.

Georgakakos, A.P. and D.H. Marks. 1987. *A New Method for Real-Time Operation of Reservoir Systems*. Water Resources Research. 23(7), 1376-1390.

Gill, P.E., W. Murray, and M.H. Wright. 1981. Practical Optimization. Academic Press, New York.

Goldfarb, D. 1970. *A Family of Variable Metric Methods Derived by Variational Means.* Mathematics of Computation, 24, 23-26.

Hall, M.C.G., and D.G. Cacuci. 1982. *Sensitivity Analysis of a Radiative-Convective Model by the Adjoint Method*. Journal of Atmospheric Science, 39.

Harbeck, G.E., G.E. Koberg, and G.H. Hughes. 1959. The Effect of Addition of Heat on Lake Colorado City, Texas. USGS Professional Paper # 272-B. Washington, D.C.

Henderson, F.M. 1963. *Flood Waves in Prismatic Channels*. Journal of the Hydraulics Division, ASCE, 89(HY4), 39-67.

Herrera, I. 1984. Boundary Methods: An Algebraic Theory. Pitman Co. London.

Hewitt, G.F., G.L. Shires, and T.R. Bott. 1994. Process Heat Transfer. CRC Press, Boca Raton, Florida.

Hills, R.G. and R. Viskanta. 1976. *Modeling of Unsteady Temperature Distribution in Rivers with Thermal Discharges*. Water Resources Research. 12(4), 712-722.

Holly, F. M., Jr., J. C. Yang, P. Schwartz, J. Schaefer, S. H. Hsu, and R. Einhellig. 1990. CHARIMA, Numerical Simulation of Unsteady Water and Sediment Movement in Multiply Connected Networks of Mobile-Bed Channels. IIHR Report No. 343, Iowa City, Iowa.

Hoybye, J.A. 1998. *Model Error Propagation and Data Collection Design. An Application in Water Quality Modelling*. Water, Air and Soil Pollution. 103(1-4), 101-119.

Ibbitt, R.P. 1972. *Effects of Random Data Errors on the Parameter Values for a Conceptual Model.* Water Resources Research, 8(1), 70-78.

Jaworski, N.A., W.J. Weber, and R.A. Deininger. 1970. *Optimal Reservoir Releases for Water Quality Control*. Journal of the Sanitary Engineering Division, ASCE. 96(SA3), 727-742.

Jazwinski, A.H. 1970. Stochastic Processes and Filtering Theory. Academic Press.

New York.

Jobson, H.E. 1973. *The Dissipation of Excess Heat from Water Systems*. Journal of the Power Division, ASCE, 99(PO1), 89-103.

Jobson, H.E. 1977. *Bed Conduction Computation for Thermal Models*. Journal of the Hydraulics Division, ASCE, 103(HY10), 1213-1216.

Jobson, H.E. 1985. Simulating Unsteady Transport of Nitrogen, Biochemical Oxygen Demand, and Dissolved Oxygen in the Chattahoochee River Downstream from Atlanta, Georgia. U.S.G.S. Water Supply Paper 2264. Washington, D.C.

Jobson, H.E. and T.N. Keefer. 1979. Modeling Highly Transient Flow, Mass, and Heat Transport in the Chattahoochee River near Atlanta, Georgia. U.S.G.S. Professional Paper 1136. Washington, D.C.

Johnson, A.I. and R.A. Clark (eds.) 1982. Proceedings: International Symposium on Hydrometeorology, June 1982, Denver. American Water Resources Association.

Kapitza, H. 1991. *Numerical Experiments with the Adjoint of a Nonhydrostatic Mesoscale Model*. Monthly Weather Review, 119(12), 2993-

Katopodes, N.D., J.-H. Tang, and A.J. Clemmens. 1990. *Estimation of Surface Irrigation Parameters.* Journal of Irrigation and Drainage Engineering, 116(5), 676-695.

Kim, K.-S. 1993. Development, Application and Analysis of the Physical Aspects of a Water Quality Modeling Framework for Highly Transient Streams. Ph.D. thesis, Department of Civil, Environmental and Architectural Engineering, University of Colorado, Boulder.

Koivo, H.N., and J.T. Tanttu. 1983. *Adaptive Prediction of Water Quality in the River Cam*. in M.B. Beck and G. van Straten (eds), Uncertainty and Forecasting of Water Quality. Springer-Verlag. Berlin. 1983.

Krajewski, K.L., W.F. Krajewski, and F.M. Holly, Jr. 1993. *Real-Time Optimal Stochastic Control of Power Plant River Heating*. Journal of Energy Engineering. 119(1), 1-18.

Kreith, F. 1973. Principles of Heat Transfer. Harper & Row, New York.

Kreith, F., and J.F. Kreider. 1978. Principles of Solar Engineering. Hemisphere Publishing. Washington, D.C.

Leonard, B.P. 1979. *A Stable and Accurate Convective Modelling Procedure Based on Quadratic Upstream Interpolation*. Computer Methods in Applied Mechanics and Engineering, 19, 59-98.

Lillehammer, A. and S.J. Saltveit (eds). 1982. Regulated Rivers. Universitetsforlaget AS, Oslo, Norway. pp540.

Lin, B., and R.A. Falconer. 1997. *Tidal Flow and Transport Modeling using ULTIMATE QUICKEST Scheme.* Journal of Hydraulic Engineering, 123(4), 303-314.

Malatre, K., and Ph. Gosse. 1995. *Is it Possible to Influence Water Temperature and Quality in the River Seine Upstream of Paris in Summer by Managing the Upstream Reservoirs*. Water Science and Technology, 31(8), 67-77.

Marchuk, G.I. 1986. Mathematical Models in Environmental Problems: Studies in Mathematics and its Applications, Vol. 16. North-Holland Publishing Co. Amsterdam.

Marino, M.A. and H.A. Loaiciga. 1985(a). *Dynamic Model for Multireservoir Operation*. Water Resources Research. 21(5), 619-630.

Marino, M.A. and H.A. Loaiciga. 1985(b). *Quadratic Model for Reservoir Management: Application to the Central Valley Project*. Water Resources Research. 21(5), 631-641.

McLaughlin, D.B. 1983. *Statistical Analysis of Uncertainty Propagation and Model Accuracy.* in M.B. Beck and G. van Straten (eds), Uncertainty and Forecasting of Water Quality. Springer-Verlag. Berlin. 1983.

Melching, C.S., C. Yen, and H.G. Wenzel. 1991. *Output Reliability as a Guide for Selection of Rainfall-Runoff Models*. Journal of Water Resources Planning and Management. 117(3), 383-398.

Miller, A.W. and R.L. Street. 1972. Surface Heat Transfer from a Hot Spring Fed Lake. Report 160, Dept. Civil Engineering. Stanford University.

Morton, F.I. 1965. *Potential Evaporation and River Basin Evaporation.* Journal of the Hydraulics Division, ASCE. 91(HY6), 67-97.

Morton, K.W. 1996. Numerical Solution of Convection-Diffusion Problems. Chapman & Hall, London

Morton, K.W., and I.J. Sobey. 1993. *Discretization of a Convection-Diffusion Equation*. IMA Journal of Numerical Analysis. 13(1), 141-160.

Moss, M.E. 1991. *Hydrologic Implications of Climate Uncertainty in the Western United States*. In Proceedings: Managing Water Resources in the West under Conditions of Climate Uncertainty, held in Scottsdale, Arizona, 14-16 November, 1990. National Academy Press, Washington D.C.

National Research Council (U.S.). 1987. River and Dam Management: a Review of the Bureau of Reclamation's Glen Canyon Environmental Studies. Committee to Review the Glen Canyon Environmental Studies, Water Science and Technology Board, Commission on Physical Sciences, Mathematics, and Resources, National Research Council. National Academy Press. Washington, D.C. 203 pages.

NEOS. 1996. The Network-Enabled Optimization System (NEOS) Optimization Tree: an Online Guide to the Field of Numerical Optimization. http://www-fp.mcs.anl.gov/otc/Guide/OptWeb/index.html.

Nemhauser, G.L, A.H.G. Rinnooy Kan, and M.J. Todd. 1989. Optimization. North-Holland, Amsterdam.

Nicholson, G.S., E.E. Pyatt, and D.H. Moreau. *A Methodology for Selecting Among Water Quality Alternatives*. Water Resources Bulletin. 6(1), 23-33.

Paily, P.P. and E.O. Macagno. 1976. *Numerical Prediction of Thermal-Regime of Rivers*. Journal of the Hydraulics Division, ASCE. 102(HY9), 257-274.

Piasecki, M. and N.D. Katapodes. 1997(a). *Control of Contaminant Releases in Rivers I: Adjoint Sensitivity Analysis.* Journal of Hydraulic Engineering, ASCE, 123(6), 486-492.

Piasecki, M. and N.D. Katapodes. 1997(b). *Control of Contaminant Releases in Rivers II: Optimal Design.* Journal of Hydraulic Engineering, ASCE, 123(6), 493-503.

Polehn, R.A., and W.C. Kinsel. 1997. *Transient Temperature Solution for Stream Flow from a Controlled Temperature Source*. Water Resources Research, 33(1), 261-265.

Ponce, V.M., R.-M. Li and D.B. Simons. 1978. *Applicability of Kinematic and Diffusion Models.* Journal of the Hydraulics Division, ASCE. 104(HY3), 353-360.

Portela, L.I., and R. Neves. 1993. Modelling of Salt Distribution in the Tejo Estuary using the QUICK Scheme. In: L.C. Wrobel and C.A. Brebbia, eds. Water Pollution II: Modeling, Measuring and Prediction. Computational Mechanics Publications, Boston, pages 121-128.

Press, W.H., B.P. Flannery, S.A. Teukolsky, and W.T. Vetterling. 1988. Numerical Recipes in C. Cambridge University Press, Cambridge, 735 pages.

Protopapas, A.L., and R.L. Bras.1993. *Effects of Weather Variability and Soil Parameter Uncertainty on the Soil-Crop-Climate System.* Journal of Climate, 6(4), 645-656.

Railsbeck, S. 1997. *Design Guidance for Short-Term Control of Flow Releases for Temperature Management*. Pacific Gas and Electric Research and Development

Report, file no. 009-97.10. San Ramon, California.

Risley, J.C. 1997. *Relations of Tualatin River Water Temperatures to Natural and Human-Caused Factors.* USGS Prof. Paper 97-4071 and 96-315.

Rutschmann, P., and W.H. Hager. 1996. *Diffusion of Floodwaves*. Journal of Hydrology, 178, 19-32.

Ryan, P.J. and D.R.F. Harleman. 1973. An Analytical and Experimental Study of Transient Cooling Pond Behavior. Ralph M. Parsons Laboratory Report 161, M.I.T. Cambridge, Mass.

Sartoris, J.J. 1976. A Mathematical Model for Predicting River Temperatures: Application to the Green River below Flaming Gorge Dam. U.S. Department of the Interior, Bureau of Reclamation, report # REC-ERC-76-7.

Schlichting, H. 1968. Boundary Layer Theory. McGraw Hill Book Co. New York.

Shanno, D.F. 1970. *Conditioning of the Quasi-Newton Methods for Function Minimization.* Mathematics of Computation, 24, 647-656.

Sinokrot, B.A. and H.G. Stefan. 1993. *Stream Temperature Dynamics: Measurements and Modeling*. Water Resources Research, 29(7), 2299-2312.

Sivapalan, M., B.C. Bates, and J.E. Larsen. 1997. *A Generalized, Nonlinear, Diffusion Wave Equation: Theoretical Development and Application*. Journal of Hydrology, 192, 1-16.

Stamou, A.I. 1992. *Improving the Numerical Modeling of River Water Quality by using High Order Difference Schemes*. Water Resources, 26(12), 1563-1570.

Stefan, H.G. and E.B. Preud'homme. 1993. *Stream Temperature Estimation from Air Temperatures*. Water Resources Bulletin, 29(1), 27-45.

Theurer, F.D., K.A. Voos and C.G. Prewitt. 1982. *Application of IFG's Instream Water Temperature Model in the Upper Colorado River.* in Johnson and Clark (eds), Proceedings: International Symposium on Hydrometeorology, June 1982, Denver. American Water Resources Association.

Thomann, R.V. and J.A. Mueller. 1987. Principles of Surface Water Quality Modeling and Control. Harper and Row, New York.

United States Bureau of Reclamation.1992. Program to Route Water from Flaming Gorge to Jensen. United States Bureau of Reclamation, Upper Colorado Region, Water Operations Branch, Salt Lake City.

United States Department of the Interior. 1993. Hydropower Licensing: the U.S. Fish and Wildlife Service Role. U.S. Fish and Wildlife Service Report 93-0644-P. U.S. Department of the Interior. Washington, D.C.

U.S. Department of the Interior, 1995. *Operation of Glen Canyon Dam: Final Environmental Impact Statement.* Bureau of Reclamation, Salt Lake City, Utah.

Vag, J.E., H. Wang, and H.K. Dahle. 1996. *Eulerian-Lagrangian Localized Adjoint Methods for Systems of Nonlinear Advective-Diffusive-Reactive Transport Equations*. Advances in Water Resources, 19(5), 297-315.

Vested, H.J., J.W. Baretta, L.C. Ekebjaerg, and A. Labrosse. 1996. *Coupling of Hydrodynamical Transport and Ecological Models for 2D Horizontal Flow.* Journal of Marine Systems, 8(3-4), 255-267.

Wang, H., and R.A. Falconer. 1998. *Simulating Disinfection Processes in Chlorine Contact Tanks using Various Turbulence Models and High-Order Accurate Difference Schemes*. Water Research, 32(5), 1529-1543.

Ward, J.V., and J.A. Stanford. 1982. *The Regulated Stream as a Testing Ground for Ecological Theory.* In: Lillehammer, A. and S.J. Saltveit (eds), Regulated Rivers. Universitetsforlaget AS, Oslo, Norway. pp540.

Warwick, J.J. and L.A. Roberts. 1992. *Computing the Risks Associated with Wasteload Allocation Modeling*. Water Resources Bulletin, 28(5), 903-915.

Wasimi, S.A. and P.K. Kitanidis. 1983. Operation of a System of Reservoirs under Flood Conditions using Linear Quadratic Gaussian Stochastic Control. Iowa Institute of Hydraulic Research Report 268. University of Iowa, Iowa City.

Webb,B.W. and D.E. Walling. 1988. *Modification of Temperature Behavior Through Regulation of a British River System*. Regulated Rivers: Research and Management, 2, 103-116.

Whitehead, P.G., and P.C. Young. 1979. *Water Quality in River Systems: Monte Carlo Analysis.* Water Resources Research. 15(2), 451-459

Whitehead, P.G. 1983. *Modeling and Forecasting Water Quality in Nontidal Rivers: The Bedford Ouse Study.* In: M.B. Beck and G. van Straten (eds), Uncertainty and Forecasting of Water Quality. Springer-Verlag. Berlin. 1983.

Wilhelms, S.C., and M.L. Schneider. 1986. *Operational Tools: Optimal Control of Reservoir Water Quality.* In: Proceedings, CE Workshop on Design and Operation of Selective Withdrawal Intake Structures, 24-28 June, 1985. San Francisco. pages 110-115.

Woodward-Clyde Consultants, 1986. Stanislaus Project Instream Temperature Study. Pacific Gas and Electric Company, San Ramon, California.

Wunderlich, W.O., and M.C. Shiao. *Long-Range Reservoir Outflow Temperature Planning*. Journal of Water Resources Planning and Management, 110(3), 285-295.

Yakowitz, S. 1982. *Dynamic Programming Applications in Water Resources*. Water Resources Research. 18(4), 673-696.

Yeh. W. W-G. 1985. *Reservoir Management and Operations Models: A State-of-the-Art Review.* Water Resources Research. 21(12), 1797-1818.

Yeh, W. W-G., and N.Z. Sun. 1990. *Variational Sensitivity Analysis, Data Requirements and Parameter Identification in a Leaky Aquifer System*. Water Resources Research, 26(9), 1927-1938.

Zhu, C., R.H. Byrd, and J. Nocedal. 1997. Algorithm 778: L-BFGS-B: Fortran Subroutines for Large-Scale Bound-Constrained Optimization. ACM Transactions on Mathematical Software. 23(4).

Zimmerman, M.J., and M.S. Dortch. 1989. *Modelling Water Quality of a Reregulated Stream Below a Peaking Hydropower Dam*. Regulated Rivers: Research and Management, 4, 235-247.

APPENDIX A

OVERVIEW OF HEAT EXCHANGE PROCESSES

A.1 INTRODUCTION

This appendix contains further details on the modeling of heat fluxes. Heat flux into and out of natural waters occurs at both the air-water and streambed-water interfaces. Fluid mechanics and boundary layer theory play a significant role in describing the physical processes of heat transfer across these interfaces. We briefly outline the physical processes governing movement of heat across these interfaces, and then provide an overview of the algorithms used in this research for modeling the most relevant components of the overall flux.

Heat transfer is the flow of energy, in the form of heat, from a source to a sink as a result of a temperature gradient. Strictly speaking, heat is transferred by either thermal radiation (transmission of electromagnetic waves) or thermal conduction (physical contact). In the case of solids, these are the only two mechanisms. However, heat transfer in liquids and gases are unconstrained in terms of their molecular movement on a macroscopic scale. This heat transfer mechanism, known as convection, is the third mechanism we will describe. It should be noted that convective heat transfer does not take place without conduction (i.e., contact between two bodies), but rather it provides the motion by which elements of differing temperatures are brought into contact (Hewitt et al., 1994).

Conductive Heat Transfer

A temperature gradient within a medium, or between two mediums, will cause movement of heat from the higher to the lower temperature region. This conduction of heat is described by Fourier's Law (here in one dimension), which states that

$$q'' = -\lambda\left(\frac{\mathrm{d}T}{\mathrm{d}x}\right) \tag{A.1}$$

where

$$\begin{aligned} q'' &= \text{heat flux (W/m}^2\text{)} \\ \lambda &= \text{thermal conductivity (W/m*K)} \end{aligned} \tag{A.2}$$

Movement of heat by conduction occurs at the molecular and atomic levels, by atomic vibration, movement of electrons, or random collisions between molecules of differing temperatures. This molecular level movement is what differentiates conduction from convection, which takes place at spatial scales several orders of magnitude larger than conduction. In this work, we are concerned with conduction both at the two system interfaces, and within the streambed itself.

Radiative Heat Transfer

All bodies which are warmer than absolute zero emit radiation. Because radiation from a body is proportional to absolute temperature raised to the fourth power, it is the predominant heat transfer mechanism in systems with high temperatures. According to the Stefan-Boltzmann law, the amount of radiation a body emits is given by:

$$J_{rad} = \varepsilon\sigma T_a^4 \tag{A.3}$$

where

$$
\begin{aligned}
J_{rad} &= \text{radiation flux} \\
\varepsilon &= \text{emissivity (0-1)} \\
\sigma &= \text{Stefan-Boltzmann constant } [5.67 \times 10^{-8}\ \mathrm{W(m^2\ K^4)^{-1}}] \\
T_a &= \text{absolute temperature (K)}
\end{aligned}
\tag{A.4}
$$

The emissivity coefficient is a correction factor which provides an adjustment for media which are not perfect black-body emitters. Water is an almost perfect emitter, with an emissivity of 0.97. We consider both longwave (atmospheric, water) and shortwave (solar) radiation in our total heat budget. The amount of incident solar radiation is highly variable both diurnally and annually, as a result of the incidence angle, and also depends largely on cloud cover.

Convective Heat Transfer and Boundary Layer Theory

The mechanics of convective heat transfer in rivers is closely tied to fluid mechanics theories set forth by Reynolds in the late 1800s. His seminal work first described laminar and turbulent flows and the transition from one to the other. Reynolds showed that at a critical value of the fluid velocity, given a pipe diameter, fluid viscosity, and density, flows change from one state to the other. The occurrence of laminar or turbulent flow is predicated on the dominance of either momentum flux or viscous shear stress. The ratio of these values is the Reynolds number. In 1908, Prandtl introduced the concept of the boundary layer, providing a theoretical link between idealized and real fluid flows. When flow travelling at a uniform velocity passes over a horizontal surface, a boundary layer develops due to the shear stress at the fluid / surface interface. In both laminar and turbulent flow, the boundary layer remains laminar, although in turbulent flow it is usually considerably narrower than for laminar flow. The extent of the boundary layer is a function of the fluid's properties and flow characteristics, and the properties of the surface over which it is passing. For a more rigorous treatment of boundary layer theory and heat transfer, the reader is referred to Schlichting (1968) and Hewitt et al. (1994). For purposes of this research, we concen-

trate on boundary layers in turbulent flow systems. Under turbulent flow, the velocity gradient near the streambed surface increases and becomes narrower, but remains laminar. The flow outside of this narrow laminar sub layer is turbulent, with an essentially uniform spatially averaged velocity throughout its depth. If the surface over which the flow is occurring is of a different temperature than the fluid, a thermal boundary layer will also form. This thermal boundary layer is often not the same thickness as the velocity boundary layer. The relationship between these two boundary layers depends on the fluid properties and the system dynamics. In natural river systems, it is rare to have laminar flows. In a river such as the Green below Flaming Gorge, Reynolds numbers are typically on the order of 10^5, which indicates turbulent flow. Because of the irregular nature of the streambed, the boundary layer at the bed-water interface is assumed negligible, and the stream is treated as a one-dimensional system with homogenous temperature in the lateral and vertical directions. The nature of heat transfer under laminar and turbulent flow regimes differ greatly. In laminar (horizontal) flow, heat is transferred vertically by conduction only. In turbulent flow, heat is transferred solely by conduction in a very narrow band adjacent to the streambed, called the boundary layer. Above the boundary layer, heat transfer occurs as a result of both conduction and turbulence in the fluid, which can quickly mix large volumes of the fluid. Most natural rivers are subject to turbulent flow regimes, thus we limit our discussion to turbulent systems. We should also make a distinction here between forced and natural convection. Under forced convection, a fluid moves due to some external force acting upon it. Natural convection refers to the movement of fluid as a result of the heating process itself, and is caused by buoyancy effects brought about by differences in density of the fluid at different temperatures. Convective heat exchange in streams is driven almost exclusively by forced, turbulent, convection (due to gravity and channel characteristics). Of particular relevance to this work is the nature of these two flow types in the areas near the streambed interface.

The physical processes of convective heat transfer between a stream and its bed may best be approximated analytically by looking at the theoretical case of fluid flow over a horizontal flat plate. The rate of heat transfer from the plate (streambed) into the fluid (stream) is proportional to the difference in temperature between the core temperature and that of the plate. At the plate surface, heat is conducted according to Equation A.1. The heat transfer coefficient may be defined by

$$h = \frac{q''}{(T_p - T_f)} \tag{A.5}$$

The coefficient is somewhat misleading in its simplicity. It is best thought of as a bulk conduction/convection coefficient which describes the total process of heat transfer into (or out of) the fluid. It is a surrogate for the complex thermal boundary layer conduction and overlying turbulent convective mixing, and is only described empirically for all but the simplest theoretical systems. The non-dimensional Nusselt number (Nu) is a useful measure of the heat transfer coefficient. It is defined by

$$Nu = \frac{\alpha L}{\lambda} \tag{A.6}$$

where L is a length term describing the distance from the origination point of the boundary layer. Equation A.6 may be physically interpreted as the ratio of the temperature gradient of the boundary layer immediately adjacent to the plate to the gradient of the temperature differential from fluid core to the plate. For a river system, the length L is somewhat ill-defined. It is also possible to relate the Nusselt number to the Reynolds (Re) and Prandtl (Pr) numbers (the Prandtl number is the ratio of diffusion of momentum to diffusion of heat in a fluid). A study by Polhausen (Kreith, 1973) develops the following empirical relationship:

$$\overline{Nu} = 0.664 Re^{1/2} Pr^{1/3} \tag{A.7}$$

Another empirical study using the Chilton-Colburn analogy of heat and mass transfer commonality yields the following relationship derived specifically for turbulent flows (Hewitt et al., 1994):

$$Nu = 0.037 Re^{4/5} Pr^{1/3} \tag{A.8}$$

Another dimensionless parameter, the Biot Number, provides a measure of the ratio of convection to conduction within the solid itself. Its relevance is that it can be used to determine the validity of a lumped parameter approximation to heat transfer in the solid. Notice that even for relatively simple systems (i.e., flow over a flat plate), analytical solutions exist only for cases of laminar flow. For this thesis, we assume a well-mixed river section both vertically and horizontally, and incorporate boundary layer effects with the use of empirically derived bulk transfer coefficients. These manifest themselves, for example, as the zero-order coefficient in the quadratic windspeed functions for evaporation and “convective” heat loss at the water surface. Specifics of the approximation used in this research are outlined in the appropriate sections below.

We now provide background for each of the major heat flux components of the temperature model. A brief description of the method is given, as well as background on the derivation, and other methods found in the literature.

The heat flux at the air-water interface is given by

$$\Delta H_a = H_{sn} + H_{an} - H_{br} \pm H_c \pm H_e \tag{A.9}$$

with

$$\begin{aligned} H_{sn} &= \text{net solar (shortwave) radiation} \\ H_{an} &= \text{net atmospheric (longwave) radiation} \\ H_{br} &= \text{longwave radiation from water} \\ H_c &= \text{conductive heat transfer} \\ H_e &= \text{evaporative heat transfer} \end{aligned} \tag{A.10}$$

Solar (Shortwave) Radiation

Net solar radiation is the sum of the incoming solar radiation minus a percent of the incoming which is reflected. The amount of reflected radiation depends on water conditions, the altitude of the sun, and cloud cover. Shortwave solar radiation is ideally measured directly at the study site. Direct observations are unavailable on the Green River, so we use an algorithmic approximation based on solar altitude, reflection coefficients, and atmospheric conditions. The solar altitude is given by (Kreith and Kreider, 1978):

$$\sin(\beta) = \sin(L)\sin(d) + \cos(L)\cos(d)\cos(h) \qquad \textbf{(A.11)}$$

where β is the solar altitude, L is the latitude of the study site, d is the sun's declination, and h is the hour angle of the sun. The hour angle is a function of river longitude (r), time zone meridian (t_m), and time of day (td):

$$h = \left[180 + r - t_m - \left(360 \times \frac{td}{24}\right)\right] \times \frac{180}{\pi} \qquad \textbf{(A.12)}$$

Reflection is often assumed to be in the range 0.02 - 0.04 of incoming solar, which is reasonable for incidence angles greater than about 35 degrees. Fresnel's reflectivity law may be used to generate more precise reflection factors at low solar altitudes (Kim, 1993).

Atmospheric longwave radiation

Atmospheric radiation depends primarily on air temperature and humidity, and can be estimated in several ways. It is commonly estimated using Brundt's formula (Edinger et al., 1974; Thomann and Mueller, 1987):

$$H_{an} = \sigma(T_a + 273)^4(C_a + 0.031\sqrt{e_a})(1 - R_l) \qquad \textbf{(A.13)}$$

where

$$\begin{aligned} \sigma &= \text{Stefan-Boltzmann constant } (4.9\times10^{-3}[J/m^2dK^4]) \\ T_a &= \text{air temperature}(^oC) \\ C_a &= \text{Brundts coefficient (0.5-0.75)} \\ e_a &= \text{air vapor pressure (mmHg)} \\ R_l &= \text{reflection coefficient (0.03)} \end{aligned} \tag{A.14}$$

This formulation relies on air vapor pressure data, which may not always be available. TVA (1972) provides an alternate form which uses percent cloud cover as a surrogate for air vapor pressure:

$$H_{an} = \sigma\varepsilon(T_a + 273)^6(1 - R_l) \tag{A.15}$$

where

$$\begin{aligned} \varepsilon &= 1 + 0.0017(cc)^2 \\ cc &= \text{cloud cover in tenths } (0 <= cc <= 10) \end{aligned} \tag{A.16}$$

and other terms are as before. Both incoming solar and atmospheric radiation terms are independent of water temperature, whereas the remaining terms are all dependent on water temperature.

Back Radiation from Water Body

Longwave radiation, in addition to being an atmospheric input, is also emitted from water. Because water is an almost perfect black-body emitter, the Stefan-Boltzmann law is again used:

$$H_{br} = \sigma\varepsilon(T_w + 273)^4 \tag{A.17}$$

where T_w is the water temperature (^oC), and ε is the emissivity of water (0.97).

Evaporation

Evaporation and conduction from a water body are similar physical processes. They involve both conduction across the interface, and convection into the atmo-

sphere. The convective process may be wind-driven (forced convection), or in the absence of wind, may be driven by density instabilities resulting from flux across the water surface (free convection) (Edinger et al. 1974). Evaporation from a water body removes 2.45 x 10^6 Joules (at 20 ^oC) of heat for each kilogram of water lost. It is most often derived empirically, though some attempts have been made to derive formulae from physical laws (e.g., Sverdrup, 1937). In the formulation we employ, evaporation is a function of wind speed, air vapor pressure, and saturation pressure of air at the water surface. It is commonly assumed that there exists a thin film of saturated air just above the water surface, and that above this surface, movement of vapor into the atmosphere is by convective forces. In most field conditions, wind-driven convection dominates (Brocard and Harleman, 1976), and Dalton's Law is used along with an empirically derived wind function (Chapra, 1997):

$$H_e = f(u_w)(e_s - e_a) \tag{A.18}$$

where

$$\begin{aligned} u_w &= \text{windspeed (m/s)} \\ e_s &= \text{saturation vapor pressure at water surface (mmHg)} \\ e_a &= \text{air vapor pressure (mmHg)} \end{aligned} \tag{A.19}$$

and from Brady et. al. (1969),

$$f(u_w) = 9.2 + 0.46u_w^2 \tag{A.20}$$

It is worth noting that Equation A.20 represents but one of numerous quadratic equations for the windspeed function. Other formulae, empirically derived, may be found in works by Miller and Street (1972), Ryan and Harleman (1973), Morton (1965), and Harbeck et al. (1959).

Conduction/Convection

Conduction and convection at the air water interface occurs if there is a difference in temperature between the two bodies. It is strongly influenced by convective wind movement over the water, which increases the total heat transfer by removing newly warmed (or cooled) air from the surface layer. Even in the absence of wind, there will be some degree of convective movement due to buoyancy effects in the atmosphere. The conductive component of the heat transfer equation is typically a function of the difference between air and water temperatures (true conduction), and the wind speed over the water surface (convection). The derivation of Equation A.21 relies on similarities between mass transfer by evaporation and heat transfer by conduction (Edinger, 1974), and leads to the use of the same windspeed function. Conduction into and out of natural waters is typically an order of magnitude less than the other terms in the heat flux equation. We use the formulation of Edinger et al. (1974):

$$H_c = 0.47 f(u_w)(T_w - T_a) \tag{A.21}$$

where

$$\begin{aligned} T_w &= \text{water temperature (C)} \\ T_a &= \text{air temperature (C)} \end{aligned} \tag{A.22}$$

and the windspeed function is computed from equation A.20.

Streambed Heat Flux

Heat transfer between streambed and stream has long been neglected as an important process in the dynamics of stream temperature models. However, it has been noted that in many natural waters, particularly those which are shallow (< 3 m) and clear, that streambed heat fluxes significantly impact diurnal heating in the overlying stream (Jobson, 1977). Heat flux into the streambed is typically assumed to be dominated by conduction, though over longer periods it may be complicated by water

movement into and out of the bed. Conduction will be the predominant mechanism over shorter periods of time (hours to days) during which convective heat flux via groundwater flow is negligible. Heat flux on the stream side of the streambed/stream interface is somewhat more complicated. In most natural rivers, flow is turbulent, which leads to a locally well mixed (vertically and laterally) system with a narrow boundary layer at the streambed. The type of approximation used for heat flux across this boundary is dependent on the relative speed with which convective mixing in the river and conduction in the streambed occur. We propose using an approximation developed by Jobson (1977) in which it is assumed that conduction within the bed is the limiting dynamic in the heat flux mechanism. If this is in fact true, then we can develop a transient heat flux equation describing the gain or loss of heat into the bed over a given time interval. The net change in total heat held by the bed becomes a gain or loss into the stream itself.

If we assume that water movement within the bed is negligible over small time periods (1 day or less), then heat transfer within the bed is a purely conductive process. The sediment heat flux can then be represented by

$$\Delta H_b = -k \left. \frac{\partial T_b}{\partial z} \right|_{z=0} \tag{A.23}$$

with

$$\begin{aligned} T_b &= \text{river bed temperature} \\ z &= \text{bed depth (= 0 at water interface)} \\ k &= \text{bed thermal conductivity} \end{aligned} \tag{A.24}$$

The temperature profile of heat in the stream bed can be solved using the methods of Carslaw and Jaeger (1959). The following derivation is taken entirely from Jobson (1977). Carslaw and Jaeger derive this expression for temperature distribution in a slab subject to heating at a boundary:

$$H(t) = C_v L\left\{1 - \frac{8}{\pi^2}\sum_{n=0}^{\infty}\frac{(-1)^n}{(2n+1)^2}\exp\left[\frac{-\kappa(2n+1)^2\pi^2 t}{4L^2}\right]\sin\left[\frac{(2n+1)\pi}{2}\right]\right\} \quad \textbf{(A.25)}$$

with

$H(t)$ = increase in heat content of bed from 0 to t as a result of a unit increase in the surface (boundary) temperature at time 0

C_v = heat storage capacity of the bed (density x specific heat) **(A.26)**

L = bed thickness

κ = thermal diffusivity

The heat flux at the interface between water and stream bed, during any timestep $i\Delta t$ to $(i+1)\Delta t$ which results from a unit change in temperature at time 0 is computed by

$$\Delta H(i) = H(i\Delta t) - H((i+1)\Delta t) \quad \textbf{(A.27)}$$

Noting that (A.25) is linear with respect to temperature, and that changes in temperature may be represented by a series of step changes, the convolution principle may be used to determine the heat flux across the stream bed / water interface, during a given timestep, for any temperature history by using

$$\Delta H_b = \sum_{j=-s}^{i}\Delta T(j\Delta t)\Delta H(i-j) \quad \textbf{(A.28)}$$

where

$\Delta T(j\Delta t)$ is the change in water temperature during period jΔt

$\Delta H(i-j)$ is given by (27) **(A.29)**

s = heat memory of the stream bed (taken as 24 hours)

Works by Jobson (1977) and Jobson and Keefer (1979) in both natural and man-made channels indicate that a “memory” of 24 hours, and a bed thickness of

0.25m is sufficient to accurately characterize the bed fluxes. Jobson notes that for a diurnal temperature variation of 10 ^{o}C in a streambed of sand, this approach yields surface heat flux results within 6% of those obtained using the computationally expensive semi-infinite medium equations.

A.2 DATA REQUIREMENTS

The ability to apply all source and sink terms to a specific location is highly dependent on the availability of data. While common meteorological data such as minimum and maximum daily air temperatures are relatively easy to come by, other model inputs such as humidity, dew point, wet and dry bulb temperatures, windspeed, shading parameters, cloud cover, etc. are often unavailable.

Because it is often more readily available than other meteorological data, air temperature is often used as a surrogate (Cluis, 1972; Paily and Macagno, 1976; Stefan and Preud'homme, 1993). For example, Paily and Macagno (1976) developed and applied a model based on a bulk heat exchange coefficient and differences between air and water temperatures. Stefan and Preud'homme (1993) used a similar model to predict water temperature in 11 rivers in the Mississippi River basin. Their bulk coefficients were derived using linear regression techniques. Findings from that study indicate that smaller, shallow streams could be more accurately modeled using air temperatures, a result which they attributed to smaller thermal inertia than is found in larger, deeper streams. Miller (1997) has also used regression techniques to develop water temperature forecasts from daily maximum, minimum, and mean air temperatures.

The model used in this work is highly data intensive. Table 1 outlines the required data. Data which are either based on physical laws and are static (e.g., Stefan-Bolzmann constant), or which are generated internally by the model (e.g., flow depth) have been excluded.

Table A.1: Data Requirements for Model Components

Model Component	Data Required
Diffusion Flow Routing	Manning's n, channel width, channel bed slope, inflow (reservoir releases), diffusion coefficient*
Advective Temperature Routing	Inflow temperature (release temperature), H_{sn}, H_{an}, H_{br}, H_c, H_e, H_b
Solar Radiation (H_{sn})	latitude, longitude, elevation (m.s.l.), time of day, cloud cover, shading factor
Atmospheric Radiation (H_{an})	air temperature, reflection coefficient, cloud cover
Back Radiation (H_{br})	water temperature
Conduction (H_c)	wind velocity, water temperature, air temperature
Evaporation (H_e)	wind velocity, wet and dry bulb temperatures, relative humidity, atmospheric pressure, air temperature
Streambed Conduction/Convection (H_b)	water temperature, streambed heat capacity, streambed conductivity

Meteorological data were gathered from multiple sites in the study area. At Flaming Gorge Dam, there is a weather station from which 7 years of data were obtained. These data include daily values for minimum and maximum air temperatures, instantaneous dry and wet bulb temperatures, daily precipitation, and wind speed. A weather station at the Brown's Park National Wildlife Refuge headquarters provides minimum and maximum daily air temperatures and precipitation data. Three other sites within Dinosaur National Monument provided data for the lower half of the study area. These sites provided daily values of minimum and maximum air temperatures, precipitation, and wind speed. One of the shortcomings of the data from the station at Flaming Gorge Dam is that it does not reflect accurately the daily temperature and windspeed from within Red Canyon. Model results indicate that heat loss from

conduction is being underestimated during nighttime hours, probably as a result of using minimum air temperature values that are too high.

Flow and water temperature data are available from numerous sources. Release volume and temperatures were obtained from the U.S. Bureau of Reclamation, which operates Flaming Gorge Dam. These data provide the upstream boundary condition for the model. Temperature data are also available for numerous sites along the Green River. These data provide a means to calibrate the model against historical observed values. There are two sets of stream temperature data that we will be primarily interested in. One set, collected by Kevin Bestgen, contains observations from several years in the early 1990s at 7 locations between 1 and 51 kilometers downstream from the dam. Those data were collected on roughly 3 hour intervals. Data further downstream, near the confluence of the Green and Yampa Rivers, are available from George Smith of the USFWS. River channel characteristics were also obtained from George Smith, as well as from Steve Brayton of the Utah Division of Wildlife Resources. Estimates of bed slope and channel width were verified against topographic maps, and through communications with George Smith, Steve Brayton, and others.

A.3 STREAMBED HEAT DIFFUSIVITY FIELD WORK

During the summer of 1998, field work was undertaken to determine bed head diffusivity coefficients for the Green River. Streambed temperatures were recorded at 20 minute intervals at depths of 4, 14, and 43 cm below the bed surface. The observations were taken at a location approximately 55 km below the dam. A stream temperature recorder approximately 15 meters from the sediment monitoring site collected hourly stream temperature data over the same period. Figure A.29 shows 8 days of sediment temperature data. Figure A.2 shows a shorter period of the same data. Using a finite difference heat diffusivity equation and regression techniques, values in the range 1×10^{-6} to 1×10^{-7} m^2/s were obtained. These values fall within the range of

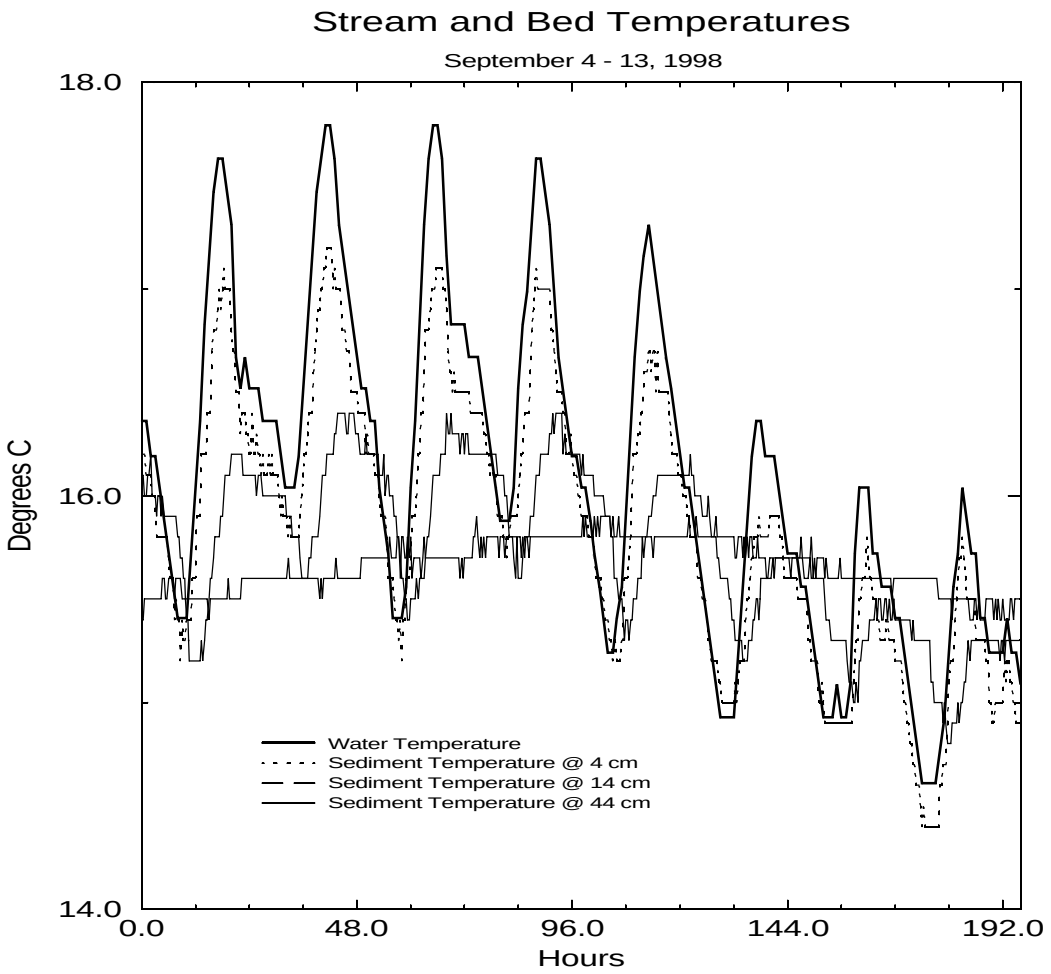

Figure A.1: 20 minute sediment temperature data and hourly stream temperature data from Brown's Park National Wildlife Refuge, approximately 55 km below Flaming Gorge Dam.

values previously observed (Jobson, 1977; Kim, 1993). The data also validate our use of 0.5 m as the depth at which a no-flux boundary can be assumed. The 43 cm observations fluctuate little if at all on a daily basis, and only vary over periods of several days to weeks as long term trends in average water temperatures change. The lag in diurnal heating with depth is apparent in Figure A.2. The maximum daily sediment temperature at a depth of 14 cm occurs approximately 6 hours later than that of the stream.

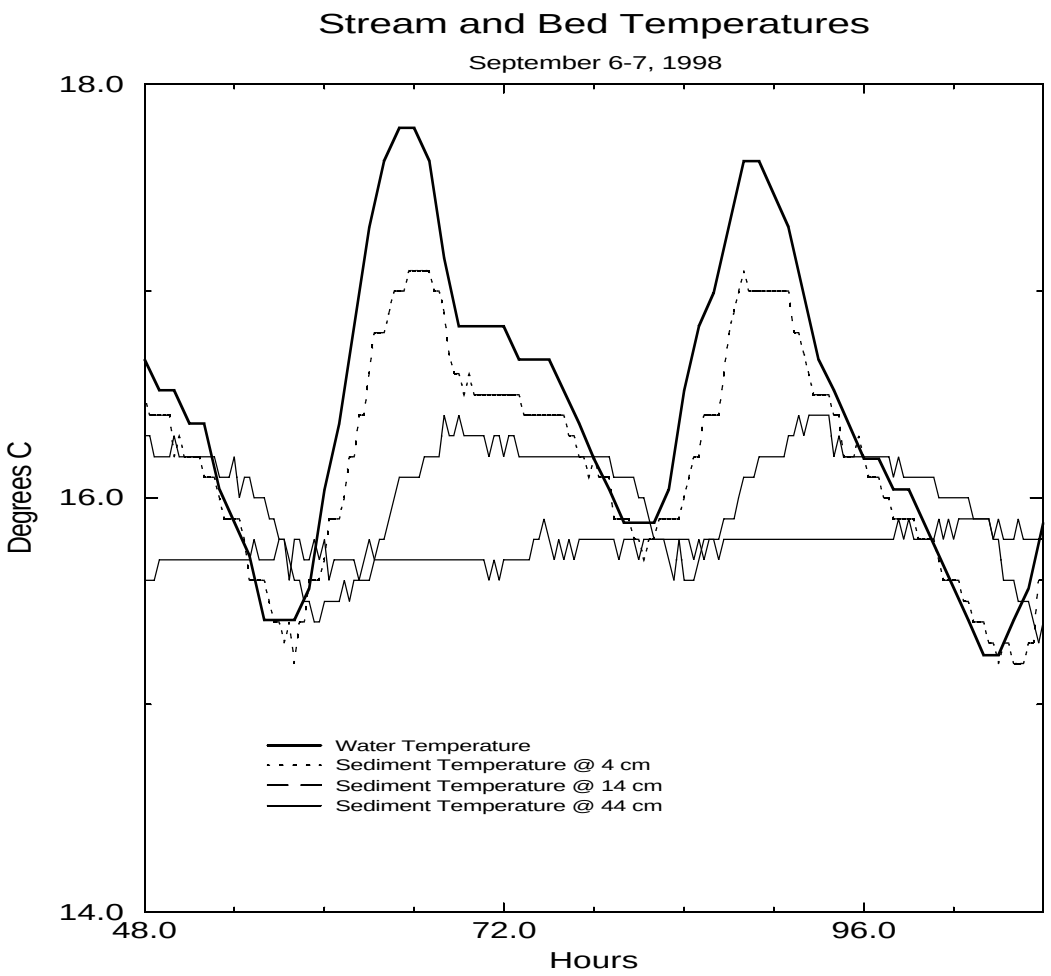

Figure A.2: Detail of Figure A.1. The diurnal lag of heat conduction into the bed is apparent from the figure.

APPENDIX B

NUMERICAL METHODS

Derivations for the three numerical methods which were tested for this thesis are provided below. The QUICKEST scheme is outlined for a full advection-diffusion problem, while the Flux corrected MacCormack and ELLAM schemes are outlined for the advection-only problem.

B.1 THE QUICKEST FINITE DIFFERENCE METHOD

The derivation of the QUICKEST scheme is taken entirely from Leonard (1979). The unique feature of the method is its use of a three-point upstream-weighted quadratic interpolation for the wall values of the independent variables in a control volume formulation of the problem. For one-dimensional flows with consistently positive flows in the x-direction, this results in the use of four nodal values per cell.

The quadratic upstream weighting concept is illustrated graphically in figure A.1, from which the value of q_r, the right wall value of the cell (denoted by the subscripted lowercase r) around node q_C, is given as

$$q_r = \frac{1}{2}(q_C + q_R) - \frac{1}{8}(q_L + q_R - 2q_C) \tag{B.1}$$

The gradient value at q_r is also shown, by the dotted line, and is given by

$$\left(\frac{\partial q}{\partial x}\right)_r = \frac{q_R - q_C}{\Delta x_r} \tag{B.2}$$

Equations for the left wall follow in similar fashion.

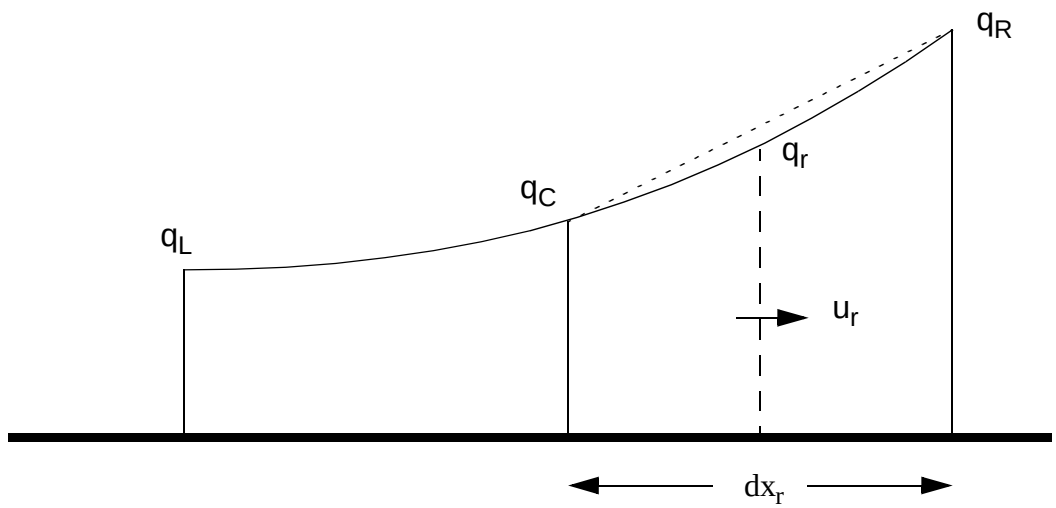

Figure B.1: Quadratic weighting scheme at right wall of control volume.

The development of the QUICKEST scheme begins by examining an advective system with constant velocity. A finite difference formulation might be written as

$$(q_i^{n+1} - q_i^n) = u(\tilde{q}_l - \tilde{q}_r)\frac{\Delta t}{\Delta x} \tag{B.3}$$

where the q terms on the right hand side (RHS) are average left and right wall values over the timestep. If we assume the profile of q sweeps downstream unchanged over a timestep (i.e., diffusion and velocity changes are ignored), then we have

$$\begin{aligned} \tilde{q}_l &= \frac{1}{2}[(q_{i-1}^n + q_i^n) - c(q_i^n - q_{i-1}^n)] \\ \tilde{q}_r &= \frac{1}{2}[(q_i^n + q_{i+1}^n) - c(q_{i+1}^n - q_i^n)] \\ c &= \frac{u\Delta t}{\Delta x} \end{aligned} \tag{B.4}$$

Eq. B.3 is then

$$q_i^{n+1} = q_i^n - \frac{c}{2}(q_{i+1}^n + q_{i-1}^n) + \frac{c^2}{2}(q_{i-1}^n + q_{i+1}^n - 2q_i^n) \tag{B.5}$$

which is formally equivalent to the central difference equation for an advection-diffusion problem, with a numerical diffusion coefficient $u^2\Delta t/2$ (Leonard, 1979). Because advection dominates over diffusion in the current problem, it is not unreasonable to make the same assumption of a fixed profile sweeping downstream for full advection-diffusion systems. Including the physical diffusion in Eq. B.5 results in

$$q_i^{n+1} = q_i^n - \frac{c}{2}(q_{i+1}^n + q_{i-1}^n) + \left(\frac{c^2}{2} + \alpha_{phys}\right)(q_{i-1}^n + q_{i+1}^n - 2q_i^n) \tag{B.6}$$

with α_{phys} the physical diffusion.

The above provides the impetus for the QUICKEST scheme, which essentially generates the same sweeping profile estimates for the quadratic upstream interpolation of Eq. B.1. When applied to the quadratic form, the final equation is

$$\begin{aligned} q_i^{n+1} = q_i^n &+ \frac{c_l}{2}\left[(q_{i-1}^n + q_i^n) - c_l(\Delta x)grad_l - \frac{\Delta x^2}{3}(1 - c_l^2 - 3\alpha)curv_l\right] - \\ &\frac{c_r}{2}\left[(q_i^n + q_{i+1}^n) - c_r(\Delta x)grad_r - \frac{\Delta x^2}{3}(1 - c_r^2 - 3\alpha)curv_r\right] + \\ &\alpha\left[\left(\Delta x grad_r - \frac{\Delta x^2}{2}c_r curv_r\right) - \left(\Delta x grad_l - \frac{\Delta x^2}{2}c_l curv_l\right)\right] \end{aligned} \tag{B.7}$$

with

$$\begin{aligned} grad_l &= (q_i^n - q_{i-1}^n)/\Delta x \\ grad_r &= (q_{i+1}^n - q_i^n)/\Delta x \\ curv_l &= (grad_r - grad_l)/\Delta x \\ curv_r &= (grad_{r+1} - grad_r)/\Delta x \\ \alpha &= \text{physical diffusion coefficient} \end{aligned} \tag{B.8}$$

B.2 THE ELLAM FINITE ELEMENT METHOD

The derivation presented here is based on the approach of Celia et. al. (1989), but is modified to exclude the diffusion term. We begin by writing the conservative advection equation using an operator representation:

$$L_x q \equiv -v\frac{\partial q}{\partial x} = \frac{\partial q}{\partial t} \tag{B.9}$$

The weak form of Eq. B.9 may be written as

$$\int_0^l \left(-v\frac{\partial q}{\partial x}\right) w(x)\,dx = \int_0^l \left(\frac{\partial q}{\partial t}\right) w(x)\,dx \tag{B.10}$$

If $q(x) \in C^1[0, l]$, that is, *q(x)* has continuity of both function and derivative over the spatial domain, and the test function *w(x)* exhibits discontinuities over the domain, $w(x) \in C^{-1}[0, l]$, then we can represent the left side of Eq. B.10 using element-wise integration:

$$\int_0^l \left(-v\frac{\partial q}{\partial x}\right) w(x)\,dx = \sum_{j=0}^{E-1} \int_{x_j}^{x_{j+1}} \left(-v\frac{\partial q}{\partial x}\right) w(x)\,dx \tag{B.11}$$

where E is the number of discrete elements in the domain. If we now integrate each elemental integral by parts, we have

$$\begin{aligned} \int_{x_j}^{x_{j+1}} \left(-v\frac{\partial q}{\partial x}\right) w(x)\,dx &= [-vwq]_{x_j}^{x_{j+1}} + \int_{x_j}^{x_{j+1}} (vq)\frac{\partial w}{\partial x}\,dx \\ &= [-vwq]_{x_j}^{x_{j+1}} + \int_{x_j}^{x_{j+1}} (L^* w) q(x)\,dx \end{aligned} \tag{B.12}$$

where L^* is the formal adjoint operator of L. The objective now is to eliminate the integral term containing the adjoint operator. This is achieved by finding *w(x)* such that it satisfies the equation $L^* w = 0$ within each element. The solution to

$$(L^*w) = v\frac{\partial w}{\partial x} = 0 \tag{B.13}$$

is simply $w(x) = c_1$, c_1 a constant. The elimination of the integral yields

$$\int_0^l (Lu)w(x)dx = \sum_{j=0}^{E-1}\left\{[-vwq]_{x_j}^{x_{j+1}}\right\} \tag{B.14}$$

Because $q(x)$ has continuity over the domain $[0,l]$, its nodal evaluations will be unique. However, $w(x)$ is not continuous, so in general, its nodal values will depend on the direction from which the node is approached. With these details in mind, we can rewrite Eq. B.14 as

$$\int_0^l (Lu)w(x)dx = \sum_{j=1}^{E-1}\{[[vw]]_{x_j}q_j\} + [-vwq]_0^l \tag{B.15}$$

where the double bracket [[*]] denotes a jump operator defined by

$$[[*]] \equiv [[*]]_{x_j^+} - [[*]]_{x_j^-} \tag{B.16}$$

We have solutions for $w(x)$ and the nodal evaluations of the adjoint equations. We must now address the temporal derivative of the right side of Eq. B.10, which involves evaluating the product of the temporal derivative and $w(x)$ over the spatial domain $[0,l]$. To achieve this, we use an approximation based on piecewise linear Lagrange polynomials:

$$\int_0^l \left(\frac{\partial}{\partial t}q(x,t)\right)w(x)dx \cong \sum_{j=0}^{E}\frac{d}{dt}[q_j(t)]\int_0^l \phi_j(x)w(x)dx \tag{B.17}$$

The integral on the right side of Eq. B.17 can be evaluated directly. Representing the integral result by α_j, and combining Eq. B.15 and Eq. B.17, we obtain

$$\sum_{j=0}^{E} \alpha_j \frac{d}{dt}[q_j(t)] + \sum_{j=1}^{E-1} \{[[vw]]_{x_j} q_j\} + [-vwq]_0^l = 0 \qquad \textbf{(B.18)}$$

Eq. B.18 is written for E elements, and the upstream boundary condition, given by the inflow to the domain, yield E+1 equations for E+1 unknowns. Using matrix notation, the problem can be represented by

$$G \cdot \frac{dQ}{dt} + H \cdot Q = 0 \qquad \textbf{(B.19)}$$

where G, H are matrices containing evaluations of α_j and *v*, *w*, respectively, and Q is the state vector containing the nodal values of *q*. The final solution is obtained by applying an Euler step function for the temporal discretization:

$$G \cdot \left(\frac{Q^{t+1} - Q^t}{\Delta t} \right) + H \cdot (Q^{t+1} - Q^t) = 0 \qquad \textbf{(B.20)}$$

B.3 THE MACCORMACK FCT FINITE DIFFERENCE METHOD

Flux corrected methods were developed as a way to counter excessive “smearing” of systems with sharp fronts. The flux correction method is essentially an “anti-diffusion” term, and can be added to any numerical scheme, including finite-element and multi-dimensional systems. We apply the flux-correction scheme to the MacCormack method, a commonly used finite difference scheme with error terms of o^2 in both space and time. The derivation that follows is based largely on Finlayson (1992). For clarity, we apply the scheme to the simpler advection equation. This in no way precludes the inclusion of a diffusion term. Rather, because the method introduces it’s own “diffusion” terms, it removes ambiguity from the derivation.

We begin with the normal MacCormack solution for the advection equation:

$$
\begin{aligned}
q^{*\,t+1}_{i} &= q^{t}_{i} - \frac{v\Delta t}{\Delta x}(q^{t}_{i} - q^{t}_{i-1}) \\
\tilde{q}^{\,t+1}_{i} &= \frac{1}{2}(q^{t}_{i} + q^{*\,t+1}_{i}) - \frac{v\Delta t}{2\Delta x}(q^{*\,t+1}_{i} - q^{*\,t+1}_{i-1})
\end{aligned}
\tag{B.21}
$$

The “final” solution for the basic method shown in Eq. B.21 becomes an intermediate solution for the FCT scheme, and is denoted by the tilde. A new intermediate variable is defined by

$$
\hat{\Delta}_{i+1/2} = \eta(\tilde{q}^{\,t+1}_{i+1} - \tilde{q}^{\,t+1}_{i}) \tag{B.22}
$$

The parameter η is often taken to be 1/8. A second intermediate solution is computed, with an extraneous diffusion term:

$$
q^{t+1}_{i} = \tilde{q}^{\,t+1}_{i} + \eta(q^{t}_{i+1} - 2q^{t}_{i} + q^{t}_{i-1}) \tag{B.23}
$$

Another intermediate variable is defined by

$$
\Delta_{i+1/2} = \eta(q^{t+1}_{i+1} - q^{t+1}_{i}) \tag{B.24}
$$

The flux correction term is then based on the value of

$$
f^{c}_{i+1/2} = sign(\hat{\Delta}_{i+1/2})max\begin{cases} 0 \\ min\begin{cases} sign(\hat{\Delta}_{i+1/2})\Delta_{i-1/2} \\ \left|\hat{\Delta}_{i+1/2}\right| \\ sign(\Delta_{i+1/2})\Delta_{i+3/2} \end{cases} \end{cases} \tag{B.25}
$$

and the final solution is given by

$$
q^{t+1}_{i} = q^{t+1}_{i} - (f^{c}_{i+1/2} - f^{c}_{i-1/2}) \tag{B.26}
$$

The scheme can be interpreted as adding artificial diffusion Eq. B.23 in order to dampen any oscillations that may form, and then removing it Eq. B.26 in order to re-sharpen the advective front.